DOI:10.15774/PPKE.ITK.2012.001

Analysis of the Heart Sounds and Murmurs of Fetuses and Preterm Infants

Ádám Tamás Balogh

A thesis submitted for the degree of
Doctor of Philosophy

Supervisors:
Ferenc Kovács, DSc
Doctor of the Hungarian Academy of Sciences
and
Tamás Roska, DSc
Ordinary member of the Hungarian Academy of Sciences

Pázmány Péter Catholic University
Faculty of Information Technology
Multidisciplinary Technical Sciences Doctoral School

Budapest, 2012

DOI:10.15774/PPKE.ITK.2012.001

DOI:10.15774/PPKE.ITK.2012.001

To my lovely wife Ramó

DOI:10.15774/PPKE.ITK.2012.001

DOI:10.15774/PPKE.ITK.2012.001

Acknowledgements

Despite having a strong fascination for becoming an engineer from childhood on, after the first semester of my undergraduate studies I became really unsure about continuing my education in electrical and computer engineering and I was thinking of changing to medical studies. However, I remained at information technology, and a few weeks later I became aware of the fetal phonocardiographic research at our faculty, something what I was really looking for – working a little bit as a physician, but being an engineer. This is why I am so deeply grateful to my supervisor Ferenc Kovács who invited me to his research group and shared with me his knowledge and his approach to scientific research, as well as for the long conversations and the support in many ways. I am also very grateful to my other supervisor Tamás Roska who, though not as directly involved with my research, has encouraged me in a great manner with his enthusiasm and fatherly guidance.

I am also very thankful to the physicians of the 1st Department of Paediatrics, Semmelweis University of Medicine, Budapest, especially to Miklós Szabó, head of department, to Kálmán Tory, who mentioned to me the idea of investigating preterm infants using phonocardiography, and Zoltán Molnár, who introduced me to the world of preterm infants and without whom the measurements could not have been performed. Special thanks go to the nurses of the neonatal intensive care unit who helped me a lot in recording the heart sounds of preterms. I also thank to Krisztina Kádár from the Gottsegen György National Institute of Cardiology, Budapest, and Zsolt Varga from the Markhot Ferenc Hospital, Eger, who gave indispensable aid to me regarding the examination of the fetuses.

A lot of the research has been performed as teamwork, and I am extremely grateful to all, former and present colleagues of the PCG research group, in particular to Katalin Barkai, Gábor Fodor, Ágnes Gál, Ádám Gazda, Barnabás Gera, Csaba Horváth, Mónika Hujter, József Joósz, Noémi Kersner, Endre Kósa, László Kozák, Andrea Nagy, Péter Talabár, Bálint Üveges, Krisztina Zsedrovitsné Gőcze and Tamás Zsedrovits. Many thanks to Balázs Jákli, Nor-

DOI:10.15774/PPKE.ITK.2012.001

bert Sárkány, Ákos Tar and József Veres from the Robotics Lab and to Attila Tihanyi for helping in the development of the measuring equipment.

Thanks to older and younger, former and present fellow PhD students and colleagues, especially to Éva Bankó, Béla Weiss, Bálint Sass, Dániel Szolgay, Norbert Bérci, Balázs Karlócai, Gergely Treplán, Dávid Tisza, Róbert Tibold, Tamás Pilissy, András Kiss, Balázs Varga, Kálmán Tornai, Vilmos Szabó, Andrea Kovács, András Gelencsér, Zoltán Kárász, László Füredi, Ádám Fekete Gábor Tornai, Csaba Nemes, Zoltán Tuza, János Rudán, István Reguly, Endre László, Csaba Józsa, György Cserey, András Oláh, Kristóf Karacs and Miklós Gyöngy.

I would like to thank Péter Szolgay, head of Doctoral School, Barna Garay and Árpád Csurgay for professional and personal help. I acknowledge also the kind help of the personnel of Students' Office, in particular Katinka Tivadarné Vida, the Dean's Office, the Financial Department and the IT Department. I am also very thankful to Viktória Sifter from the Library.

I would like also to express my deepest gratitude to my family and to all my friends, who helped and supported me in many-many ways, often not even knowing of it. I thank to my sister, Zsuzsi, in helping correcting many mistakes of my dissertation.

And, although it cannot be formulated in words, thank you, my lovely Ramó. I am so very grateful to all the Blessings I have received.

DOI:10.15774/PPKE.ITK.2012.001

Abstract

Cardiac auscultation is one of the oldest examination methods. Despite the development of modern imaging techniques the stethoscope is still considered a symbol of the doctor's profession. At the beginning of the 21^{th} century auscultation has found its main role in primary and in home health care when decisions have to be made about any further, more extensive examinations or special care. However, it seems that the real potential of heart sound analysis is still not exploited, especially in the field of fetal-neonatal examinations.

The aim of this thesis work has been twofold. First, recent studies showed that the fetal heart sound signal contains much more information than currently utilized in routine cardiotocographic examinations. Although a multitude of tools have been developed in the recent decades for the analysis of phonocardiographic (PCG) signals, their adaptation to fetal PCG is not straightforward because of differences in the cardiac anatomy, physiology and in the properties of the recorded signal (for instance bandwidth). Another major issue is the high level of noise. In this dissertation I present results on improved fetal heart rate calculation based on a method in the time-frequency domain. Furthermore, I describe a heart sound model which can be applied for parameter estimation of the first heart sound. The most important result outlined is the investigation of fetal heart murmurs, which could be a tool contributing to the widespread screening for congenital heart diseases prenatally.

A second aim of this work has been the application of phonocardiography to preterm infants with patent ductus arteriosus (PDA). I investigated the possibility of monitoring the state of the PDA through parameters of the heart sound signal. For this reason I introduced a method for sensitive detection of the murmur produced by turbulent blood flow through the ductus arteriosus and extracted parameters of the murmur which showed a relationship with important medical parameters. Another approach was the examination of the separation of the aortic and pulmonary components of the second heart sound (splitting). I applied a heuristic decomposition method and verified this procedure on an adapted heart sound model for preterm neonates. Based on this analysis I found that there is an increased splitting around the time of the closure of the PDA in the case of preterm infants receiving medication for closure.

DOI:10.15774/PPKE.ITK.2012.001

DOI:10.15774/PPKE.ITK.2012.001

Contents

DOI:10.15774/PPKE.ITK.2012.001

DOI:10.15774/PPKE.ITK.2012.001

DOI:10.15774/PPKE.ITK.2012.001

DOI:10.15774/PPKE.ITK.2012.001

List of Figures

DOI:10.15774/PPKE.ITK.2012.001

DOI:10.15774/PPKE.ITK.2012.001

DOI:10.15774/PPKE.ITK.2012.001

DOI:10.15774/PPKE.ITK.2012.001

List of Tables

DOI:10.15774/PPKE.ITK.2012.001

DOI:10.15774/PPKE.ITK.2012.001

List of Abbreviations

A_2	Aortic component of the second heart sound
ASD	Atrial septal defect
BPM	Beats per minute (heart rate)
CF	Confidence factor for heart rate calculations
CFD	Computational fluid dynamics
CHD	Congenital heart disease
CTG	Cardiotocography
D_{PDA}	Diameter of the PDA
ECG	Electrocardiography
FFT	Fast Fourier transformation
FHR	Fetal heart rate
fPCG	Fetal phonocardiography
HiR	Hit rate
HRV	Heart rate variability
IUGR	Intrauterine growth restriction
LA/Ao	Left atrial to aortic root ratio
$LSEV_{max}$	Average maximal late systolic envelope value
MCG	Magnetocardiography
NL	Noise level of a PCG recording
NRMSE	Normalized root mean square error
NST	Nonstress test
P_2	Pulmonary component of the second heart sound
PCG	Phonocardiography
PDA	Patent ductus arteriosus
S1	First heart sound
S2	Second heart sound
SI	Splitting interval
SNR	Signal-to-noise ratio
STFT	Short time Fourier transform
STV	Short-term variability
T_{bb}	Beat-to-beat time
TOCO	Uterine contraction
TOF	Tetralogy of Fallot
v_{max}	maximal blood velocity through the PDA
VSD	Ventricual septal defect
WVD	Wigner-Ville Distribution

DOI:10.15774/PPKE.ITK.2012.001

DOI:10.15774/PPKE.ITK.2012.001

Chapter 1

Introduction

"Itt nem vagyok idegen
Fekszem a szíveden
és hallom, hogy dobog."

Ákos – Adj hitet!

"And the sound of your heart," he continued.
"It's the most significant sound in my world."

Stephenie Meyer – Eclipse

1.1 Preface

Phonocardiography (PCG) deals with processing of the acoustic signals produced by the mechanical actions of the heart resulting in the vibration of the valves, heart muscle tissues and great vessels [13]. One of the central issues is to extract the different heart sounds from a noisy recording and relate them to the corresponding cardiac event. Moreover, heart sounds can be further analysed and certain features can be extracted for estimating the underlying cardiac parameters.

The importance of the heart was already realized in the fourth century B.C., although with some misconceptions: Aristotle argued that it was the seat of intelligence, motion and sensation [14]. From the medical perspective, Hippocrates noted already an early form of auscultation by holding an ear against the chest, but in his works he described only breathing sounds. Blood circulation was first described by William Harvey, an English Physician in 1628. In the same century, the polymath Robert Hooke (1635-1703) described

DOI:10.15774/PPKE.ITK.2012.001

the diagnostic potential of heart sounds [15]:

> *"I have been able to hear very plainly the beating of a Man's Heart... Who knows, I say, but that it may be possible to discover the Motions of the hemal Parts of Bodies... by the sound they make, that one may discover the Works performed in the several Offices and Shops of a Man's Body, and thereby discover what Instrument or Engine is out of order."*

These investigations lead to the invention of the stethoscope in 1816 by R. T. H. Laennec, and a century later the fetoscope for fetal heart sound examination. Nowadays, because of new advances in cardiac imaging, cardiac auscultation has become a preliminary test in the primary health care. On the other hand, due to the limited financial and human expert resources and the development of modern low cost computational devices in information technology, phonocardiography emerges also as a topic of current research and a possible tool aiding clinical decision making.

When describing the state of the art of PCG it is often compared to electrocardiography (ECG), a similar noninvasive examination method, so to say the electronic counterpart of PCG. A main difference is that greater success was achieved in standardizing ECG in contrast to classical PCG [13]. However, due to improvements in sensor technology and the availability of inexpensive computing devices, the concept of intelligent stethoscope gains importance, especially in telemedical applications [10,16–18], screening of children [19–23] or even in anesthesiology [24]. The engineering part of these tasks motivates also the development of methods for phonocardiographic signal processing using approaches in the time domain [25–27], in the frequency and in the time-frequency domains [28–32], or in the field of nonlinear dynamics [33–35]. PCG is regarded also as a promising tool for early identification of coronary artery disease [36, 37]. Another current research topic, where PCG comes into view, is the assessment of malfunctioning prosthetic heart valves [38,39]. All these current examples show the potential of PCG in present healthcare.

That phonocardiography offers unexplored possibilities is especially valid for the examination of fetuses because of their hidden position enabling the usage of only a limited number of monitoring techniques. Furthermore, due to its passive nature causing no irradiation at all, fetal phonocardiography can be applied for long-term monitoring. The development of adequate methods, which are certainly needed because of the great amount of data, could enable nearly continuous monitoring of the wellbeing of the fetus. Furthermore, the detection of abnormal heart sounds could contribute to the early diagnosis of cardiac anomalies.

Computerized phonocardiography is also a tool for quantitative and objective analysis which is missing in classical auscultation. This can be exploited, for instance for the monitoring of certain cardiac diseases by assessing the underlying cardiac dynamics.

DOI:10.15774/PPKE.ITK.2012.001

Nonetheless, for achievements in PCG the knowledge of the cardiologists, electric, computer and mechanical engineer has to be combined, making it an exciting and difficult multidisciplinary field of science.

1.1.1 Motivations and aims

Phonocardiography is not only the computerized form of auscultation. It opens new possibilities for the noninvasive examination of the functioning of the heart because, for instance, an important part of the intensity and frequency distribution of the heart sounds and murmurs is out of the human hearing range (Fig. 1.1), especially in the case of noise-contaminated fetal or preterm heart sound recordings.

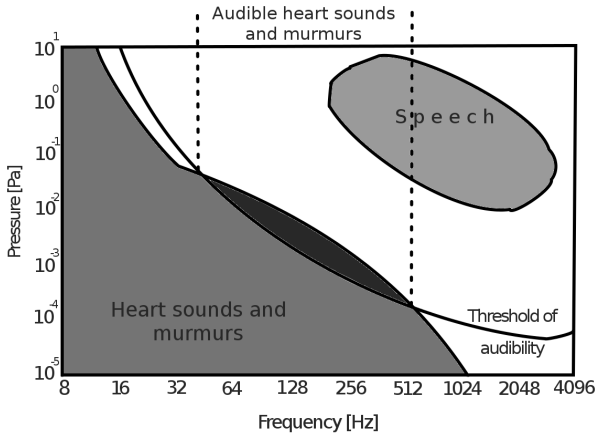

Figure 1.1: Intensity of heart sounds and murmurs in correspondence with the threshold of audibility and speech. Figure redrawn from Leatham [40].

Some other advantages of PCG have been already mentioned earlier and will also be highlighted in the following sections. There is a great variety of questions in this field which can be addressed from both a medical and an engineering point of view. The focus of my research can be summarized as follows: *Investigation of methods for the computerized analysis of phonocardiographic recordings from fetuses and preterms for aiding the diagnosis and monitoring of cardiac anomalies and diseases, with special attention to the extraction of parameters from the heart sounds and murmurs.*

In the following sections an introduction is given to the application of phonocardiography in the case of fetuses and preterm neonates.

1.1.2 Phonocardiography in the case of fetuses

Fetal examinations are an important field of healthcare, but due to the hidden position of the fetus, special measuring problems appear. It is a somewhat surprising that the

DOI:10.15774/PPKE.ITK.2012.001

observation of fetal heart sounds – despite its quite obvious medical significance – has not been described before the 17^{th} century. The first note on fetal heart tones is a poetry from a french man, Phillipe LeGaust, who was a colleague of a physician, Marsac, credited with first having heard the fetal heart. Nonetheless, this observation remained unnoticed until around 1820 when a Swiss and a French obstetrician, independent from each other, described the potential diagnostic significance of fetal heart sounds, but listening to the fetal heart tone became clinical practice only after 1833 when Evory Kennedy of Dublin published an extensive book in order to convince clinicians of the value of the aforementioned findings [41].

The first fetal heart sound examinations were performed by placing the ear on the maternal abdomen. Later, much attention was paid to whether auscultation with Laennec's instrument, the stethoscope, is more appropriate than auscultation with direct ear contact. In 1917, David Hillis, an American obstetrician described an instrument called head stethoscope or fetoscope, which is a stethoscope attached to the head of the obstetrician keeping his hand free during the auscultation. Because DeLee, chief of staff at the same institute, claimed the innovation to be his idea, this instrument subsequently came to be known as the DeLee-Hillis stethoscope, and has changed little since its early development [42].

Figure 1.2: The DeLee-Hillis stethoscope (fetoscope) for fetal auscultation, keeping the hands of the obstetrician free during the examination.

The first commercially available electronic fetal heart rate monitor was developed by Konrad Hammacher and Hewlett-Packard in 1968, using external tocography and phono-

DOI:10.15774/PPKE.ITK.2012.001

cardiography. Subsequent improvements allowed the addition of external ultrasound and intravaginal fetal electrocardiographic monitoring. After several decades of improvement, the most widely used noninvasive method for cardiotocography (CTG), which focuses on measuring the fetal heart rate and on simultaneous indication of the womb contractions (TOCO), is the ultrasound Doppler CTG. The measurement is based on the Doppler principle detecting the movement of the heart wall by the frequency change of the reflected ultrasound beam [43].

From the 1970s on ultrasound-based equipment became one of the most important tools for obstetrician examinations. At present, ultrasound echocardiography is the most informative noninvasive method providing reliable data about the morphology of the heart with possible malformations, furthermore about blood flow velocities. The disadvantage of this examination is that the equipment is expensive and well-skilled expertise is needed for obtaining and evaluating the data, which limits its usability for widespread screening. The more simple measurement of cardiotocography is the traditional nonstress test (NST) in the third trimester by which some basic fetal parameters may be obtained reflecting the actual status of the fetus. These parameters are derived from a 20-minute long record producing the fetal heart rate (FHR)-diagram (Fig. 1.3.). Among the main features are the visually well observable accelerations of the heart rate. A further characteristic feature of the diagram is the fluctuation from which the heart rate variability (HRV) is calculated, which is related to the neuronal control of the heart rate. The third parameter is the mean value (baseline) of the heart rate calculated as the average value but ignoring the outstanding sections (such as the accelerations) of the diagram. The abrupt decrease of the FHR (deceleration) might indicates an abnormal situation of the pregnancy, especially when it follows a womb contraction in a given delay [42]. All these parameters have official definitions [44], but there is still much research and controversy on the significance of FHR.

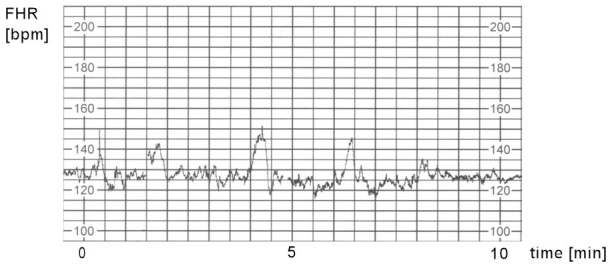

Figure 1.3: Fetal heart rate (FHR) diagram from a 10-min long recording. Three accelerations are observable.

Although the ultrasound Doppler CTG is a robust method, it has some limitations. It

DOI:10.15774/PPKE.ITK.2012.001

is still a topic of scientific debate whether ultrasound exposure has an adverse effect on the developing fetus [45–48], which should also be taken into account in the case of echocardiographic examinations. Furthermore, when compared with direct fetal ECG – the most accurate method for FHR determination – the beat-to-beat time (T_{bb}) values show an average absolute error of ΔT_{RR}=2.98 ms with a standard deviation of σT_{RR} =4.18 ms, and a significant decrease in the short term HRV parameters of even 40 % [49]. It should be also mentioned that this method does not provide any information about the inner part of the heart, for instance about the operation of the valves or about the presence of a septum defect or other abnormality.

There are three other methods to carry out CTG measurements, namely electrocardiography (ECG), magnetocardiography (MCG) and phonocardiography, which are described in turn below.

Fetal electrocardiography (fECG) is one of the gold standards for determining the fetal heart rate and thus obtaining fetal HRV parameters. A disadvantage is that in the noninvasive scenario the electrodes are attached to the maternal abdomen which introduces heavy signal processing requirements for extracting the weak fetal ECG signal from the noisy recordings containing also the strong maternal ECG signal and electromyographic signals [50, 51]. Furthermore, in the last month and in the 28^{th} to 34^{th} weeks of the pregnancy the reliability of this fECG decreases to 60 % due to the presence of the vernix caseosa[1] [52–56]. However, its passive nature enables very long measurements, which can be utilized for studying the FHR variability [57], and the analysis of ST segments enables the more reliable diagnosis of perinatal fetal hypoxia [58].

Magnetocardiography can also be used for noninvasive CTG measurements. The problems with this method are the expensive equipment and the skilled personnel required, but the obtained R-R time intervals and the corresponding FHR values are very accurate and suitable for deriving further parameters. As an example, maternal-fetal heart rate synchronization has been investigated with fMCG [59]. In another study the changes in the low frequency bands of the spectral density of the R-R interval function with gestational age were examined in order to find relations to the development of the fetus [60].

The three formerly mentioned methods for CTG measurements, perhaps except fECG, have some limitations regarding the following aspects:

- long-term measurements,
- widespread screening of pregnant women,
- evaluation of further features, for example heart murmur.

Regarding long-term measurements it should be noted that a 20-minute measurement is

[1]The vernix caseosa is a waxy or cheese-like white substance found coating the skin of newborn human babies

DOI:10.15774/PPKE.ITK.2012.001

rather short to get a true information about the fetal status. This is partly because the fetal status is dependent on the current environment, such as time of day, state of the mother, and so on. Because of ultrasound irradiation on the intrauterine environment long-term ultrasound-based CTG measurement, including its home monitoring application, is not preferred. The long-term application of MCG is safe and suitable, the only obstacle is the very complex measuring scenario. Fetal ECG fulfils most of the requirements, although the low SNR, especially in the presence of the vernix caseosa, limits the capability of identifying the effect of cardiac abnormalities on the electric waveform.

A re-emerging method for CTG measurements is fetal phonocardiography (fPCG). This is a simple technique for recording transabdominally the acoustic signal of the fetal cardiac system. The signal is usually corrupted by noise originating from fetal motions and from the maternal heart and digestive system, however, new advance in signal processing show a promise for identifying significant features of the fPCG signal related to the fetal wellbeing.

There are relatively few scientific contributions to fPCG. In one of the earliest contributions to fetal PCG, patterns of the fetal phonocardiogram were correlated with fetal breathing movements and other fetal movements [61]. For denoising the fPCG signal several methods were investigated, for example the wavelet transform [62] or adaptive filtering [63].

The beat-to-beat time (T_{bb}) measured simultaneously with fPCG and fetal ECG was compared by Ortiz *et al.* [64]. They found that the average T_{bb} time correlated well, and heart rate variability measures in the very low and low frequency range agreed between the two methods. On the other hand, the power spectral density of the HRV differed in the high frequency range (above 0.3 Hz), which was attributed to physiological differences between the two measured phenomena and to possible errors resulting from the signal processing. The first one is not completely justified, in the case of the latter there is a possibility for improvement, attempted also in the present work.

Screening for congenital heart diseases

A further important topic in obstetrics is the detection of diseases, in particular cardiac diseases because any abnormality in the fetal circulation might have serious consequences, for instance the injury of the brain [65]. Comprehensive echocardiographic examination is the most accurate method for detecting cardiac malformations during pregnancy, but it is expensive and needs skilled expertise. Since the prevalence of congenital heart diseases (CHD) is estimated to be around 8/1000 live births [66, 67], there is a necessity for examination methods which can be used for widespread screening. A detailed echocardiography examination is usually suggested based on risk factors or on an abnormal four-

DOI:10.15774/PPKE.ITK.2012.001

chamber view, and some reports suggest that the inclusion of the three-vessel view in the screening would also increase the detection rate [68]. Risk factors, such as advanced maternal age, family history of genetic disorders, gestational diabetes or multiple pregnancy define the high-risk population, whose screening is worldwide more or less solved [69].

On the other hand, detection of CHDs in the low-risk population, where most fetal cardiac malformation cases occur and only routine screening is performed with greatly varying training of the operator, remains still a challenge [69,70]. It is problematic because moderate symptoms of anomalies remain usually unnoticed. Based on present screening methods the rate of prenatally identified cardiac abnormalities is still only around 50 % or even less [71], whereas recent studies indicate that prenatal diagnosis of congenital cardiac defects is important during delivery [72], and improves outcome, for instance in the case of duct-dependent heart defects [73,74]. These studies underline the importance of widening the possible techniques for fetal heart examinations in order to minimize the number of unforeseen cases requiring urgent treatment after delivery.

Echocardiography, being expensive, is not a suitable tool for prenatal screening of the low-risk population, but is unconditionally necessary for the detailed examination of the patients found positive by some screening. The capability of Doppler CTG for discovering additional features is limited to the investigations based on the time- and frequency-analysis of the FHR data, which is useful for assessing intrauterine growth restriction (IUGR) and the neural development of the fetus. However, cardiac anomalies usually do not manifest themselves in the FHR and a further problem is that FHR variability measures calculated from T_{bb}s of the Doppler CTG proved of decreased accuracy [49]. As already mentioned, fetal ECG and MCG methods are much more reliable concerning the timings and the signal shapes, they are also a topic of current research, but some major limitations are present, for instance due to the measuring scenario and the vernix caseosa.

It appeared based on the analysis of the recordings of the high-volume CTG measurements from the last ten years that the PCG method is capable of detecting some additional features of the fetal heart as well, such as the splitting of heart sounds – related to abnormal pressure ratios – and murmur – originating form a turbulent blood flow –, which may be used for indications of some CHDs.

1.1.3 Phonocardiography in the case of preterm infants

Phonocardiography can be applied also in other fields of healthcare. One of them, investigated in this work, is the examination of preterm neonates, in particular preterms with a certain congenital heart disease called patent ductus arteriosus (PDA). This disease affects a certain essential fetal vessel, the ductus arteriosus, which should close after

DOI:10.15774/PPKE.ITK.2012.001

birth (Fig. 1.4). The vital decision a physician faces is whether and how to treat this disease. Unfortunately there are only a limited number of possibilities for clinical assessment for aiding this decision. However, the application of phonocardiography is still not exploited in this field.

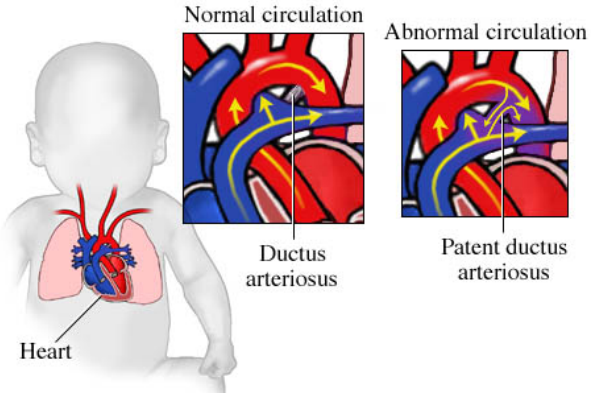

Figure 1.4: The difference between normal circulation and abnormal circulation due to patent ductus arteriosus. This essential fetal vascular structure has to close after birth otherwise allowing harmful systematic-to-pulmonary communication. Reprinted from [75].

In general the prevalence of PDA is around 2 per 1000 births, but in the case of preterms there is an increased risk for PDA which is due to physiological factors related to prematurity [76]. Some studies show that 65 % of preterm neonates with birth weight $\leq$ 1000 g will have PDA and a gestation of $\leq$ 30 weeks is also a recognized risk factor [77,78]. PDA is about twice as common in girls than in boys.

The main diagnosis is done with echocardiography, which needs expertise, and sophisticated and expensive equipment. Furthermore, the assessment of hemodynamical significance is still not obvious [77,79], which means that the type and the timing of the treatment is also ambiguous [78,80,81]. These aspects underline the need for simple tools helping the diagnosis and the monitoring of the PDA in preterms.

Recent advances in neonatal monitoring provide new tools and equipment for the surveillance of preterm newborns [82,83], however, these studies usually deal with body temperature, electro-cardiogram, respiration and the degree of blood oxygen saturation monitoring. Although PDA may influence these values, its effect is rather indirect. Skin reflectance has also been suggested as a more direct examination for diagnosing hemodynamical significance [84], and pulse wave analysis possesses also diagnostic value not yet exploited [85,86]. Phonocardiography comes into view based on the observation that one of the fundamental symptoms is murmur. It could help in the quantitative assessment of murmur parameters since the murmur is often difficult to hear in the noisy environment of the neonatal intensive care unit. Although earlier studies investigated the murmurs

DOI:10.15774/PPKE.ITK.2012.001

related to PDA in preterm infants [87], none of them tried to find a relationship between various parameters of the heart sound and of the patent ductus arteriosus in the case of preterm neonates.

Some recent works investigated also the application of biomarkers for diagnosing hemodynamically significant PDA [88]. Although echocardiography probably will remain the gold standard for the assessment of PDA, an appropriate combination of ultrasound, biomarkers, and clinical signs might improve the outcome [89], since the underlying main problem is that there is still a lack of understanding of neonatal circulation, and there is a "need to move the research beyond simply showing change in a physiological variable in response to a treatment" [90].

The main idea behind investigating murmurs is to access the blood flow dynamics through analysis of the generated sound, which is also referred as phonoangiography [91]. However, it is a very difficult problem to relate acoustic parameters with parameters of a turbulent fluid flow, not to mention the noise which affects the measurements.

Another feature is the investigation of the heart sounds. Normally, these are made up of the closure sounds of the valves on the left and right side of the heart. In the case of the second heart sound these are the aortic and the pulmonary valves. The pressure ratios between the arteries and the ventricles determine the exact closure time of these valves. Because the patent ductus arteriosus connects the two main arteries, its will have an influence on the pressure ratios between the arteries and the ventricles, thus also on the second heart sound. During the closure of the PDA the pressure rates will apparently change, which could be reflected in the time interval between aortic and pulmonary components of the second heart sound.

1.2 Methods

All fetal phonocardiographic (fPCG) data was recorded with a phonocardiographic cardiotocographic (CTG) device (Fetaphon-2000^{TM}, Pentavox Ltd.) domiciliary or in clinical environment, in the case of the latter one mostly at the Hungarian Institute of Cardiology, Budapest. The length of these recordings was usually 20 minutes corresponding to the length of conventional CTG examinations. The fPCG device uses a sampling frequency of 333 Hz and a resolution of 8 bits. The recorded data was transferred via a mobile network and stored on an evaluation centre.

Phonocardiographic data of preterm infants was recorded using a self-made electronic stethoscope at the 1st Department of Paediatrics, Semmelweis University of Medicine, Budapest. After preprocessing, the data was archived for further analysis with a sampling frequency of 3000 Hz and a resolution of 16 bits. The length of the measurements was usually 30 seconds long. Informed consent was obtained in all cases.

DOI:10.15774/PPKE.ITK.2012.001

The difficulty in phonocardiographic signal processing arises from the nonstationarity of the signals, often resulting in very short transients, and a low signal-to-noise ratio. Some of the noise can be filtered out using traditional linear filters, but noise components often overlap with heart sound components not only in the time, but also in the frequency domain. I applied a wide variety of tools for biomedical signal processing, not all of them producing acceptable outcomes. In this work I present the results of the following approaches:

- **Time domain methods**: linear filtering, improved ensemble averaging [92], heuristic methods
- **Time-frequency domain methods**: short time Fourier transform [93], wavelet transform [94], Wigner-Ville distribution [95]
- **Signal modelling and model fitting**: linear and nonlinear chirp models [28, 96], time-frequency domain based parameter estimations [97], Monte Carlo method [98]

A more detailed description of the aforementioned methods can be found in Chapter 3.

There are several important phonocardiographic features which have to be assessed. In the case of fetal CTG measurements the fetal heart rate (FHR) is one of the most important ones, which can be calculated based on the cyclostationary period of the fPCG signal. Moreover, recent studies suggest that based on the variability of the beat-to-beat times the development of the fetal nervous system can be assessed [99] and further details of the fetal wellbeing (e.g. detection of IUGR) can be monitored [100], emphasizing the importance of exact FHR determination.

Splitting, that is the temporal separation of different heart sound components, is often one symptom of cardiac anomalies [101]. Quantitative analysis is very difficult because of the overlapping components. Approaches based on models of the heart sounds show a possibility of estimating not only the splitting but also other parameters of the heart sounds.

The detection of murmurs is crucial for early diagnosis of cardiac diseases, but it is also a difficult task due to the presence of noise, especially in the case of the PCG signals of fetuses and preterm infants. Nevertheless the detection is only the first step in clinical applications because based on extracted parameters of the underlying cardiovascular phenomena can be monitored or classification of the heart diseases is possible in some cases.

In this dissertation I present novel results for investigating these aspects based on the methodology mentioned above.

For processing and analysis of the data and visualisation of the results I implemented all algorithms in different versions of Matlab (The MathWorks Inc., Natick, MA, USA).

DOI:10.15774/PPKE.ITK.2012.001

1.3 Framework of the dissertation

Except the chapters describing the biological and methodological background, this work is divided into two major parts. The first one explains the application of phonocardiography in the case of fetuses, the second one deals with PCG results in the case of preterm infants. These two parts can be read separately; in the one or two cases it is needed, reference to corresponding sections is given.

The chapters are organized as follows: Chapter 2 gives a detailed description of the anatomy and physiology of the human cardiovascular system, of possible cardiac abnormalities and diseases and of the generation of heart sounds and murmurs.

In Chapter 3 the theory and methods are introduced for the analysis of nonstationary signals, such as phonocardiographic signals.

Chapter 4 deals with phonocardiography of fetuses, starting with the determination of the heart rate, followed by the investigation of heart sound models, and ending with the detection of fetal heart murmur.

In Chapter 5 the heart sounds of preterm infants having a certain congenital heart disease, called patent ductus arteriosus, are analysed. The focus is on investigating heart murmur and heart sound splitting related to PDA.

Finally, in Chapter 6 conclusions are drawn and possible further work is addressed. A summary of the achieved results in form of theses is also given in this chapter, concluded with the delineation of possible applications.

1.3.1 General notes

Because most of the work was carried in out in collaboration, in the rest of the dissertation – except in the summary in Chapter 6 – I will use “we” instead of “I”. My contributions are enumerated in Chapter 6 in a rigorous manner. The results of the work of the other members of the research group can be found in [102–109].

DOI:10.15774/PPKE.ITK.2012.001

Chapter 2

Origin of Heart Sounds & Murmurs

In order to fully understand the genesis and significance of heart sounds some biological knowledge is required. The following sections try to give a short introduction on the anatomy and development of the human heart and on cardiovascular dynamics including the genesis of heart sounds. Furthermore, possible malformations and abnormalities will be discussed, with special attention on the resulting acoustic manifestations.

2.1 The anatomy of the human heart

The heart is one of the most important organs in the human body; it is the pump of life, providing nutrients and oxygen for the tissues and organs through continuous blood flow while removing carbon dioxide and other by-products. Cardiac arrest without emergency treatment will result in death after a couple of minutes. This is why early diagnosis of cardiovascular diseases is so important.

The human heart is essentially a muscle, in adults somewhat larger than a fist. It consists of four main parts, the so called chambers: two upper atria and two lower ventricles. The septum divides it into a larger and stronger left and a smaller and weaker right side. This partition is essential for the effective circulation of the blood. The pulmonary vein, returning oxygenated blood from the lungs, empties into the left atrium. The atria act as a collecting reservoir, making faster filling of the ventricles possible. The ventricles act as pumps pushing out the blood into the great arteries. In the case of the left ventricle, the receiving great artery is called the aorta, which forwards the oxygen-rich blood to the body. The pulmonary artery, emanating from the right ventricle, transports de-oxygenated blood to the lungs again. A schematic drawing of the human heart is shown in Fig. 2.1.

DOI:10.15774/PPKE.ITK.2012.001

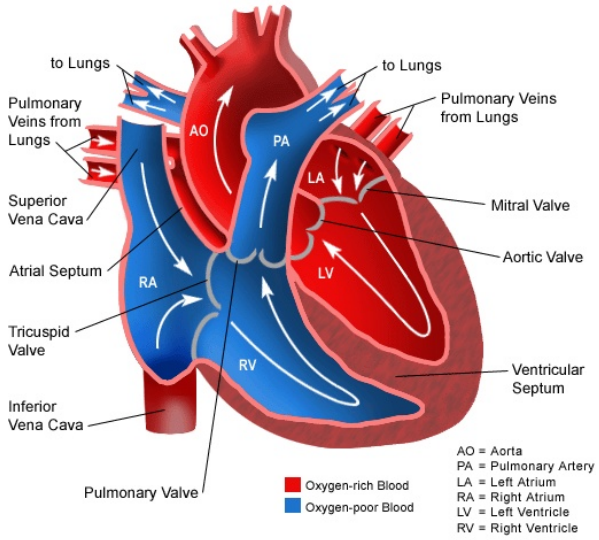

Figure 2.1: The schematic representation of the human heart. The white arrows show the flow direction of the blood. Figure reprinted from [110].

2.1.1 Heart valves

Heart valves are passive elements consisting of connective tissue, responsible for the unidirectional blood flow. The atrioventricular valves, that is the mitral and tricuspid valves separate the atria and ventricles, whereas the semilunar valves, called the aortic and pulmonary valves are located at the outflow of the ventricles. There is a single fibrous ring around each of the heart valves, and these rings are connected forming a fibrous skeleton. This framework has several physiological functions: it is the base to which the heart valves and great arteries attach, and it protects the valves from overstretching as the blood passes through them; furthermore, it behaves as an isolating layer between the atria and ventricles preventing them from simultaneous contraction (the heart has its own electric circuit, responsible for the appropriate timing of the electric signals) [111].

All four valves consist of so called leaflets or cusps (Fig. 2.2). Except the mitral valve, all other valves have three cusps. The main difference between the atrioventricular and semilunar valves is that the atrioventricular valves are connected to the ventricular wall via the chordae tendineae. These tendons prevent the valves from turning over into the atria when the ventricles contract to push the blood out into the great arteries. There is less danger of prolapse in the case of the semilunar valves since they have to resist much smaller pressure gradients.

DOI:10.15774/PPKE.ITK.2012.001

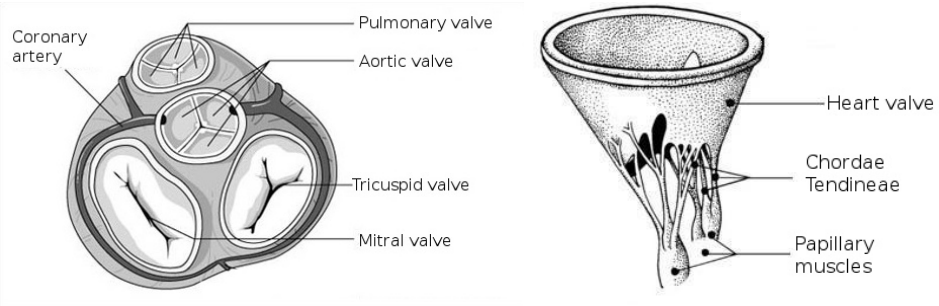

Figure 2.2: The cross-section of the heart showing the four heart valves (left) and an atrioventricular valve with the attached chordae tendineae connecting the valve leaflets to the papillary muscles and the ventricle wall (right). Taken from [112].

2.1.2 The fetal and neonatal circulation

The development of the fetal heart begins during the third week of gestation. In the beginning, the cardiac precursor cells form a single tube. The beating of the fetal heart, which happens based on the intrinsic spontaneous contraction of the myocardium, i.e. the heart muscle, starts around day 21 of gestation, however, blood circulation starts only a week later [113]. During the 4^{th} week of gestation constriction of the tube define the separate components of the hearts, which will develop later on as the atria and ventricles. The looping of the heart tube initiates the final development of the normal heart structure. The 4-chamber heart evolves by the end of week 7. This is also about the first time when a heartbeat can be detected and viability can be assessed. The development of the heart is extremely sensitive during weeks 4-7 of gestation. This is why certain maternal infections, medication or metabolic diseases in this period can contribute to the development of congenital heart diseases.

In contrast to the human adult circulation, where oxygenated and de-oxygenated blood is well separated, in the case of the developed fetal circulation this is not the situation (Fig. 2.3). This is necessary because the fetal lungs are in a collapsed state and the reoxygenation of the blood occurs in the placenta. The umbilical arteries, emanating from the descending aorta just after the bifurcation, transport deoxygenated blood to the placenta. Most of the returning oxygen-rich blood is emptied into the inferior vena cava through the ductus venosus from the umbilical vein. As the inferior vena cava enters the right atrium, the blood is guided toward the oval foramen – an opening between the two atria, vital before birth – by the valve of the inferior vena cava, and most of the blood passes directly into the left atrium. This is needed because this way it is possible to supply the fetal brain with as much oxygenated blood as possible, since from the left atrium the blood travels directly to the head and arms via the left ventricle and arteries arising at

DOI:10.15774/PPKE.ITK.2012.001

the top of the aortic arch [114].

The fetal pulmonary circulation has a high resistance to flow, therefore the blood pumped out of the right ventricle travels through an additional vessel, the ductus arteriosus, which closes after birth, into the aorta. It is noteworthy that the ductus arteriosus connects to the aorta just after the aortic arch. This is important since – as already mentioned – arteries arising from the top of the arch transport blood to the brain. The blood coming through the ductus arteriosus is less oxygenated than the blood coming from the left ventricle. In such a way the fetal brain receives as much oxygen as possible (note the color coding for blood oxygen level in the schematic Fig. 2.3), which is clearly an evolutionary advantage.

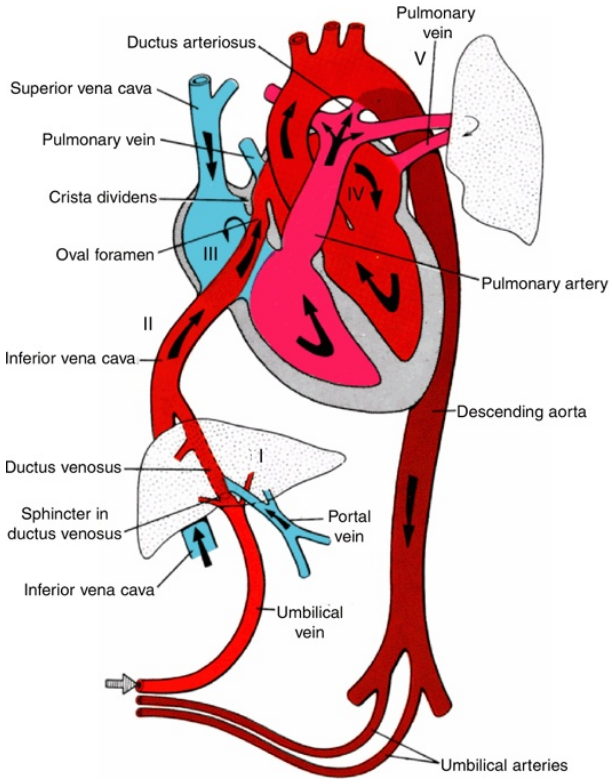

Figure 2.3: Fetal circulation. Arrows show the direction of blood flow. Note the locations where oxygenated blood mixes with deoxygenated blood: the liver (I), the inferior vena cava (II), the right atrium (III), the left atrium (IV), and at the entrance of the ductus arteriosus into the descending aorta (V). Taken from [114].

After birth, the transition to adult circulation is usually surprisingly rapid. The first intake of breath forces the lungs to expand, resulting in normal pulmonary circulation. Due to the changed blood pressure ratios and some other physiological factors the oval foramen and the ductus arteriosus functionally closes during the first day of life.

DOI:10.15774/PPKE.ITK.2012.001

2.2 The dynamics of the heart

In order to maintain continuous blood flow in the circulatory system, the heart contracts periodically, on average 72 times per minute in the case of adults. However, the heart muscles of the human heart do not contract simultaneously, the contractions occur in two main phases, which are called systole and diastole. At the beginning of the heart cycle, as the ventricles contract, the pressure inside these lower heart chambers increase exceeding the atrial pressure which produces the closing of the atrioventricular valves, marking the beginning of the systole. Slightly later the semilunar valves open, allowing the ventricular blood to enter the great arteries. As the ventricles relax at the end of the systole, the pressure gradient between the great arteries and the ventricles becomes negative, which would cause the arterial blood to flow back into the ventricles. This is prevented by the closing of the aortic and pulmonary valves, which is the beginning of the diastole. As the pressure inside the ventricles decreases further, the atrioventricular valves fall open, which makes the refilling of the ventricles possible (see Fig. 2.4). At the end of the diastole the atria contract pushing even more blood into the ventricles before the cycle starts all over again [115].

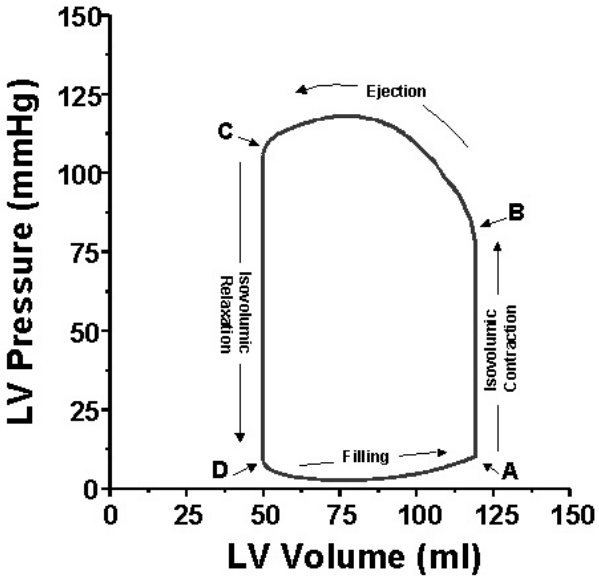

Figure 2.4: The pressure-volume curve of the left ventricle. Point A marks the beginning of the systole (the closing of the mitral valve), point B corresponds to the opening of the aortic valve. Point C denotes the end of the systole and beginning of the diastole (closure of the aortic valve) and point D indicates the opening of the mitral atrioventricular valve. Figure reprinted from [116].

DOI:10.15774/PPKE.ITK.2012.001

2.3 Heart sounds & murmurs – terminology and definitions

Mechanical actions of the heart produce audible noises. These noises are called heart sounds, and are produced by vibration of the valves, heart muscle tissues and great vessels [117]. The cardiovascular sounds are weak compared to other physiological sounds, such as speech, stomach rumbling and breathing noise. They produce frequencies in the range of 1-1000 Hz, however the main components lie in the lower part of this bandwidth, which is also around the lower limit of the human hearing (Fig. 1.1).

2.3.1 Heart sounds

There are two major heart sounds, which are always present, and two less dominant heart sounds, which can be observed only in a restricted group of people. As shown in Fig. 2.5, the first heart sound (S1) is produced at the beginning of the systole, and is caused by the closing of the atrioventricular valves and vibration of the ventricle walls. The second heart sound (S2) coincides with the end of the systole and beginning of the diastole, and it is generated by the closing of the aortic and pulmonary valves and by the fast deceleration of the arterial blood. The third (S3) and forth (S4) heart sounds occur during the diastole. The S3 sound is believed to be initiated by the sudden deceleration of atrioventricular blood flow when the ventricle reaches its limit of distensibility, causing vibrations of the ventricular wall. Finally, the S4 sound is produced by the end-diastolic atrial contractions, resulting in vibrations of the ventricle wall like in the case of the S3 sound [13].

The S3 and S4 are rarely observed in the neonatal period. In the case of fetal and preterm heart sound recordings only the S1 and S2 sounds can be detected, due to the low signal-to-noise ratio. Segments of typical fetal and neonatal recordings are shown in Fig. 2.6.

The origin of heart sounds

In general there are two main theories regarding the generation of heart sounds, but it is still a topic of scientific debate [118]. The first one argues that the closing of heart valves generates vibrations similarly to the closing of a door, which can be perceived at the thorax. This is called the *valvular theory*, meaning that the vibrations of the valves are dominant, and it is supported by the echocardiographic findings demonstrating the coincidence between the timing of the valve vibrations and the heart sounds [119]. On the other hand, the *cardiohemic theory* states that no cardiac structure can vibrate on its own, because the blood is an incompressible fluid coupling the different cardiovascular structures. According to this theory not only the vibration of the valves is important, but the thoracic heart sound is a result of vibrations of the entire cardiohemic system: the heart cavities, the valves and the blood [118].

DOI:10.15774/PPKE.ITK.2012.001

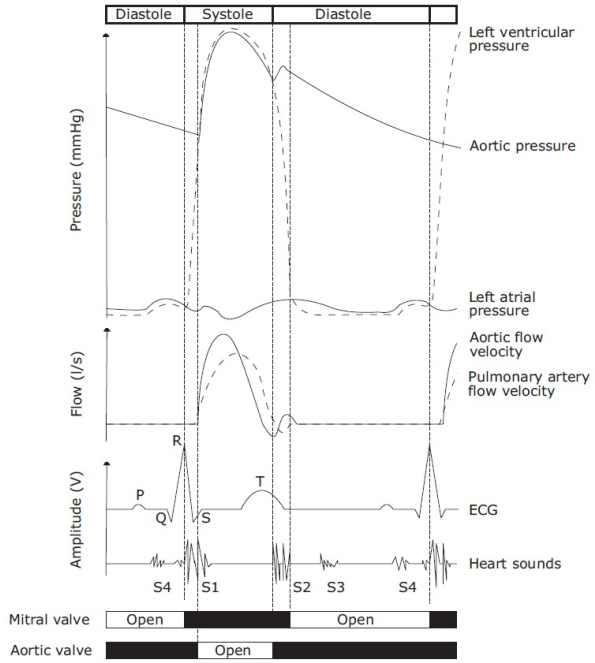

Figure 2.5: The Wiggers diagram: a comprehensive representation of the dynamics of a single heart cycle. Note the temporal synchronisation between the different signals. Taken from [35].

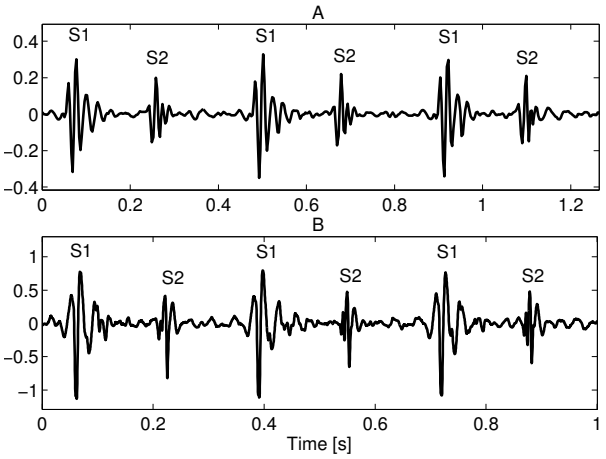

Figure 2.6: Three heart cycles of typical (A) fetal and (B) preterm neonatal heart sound recordings. See Sections 4.1 and 5.2.1 for for further details regarding the equipment and methods employed in acquisition.

DOI:10.15774/PPKE.ITK.2012.001

Splitting of heart sounds

A feature which has clinical significance is the splitting of heart sounds. As described earlier, the S1 and S2 sounds are the result of valve closure and vibration occurring at both sides of the heart, which yield two components for both heart sounds. There is usually just a very short delay between the timing of these components producing in general a single heart sound. Nevertheless, if – due to some reason – the closing of the valves happens significantly earlier or later on one side, then this single heart sound will change into two sounds – a split heart sound.

The genesis of the S1 is surrounded by some controversy [120,121], however, the closing of the atrioventricular valves is beyond all doubt involved in the generation of the first heart sound. The mitral valve closes usually slightly earlier than the tricuspid valve on the right side, but in general they cannot be separated. Splitting of the S1 sound has also important clinical implications, such as left or right bundle brunch block. An example of fetal S1 split is shown in Fig. 2.7.

It is well supported that the S2 sound is composed of a component produced by the closure and vibration of the aortic valve and surrounding tissues (A_2), followed by a sound resulting from the closure and vibration of the pulmonary valve and surrounding tissues (P_2). The A_2 component usually precedes the P_2 component; their temporal separation is denominated as the S2 split. In adults, the separation increases during inspiration up to 80 ms, known as physiological split, due to an increased amount of blood returning to the right ventricle and a decreased amount of blood returning to the left ventricle, which results in a delayed P_2 component and an earlier A_2 component, respectively. During expiration the splitting decreases again, resulting in the sensation of a single sound. Reversed splitting, that is splitting only during expiration might indicate aortic stenosis or left bundle branch block. On the other hand, splitting during inspiration *and* expiration is often a symptom of pulmonary stenosis, atrial septal defect or ventricular septal defect (cardiovascular diseases are described in more detail in section 2.4).

2.3.2 Heart murmur

Murmur arises from the acoustic radiation of turbulent blood flow caused, for instance, by a constriction in the artery or an insufficiently functioning heart valve (Fig. 2.8). Section 5.1.1 describes the generation of heart murmur in more detail. Since turbulence is a chaotic dynamic state, the resulting heart murmur differs greatly from the heart sounds which have "only" an oscillating background. Although simulation of flows in cylindrical tubes with certain constrictions give new insight into the dynamics behind heart murmur (see Fig. 2.9), there is still a great lack of understanding, which hinders the exploitation of the diagnostic value of heart murmur.

DOI:10.15774/PPKE.ITK.2012.001

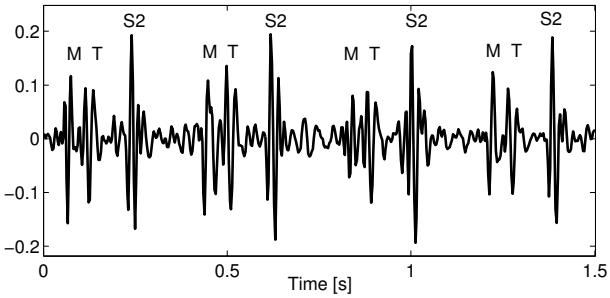

Figure 2.7: Fetal heart sound record with 60 ms S1 split, separating the mitral (M) and tricuspid (T) component of the first heart sound.

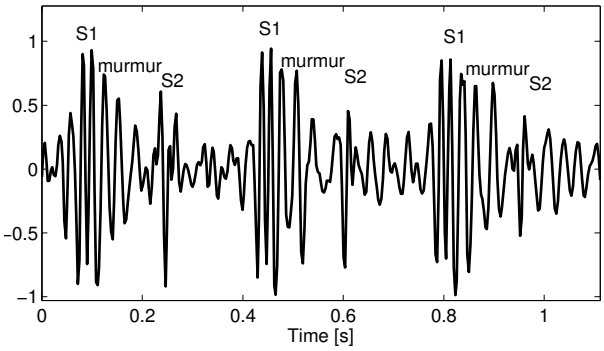

Figure 2.8: Fetal heart sound record with a significant systolic murmur due to turbulent blood flow through collateral arteries.

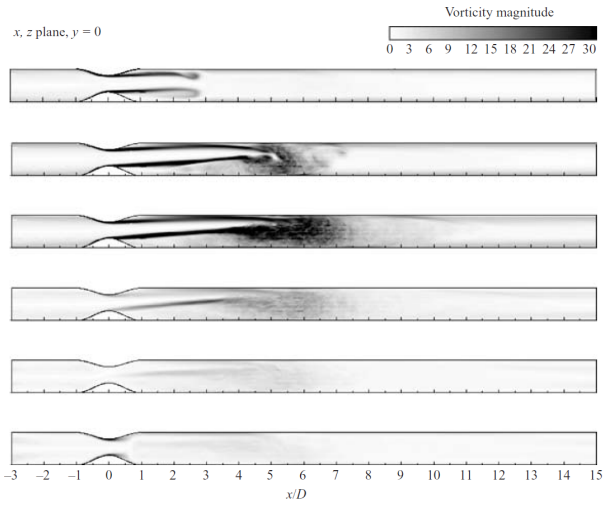

Figure 2.9: Sequence of normalized averaged vorticity magnitude contours for pulsatile flow through the 75 % eccentric stenosis. Taken from [122].

DOI:10.15774/PPKE.ITK.2012.001

Although the presence of murmur is always related to some deviation resulting in turbulent blood flow, if the real cause is hemodynamically insignificant, it is regarded as *innocent murmur*. In contrast, murmur related to some cardiovascular disease is called *pathological murmur* [117].

Usually five properties of heart murmur are assessed during auscultation in clinical practice [123]:

- **Timing and duration**: murmurs should be identified as being systolic or diastolic (or rarely, continuous). The duration can then be subdivided into further subcategories, such as early, mid, late systolic or even holosystolic.

- **Intensity**: the intensity of a murmur is graded on a scale of 1-6, where grade 1 is a quiet murmur that can be heard only after careful auscultation over a localised area and grade 6 is a murmur sufficiently loud to be heard with the stethoscope raised just off the chest surface.

- **Point of maximal intensity and radiation**: point of maximum refers to where the murmur can be heard best. Several locations on the chest are defined which correspond to specific parts of the heart. Regarding the radiation, a general rule of thumb is that the sound radiates in the direction of the blood flow.

- **Shape**: the shape describes the intensity change of the murmur during the cardiac cycle and it is related to the corresponding flow velocities. It is described by musical notions, for example crescendo or decrescendo, but the intensity can also remain fairly constant.

- **Character**: it is described by the pitch of the murmur and based on the spectral configuration. For example, in the case of a musical murmur typically a dominant tone is present, but usually many frequencies build up the murmur, making it blowing, harsh, or rumbling.

2.4 Heart diseases

The anatomy and functioning of normal fetal, neonatal and adult circulation have been described in the previous sections, but a great part of this work deals with heart sounds related to different pathological cases. This necessitates an introductory section on different cardiovascular diseases.

DOI:10.15774/PPKE.ITK.2012.001

2.4.1 Heart valve diseases

Heart valves have the two major functionalities of blocking the back flow and enabling the forward flow of the blood in the different phases of the heart cycle. Consequently it is not surprising that there are two major abnormalities which affect heart valves: *stenosis*, which is abnormal narrowing, hindering normal forward flow, and *insufficiency*, which corresponds to the insufficient closing of the heart valve enabling back flow [124]. Although abnormalities of all for heart valves are possible, the valves on the left side of the heart are more frequently affected by valvular diseases, since the left side has to support the continuous blood flow in the greater systematic circulation.

Stenosis

Heart valve stenosis is an abnormal narrowing of the valvular orifice due the thickening or calcification. Formerly it was often caused by rheumatic fever, but it has become a rare disease nowadays in the western world, except in early life. The stenosis of the aortic valve increases the workload of the left ventricle since the muscles have to push with a greater force to maintain cardiac output. This will result in the thickening of the left ventricle wall, called hypertrophy. In serious cases, with no surgical replacement of the valve it may lead sudden cardiac arrest. Since the blood flow velocities are high during the systole when the blood flows through the aortic valve, the flow becomes turbulent, and a strong systolic crescendo-decrescendo murmur develops, which is a usual symptom of aortic stenosis.

Mitral stenosis hinders the normal filling of the left ventricle during the diastole. It is caused by scarring of rheumatic fever, causing the valve flaps getting stuck together by adhesions. This causes the blood being backed up in the lungs, resulting in congestive heart failure, which is a condition in which the heart cannot supply the body's need. The only treatment of mitral stenosis is surgical opening of the valve. Similar to aortic stenosis, murmur may arise as a physical symptom, but in this case at the end of the diastole when the atrium contracts. Another sign is an unusually loud S1 sound because of increased force in closing the mitral valve.

Pulmonary and tricuspid stenosis is a rare, congenital phenomenon that often requires surgery.

Heart valve insufficiency

During aortic insufficiency, or regurgitation, when the aortic valve leaks blood back into the left ventricle, the chamber has to work harder than normal. It has to pump the blood that leaked back out again together with the usual volume of blood it would have

DOI:10.15774/PPKE.ITK.2012.001

pumped anyway. It may become serious if the amount of blood leaking back is significant, overloading the left ventricle. If the valve is not replaced early enough, the ventricle wall may be stretched past the point of no return, meaning that the heart muscles can not recover even after surgery and progressive heart failure may develop. A common symptom is early, decrescendo diastolic murmur, resulting from the turbulent blood flow through the insufficiency.

Mitral Regurgitation causes similarly the stretching of the left atrium, thus timing of the surgical replacement is crucial. A further problem is that muscles of the left ventricle become weakened since they pump great amount back into the lower pressure system of the atrium. This may have as a result that after surgery the ventricle simply can't handle the load introduced by the greater pressure in the aorta. Since the blood is backed up in the lungs, similarly to the mitral stenosis, congestive heart failure may develop. A high-pitched holosystolic murmur is a major sign of mitral insufficiency.

Tricuspid and pulmonary insufficiency are usual consequences of other cardiac abnormalities, for instance increased pulmonary arterial pressure from patent ductus arteriosus may induce pulmonary insufficiency.

Mitral valve prolapse Mitral valve prolapse is characterized by the displacement of a weakened mitral valve leaflets into the left atrium. At the peak of systolic pressure, a weakened mitral valve may pop back into the atrium a little, which may produce an acoustic sign, named systolic click. If the prolapse is larger, there may be late-systolic murmur as a little blood leaks back into the atrium. Severe mitral valve prolapse, with further risk of complications is rare.

2.4.2 Congenital heart diseases

A congenital heart disease (CHD), also known as congenital heart defects, are structural problems arising from abnormal formation of the heart or major blood vessels. The incidence is around 8 per 1000 live birth, but this measure includes some defects that resolve spontaneously or do not require treatment [67]. Some of the diseases mentioned in the previous section may present as being congenital, for instance aortic valve stenosis with a bicuspid aortic valve, that is having only two flaps. A short description of some of the most frequent severe CHDs is presented hereunder. For more details the reader is referred to [101, 125].

Septal defects

In a healthy adult heart there is no communication between the two sides of the heart. In contrast, in the case of septal defects due to some reason (e.g. genetic) there is a failure of

DOI:10.15774/PPKE.ITK.2012.001

closure of the septum between the two sides of the heart during fetal development. This defect, i.e. hole, may lie between the atria or ventricles, the latter is more frequent.

Ventricular septal defect The pressure in the left ventricle is about five times higher than the pressure in the right ventricle throughout systole. If there is a hole in the septum between the ventricles, blood will flow from the left ventricle to the right, into the lungs, and back around to the left ventricle. If the defect is small the ventricle can compensate the little amount of leaking blood, furthermore small congenital VSDs often close on their own. However, if the ventricular septal defect (VSD) produces a significant left-to-right shunt, the small pulmonary arteries may be overloaded and the pulmonary flow velocity increases, even becomes turbulent, resulting in the thickening of the pulmonary vessel walls. This in turn increases the pulmonary pressure in such a way that the flow through the septal defect reverses, that is it becomes right-to-left, which will cause cyanosis of the patient, since deoxygenated blood circulates throughout the body (this process is called the Eisenmenger syndrome). Nevertheless, if a severe VSD is diagnosed early enough, surgical treatment is a safe remedy. A frequent symptom is holosystolic murmur arising from the turbulent flow through the septal hole.

Atrial septal defect A similar disease to the previously mentioned VSD is the atrial septal defect (ASD), but it is usually less dangerous. In the case of this defect there is a communication between the two atria. Since on the left, systematic side the pressure is normally greater than on the right, pulmonary side, a left-to-right shunt evolves in this situation, which means that a certain amount of reoxygenated blood arriving from the lungs into the left atrium flows back through the atrial hole to the lungs via the right atrium and ventricle. This results in a similarly increased pulmonary blood volume, which, however, produces rarely the thickening of the small pulmonary arteries, like in the case of severe VSD. The main reason is that even if the ASD is significant, it increases only the blood volume in the pulmonary circulation, in contrast to the VSD where the blood flow is also increased, which can become even turbulent. Even though an ASD can produce complications, especially in elderly people. Fortunately it is easy to close an atrial septal defect surgically. Physical symptoms may include a systolic ejection murmur due to the increased flow of blood through the pulmonary valve. A frequent sign is the fixed splitting of the S2 sound.

Patent ductus arteriosus

As already described, the ductus arteriosus itself is an essential fetal vascular structure (Fig. 2.3, 1.4). It connects the main pulmonary artery with the descending aorta

DOI:10.15774/PPKE.ITK.2012.001

and shunts 90 % of the blood coming from the right ventricle into the aorta due to the high resistance of the pulmonary circulation. Closure during pregnancy is a very rare phenomena with adverse effects and may lead even to right heart failure [126]. In the case of normal neonates, with the first intake of breath the lungs expand and the resistance of the pulmonary circulation decreases greatly allowing the development of the normal human circulation. Under normal conditions functional complete closure occurs within the first day after birth [127]. The functional closure is an active process caused by smooth muscle constriction since the ductus arteriosus has a predominantly muscular media with circumferential fibres [128]. The increased level of oxygenated blood and the decreased level of prostaglandins are two main factors contributing to this process [129, 130]. The anatomical closure due to remodeling makes these changes irreversible.

The persistence of the ductal patency is abnormal and is regarded as a congenital heart disease called patent ductus arteriosus (PDA). In this respect, it differs from the other congenital defects because there is no abnormal formation of the heart structure before birth, there is only an abnormality in the final stage of cardiovascular development, i.e. at birth. If the ductus arteriosus remains open after birth a left-to-right shunt evolves due to the higher pressure in the aorta. This means an increased pulmonary fluid volume which may cause respiratory problems. Also the left atrium and ventricle have to compensate the increased fluid volume returning from the lungs and the "pressure leakage" in the aorta which may cause hypertrophy of the left atrium and ventricle. Nevertheless the physiological impact and clinical significance of a PDA depends above all on its size and the state of the underlying cardiovascular system.

A typical symptom is machinery continuous, systolic-diastolic murmur, best heard at the upper left sternal border, furthermore an overactive precordium, tachycardia and bounding peripheral pulses due to the rapid decrease of the diastolic pressure through the ductus. That means that there is an increased difference between the systolic and diastolic blood pressures compared to healthy individuals, for instance in the case of neonates 2:1 ratio instead of 3:2).

The closure of the PDA may occur spontaneously or due to a surgical or transcatheter intervention. In the case of preterm infants pharmacological closure is also possible [131].

In Chapter 5 we describe in more detail the phonocardiographic analysis of preterm infants with PDA.

Tetralogy of Fallot

Tetralogy of Fallot (TOF) is a combination of four different defects: pulmonary stenosis, overriding aorta, ventricular septal defect and hypertrophy of the right ventricle. The pulmonary stenosis is regarded as the major cause of the malformations, with the other

DOI:10.15774/PPKE.ITK.2012.001

associated malformations acting as compensatory mechanisms. An overriding aorta is a malposition of the aortic valve with a connection to both ventricles. This means in more detail that as the right ventricle contracts the deoxygenated blood is pushed back into the systematic circulation through the aorta due to the high resistance of the pulmonary artery caused by the stenosis. This right-to-left shunt is more enforced due to the ventricular septal defect. A further consequence is right ventricular hypertrophy, in other words the thickening of the right ventricle wall, as this chamber tries to maintain sufficient pulmonary blood volume. A systolic murmur might present due to the turbulent flow through the pulmonary stenosis or the VSD. Usually surgical reconstruction is required.

In the most severe form of TOF the pulmonary outflow is not only stenosed but completely missing, which is called pulmonary atresia. Although usually collateral arteries develop emanating from the aorta to the pulmonary artery and lungs, enabling certain degree of reoxygenation of the blood, reconstruction of a viable circulation is not always possible.

DOI:10.15774/PPKE.ITK.2012.001

DOI:10.15774/PPKE.ITK.2012.001

Chapter 3

Methods for Phonocardiographic Signal Analysis

In this chapter the theory of methods for the analysis of phonocardiographic signals is described.

3.1 Cyclostationary processes

Phonocardiographic (PCG) signals, similarly to most of the biomedical signals, are non-stationary signals meaning that their spectral content changes rapidly over time. They can be regarded as stationary only in a short time window [132]. On the other hand, due to the cyclic work of the heart, PCG signals exhibit also a sort of periodic property called cyclostationarity.

A time series $x(n)$ with mean $\mu_x(n)$ and covariance $c_{xx}(n,\tau)$ is wide-sense cyclostationary if and only if there exists an integer P such that $\mu_x(n) = \mu_x(n + l \cdot P)$ and $c_{xx}(n,\tau) = c_{xx}(n+l \cdot P,\tau),\ \forall n, l \in \mathbb{Z}$. The smallest of all such Ps is called the period [133].

It can be explained the following way: heart valves repeat their actions in each cycle, and the heart rate generally does not change abruptly. Thus heart cycles are quasi-periodic. It means that heart sounds are quasi-cyclic stationary.

It should be noted that due to the nonstationarity the covariance function has not only a time-lag variable (τ) but depends also on the time variable (n). Obviously this is valid also for the normalized covariance function, the *autocorrelation function* which is defined

DOI:10.15774/PPKE.ITK.2012.001

according to the Pearson formula for the time instant n as follows:

$$C_P[n,k] = \frac{\sum_{i=n}^{n+N-1} x[i] \cdot x[i+k]}{\sqrt{\sum_{i=n}^{n+N-1} (x[i])^2} \cdot \sqrt{\sum_{i=n}^{n+N-1} (x[i+k])^2}}, \tag{3.1}$$

where $x[n]$ is the zero-mean signal, k is the time-lag and N is the size of the correlation time window. Note that $C_P[n,k] \in [0,1], \forall n,k \in \mathbb{Z}$, and it can also be regarded as the cosine of the angle between the vectors $\mathbf{x} = [\, x[n], x[n+1] \dots x[n+N-1] \,]$ and $\mathbf{y} = [\, x[n+k], x[n+k+1] \dots x[n+k+N-1] \,]$.

The period of the autocorrelation function is equal to the cyclostationary period. It can usually calculated by calculating the time-lag difference between the local maxima.

In general, the complexity of the computation of the autocorrelation function for one time instant is $\mathcal{O}(n^2)$, but relying on the Wiener–Khinchin theorem an efficient way with $\mathcal{O}(n \log(n))$ exists by applying the Fast Fourier Transformation (FFT) [134]:

$$\begin{aligned} &1. \quad \mathbf{X} = \mathrm{FFT}\{\mathbf{x}\}, \\ &2. \quad \mathbf{S} = \mathbf{X} \cdot \mathbf{X}^*, \\ &3. \quad \mathbf{c} = \mathrm{IFFT}\{\mathbf{S}\}, \end{aligned} \tag{3.2}$$

where $\mathbf{x} = [\, x[n], x[n+1] \dots x[n+N-1] \,]$, * denotes the complex conjugate, IFFT is the inverse transform and $\mathbf{c}$ is the vector of correlation values at different time lags without normalization.

Another correlation measure is the modulus difference, which has the advantage that its calculation involves practically only additions and just a very few multiplications which might be preferable in the case of certain computing architectures. The modulus difference is another approach to calculating the period of a cyclostationary process [135]. It is defined for the time instant n as follows:

$$\Delta[n,k] = \frac{\sum_{i=n}^{n+N-1} |x[i] - x[i+k]|}{\sum_{i=n}^{n+N-1} |x[i]| + \sum_{i=n}^{n+N-1} |x[i+k]|}, \tag{3.3}$$

where $x[n]$ is the zero-mean signal, k is the time-lag and N is the size of the time window. Note that $\Delta[n,k] \in [0,1], \forall n,k \in \mathbb{Z}$ and it is an inverse correlation measure. For better

DOI:10.15774/PPKE.ITK.2012.001

comparison with $C_P[n,k]$, usually

$$C_\Delta[n,k] = 1 - \Delta[n,k] \tag{3.4}$$

is applied, where again the time-lag difference between local maxima have to be regarded when estimating the cyclostationary period.

Ensemble averaging

If several recordings of the same event can be performed then averaging of the signals often improves the signal-to-noise ratio (SNR). The technique, which is based on this assumption, is called *ensemble averaging*. It is often applied in the case of biomedical signals, such as evoked potentials [92]. In the case of cyclostationary signals it is also possible to form an ensemble. This is accomplished by selecting segments of length N, $N < P$, from every cycle, where P is the cyclostationary period. This could be the first heart sound in the case of phonocardiographic signals. Let us assume that in this window the signal $s[n]$ remains very similar from cycle to cycle and the recorded data $x[n]$ is only affected by additive noise $\nu[n]$:

$$x_i[n] = s[n] + \nu_i[n], \tag{3.5}$$

where $i = 1, 2, \ldots M$ denotes the different cycles of the cyclostationary signal and $n = 0, 1, \ldots N-1$. By assuming $\nu[n] \sim \mathcal{N}(0, \sigma)$ averaging will obviously suppress the additive noise:

$$\hat{s}[n] = \frac{1}{M} \sum_i x_i[n] \approx s[n] + \frac{1}{M} \sum_i \nu_i[n] \approx s[n]. \tag{3.6}$$

Further improvements of this method will be described in Section 4.4.2.

3.2 Spectral analysis of nonstationary signals

Spectrum calculation and analysis is one of the most important cornerstones in signal processing. Unfortunately in the case of nonstationary signals, classical Fourier analysis becomes a cumbersome tool and fails in representing the underlying characteristics in an appropriate form. For instance, to represent a transient phenomenon, such as a heart sound, the Fourier transform would require many coefficients to represent this localized event. An answer to the need for more useful tools in the field of nonstationary signal processing is the development of a multitude of different transforms, such as the short time Fourier transform, wavelet transform or Wigner-Ville distribution. A short introduction to the theory of these methods is given below.

DOI:10.15774/PPKE.ITK.2012.001

3.2.1 The short time Fourier transform

For better understanding let us start with the conventional Fourier transform of an $x(t)$ real-valued signal

$$\mathcal{F}\{x(t)\}(f) = \int_{-\infty}^{\infty} x(t)e^{-i2\pi ft}\mathrm{d}t, \tag{3.7}$$

where $e^{-i2\pi ft}$ is the Fourier basis.

Since in the case of nonstationary signals the frequency content changes over time, it seems reasonable to investigate the Fourier transform of a nonstationary signal only in a short time segment. This is the idea of windowed Fourier transformation, which was introduced by Dennis Gabor[1] in 1946 by defining time-frequency atoms, which are signals localized in time and in frequency [93]:

$$g_{u,f}(t) = g(t-u)e^{i2\pi ft}. \tag{3.8}$$

By decomposing a $x(t) \in \mathbf{L^2}(\mathbb{R})$ signal into such time-frequency atoms one arrives at the 2D representation of the signal, the windowed, or *short time Fourier transform* (STFT):

$$\mathcal{S}\{x(t)\}(u,f) = \langle x(t), g_{u,f}(t)\rangle = \int_{-\infty}^{\infty} x(t)g(t-u)e^{-i2\pi ft}\mathrm{d}t. \tag{3.9}$$

One can also define the energy density of the given $x(t)$ signal by considering the squared magnitude of the STFT. This is called the *spectrogram*:

$$\mathcal{P}_{\mathcal{S}}\{x(t)\}(u,f) = |\mathcal{S}\{x(t)\}(u,f)|^2 = \left|\int_{-\infty}^{\infty} x(t)g(t-u)e^{-i2\pi ft}\mathrm{d}t\right|^2. \tag{3.10}$$

The spectrogram shows how much energy the time-frequency atom centred around (u,f) takes out of $x(t)$, making the spectral changes of a nonstationary signal observable in a quite straightforward way. However, it should be noted that this enhanced representation comes at some expense: the increased temporal resolution decreases the frequency resolution. This is explained by the Heisenberg uncertainty principle, which states that the temporal spread of a function and its frequency spread in the Fourier domain cannot be simultaneously arbitrarily small [94]. More precisely this means that the $g_{u,f}$ time-frequency atom cannot have an arbitrarily small temporal width, σ_t, and frequency width, σ_f, at the same time. The area of the non-zero time-frequency domain of $g_{u,f}$, the so

[1] Original name: Gábor Dénes, born 5 June 1900 in Budapest, Hungary, died 9 February 1979 in London, United Kingdom

DOI:10.15774/PPKE.ITK.2012.001

called Heisenberg rectangle has a lower bound:

$$\sigma_t \sigma_f \geq \frac{1}{2}. \tag{3.11}$$

The above area is minimum when $g(t)$ in Eq.(3.8) is a Gaussian, in which case the atoms $g_{u,f}$ are called Gabor functions. In the case of heart sounds, Jamous *et al.* showed that the optimal range of time-window duration for analysing PCG signal with STFT is between 16 and 32 ms [132]. For fetuses and neonates due to the smaller sizes of the cardiac structures, it is probable at the lower limit of this interval. However, in general it is a difficult task to select the appropriate time window.

3.2.2 The wavelet transform

Another approach for arriving at the time-frequency domain is the wavelet transform. This transform is very useful in large number of applications, including the current one of fetal PCG signal processing, as we shall see in Section 4.2.3.

The wavelet transform is a very similar approach to the short time Fourier transform. It is similarly a linear transform, however, there are two main differences: first of all the wavelet transform may use a different basis function than the windowed sinusoids and secondly, the temporal width and frequency width of the analysing window varies with frequency.

In the case of the STFT the analysing functions are windowed complex exponentials, i.e. $g(t-u)e^{-i2\pi ft}$, in the case of the wavelet transform they are called wavelets. A wavelet is a $\Psi \in \mathbf{L^2}(\mathbb{R})$ function with zero average, concentrated around $t = 0$ and its square norm is equal to 1:

$$\int_{-\infty}^{\infty} \Psi(t)\mathrm{d}t = 0, \tag{3.12}$$

$$||\Psi|| = 1. \tag{3.13}$$

There are several functions which satisfy the conditions above, a good example is the second derivative of a Gaussian, called Mexican hat. Other wavelets can be easily found in the rich literature of wavelet transforms [94, 136].

The different time-frequency atoms are obtained by translating Ψ, the mother wavelet, by $u \in \mathbb{R}$ and scaling it by $s \in \mathbb{R}^+$:

$$\Psi_{u,s}(t) = \frac{1}{\sqrt{s}} \Psi \left(\frac{t-u}{s} \right). \tag{3.14}$$

DOI:10.15774/PPKE.ITK.2012.001

Finally, the wavelet transform takes the following form:

$$\mathcal{W}\{x(t)\}(u,s) = \langle x(t), \Psi_{u,s}(t)\rangle = \int_{-\infty}^{\infty} x(t)\frac{1}{\sqrt{s}}\Psi\left(\frac{t-u}{s}\right)\mathrm{d}t. \tag{3.15}$$

As already mentioned, in contrast to the Gabor functions the temporal and frequency widths of the wavelets depends on the scale parameter. In particular, the temporal width *in*creases and the frequency width *de*creases with increasing scale. This is reasonable since for observing fast variation obviously a smaller temporal window is more appropriate than for observing slow oscillations.

The signal can be reconstructed from its wavelet transform if the applied wavelet satisfies a weak admissibility condition, even when the wavelet basis functions are not orthonormal. The reconstruction is possible using the following formula:

$$x(t) = \frac{1}{C_\Psi}\int_0^{\infty}\int_{-\infty}^{\infty}\mathcal{W}\{x(t)\}(u,s)\frac{1}{\sqrt{s}}\Psi\left(\frac{t-u}{s}\right)\mathrm{d}u\frac{\mathrm{d}s}{s^2}, \tag{3.16}$$

where C_Ψ is a constant that depends on the wavelet used. It has to satisfy the admissibility condition, that is it has to be finite, and it is defined as follows:

$$C_\Psi = \int_0^{\infty}\frac{\left|\hat{\Psi}(\omega)\right|^2}{\omega}\mathrm{d}\omega < +\infty, \tag{3.17}$$

where $\hat{\Psi}$ is the Fourier transform of Ψ. This conditions implies that $\hat{\Psi}(0) = 0$, which explains why wavelets must have a zero average.

As in the case of most real world signals, such as a fetal PCG signal, we usually have to operate with digital samples. The discretized version of the continuous wavelet transform enables the computation of the continuous wavelet transform by computers, but it is not a true discrete transform, it is only a sampling of the time-scale plane [94].

The continuous wavelet transform, even when sampled to a certain degree, yields a very redundant representation of the investigated signal. The discrete wavelet transform (DWT) computes the time-scale plane sampled on a dyadic grid, which is still enough for the reconstruction of the original discrete signal, and it can be implemented in a very efficient way with a complexity of only $\mathcal{O}(n)$. Since this is not the major topic of this work, for further details the reader is referred to the explanation in [137].

3.2.3 Overcomplete representations

In the previous sections we defined two time-frequency representation of the signal x. These approaches can be written in more general as the decomposition of x into the linear combination of so called atoms γ_i of a dictionary Γ. Because in this section the emphasis

DOI:10.15774/PPKE.ITK.2012.001

is on the realization, the following definitions and calculations are shown in discrete time:

$$x[n] = \sum_{\gamma_i \in \Gamma} a_i \gamma_i[n], \tag{3.18}$$

where a_i is the coefficient of the atom γ_i.

The atoms γ are the sinusoids in the case of the Fourier transform and wavelets in the case of the wavelet transform. In those scenarios the atoms form a basis. However, the dictionary can also be overcomplete, meaning that the atoms are not linearly independent and hence the decomposition is non-unique. For instance, an overcomplete dictionary can be defined by combining Gabor atoms and a certain wavelet family. Overcompleteness gives the possibility of adaptation because we can choose among many representations the one that is best suited to our purpose [138].

Here we show only two principles for resolving the non-uniqueness. The first is the *Methods of Frames* which minimizes the l^2 norm of the coefficients a_i:

$$\min ||\mathbf{a}||_2 \text{ subject to } \sum_{\gamma_i \in \Gamma} a_i \gamma_i[n] = x[n], \tag{3.19}$$

where $\mathbf{a}$ is a vector containing the coefficients a_i. This is a quadratic optimization problem and can be solved using linear algebra.

The second approach is called *Basis Pursuit*. In this case the minimization is performed with respect to the l^1 norm:

$$\min ||\mathbf{a}||_1 \text{ subject to } \sum_{\gamma_i \in \Gamma} a_i \gamma_i[n] = x[n]. \tag{3.20}$$

Changing from the l^2 norm to the l^1 norm has major consequences. The Basis Pursuit method involves nonlinear, convex optimization. Fortunately it can be reformulated as a linear program, and due to advances in the last decades, efficient interior point algorithms exist for solving large scale linear programs [138].

Optimization with respect to the l^1 norm has the major advantage that it leads to a sparse representation of the signal of investigation. This can be exploited for example for compression but it is also the basis of *compressed sensing* [139].

3.2.4 Quadratic time-frequency distributions

Quadratic time-frequency distributions describe the energy distribution of the signal in the time-frequency domain. One of such distributions have already been introduced: the spectrogram. In the section below we will see how all these distribution are related to each other through the Wigner-Ville distribution.

DOI:10.15774/PPKE.ITK.2012.001

The analytic signal and the Hilbert transform

In order to give a constructive introduction to the Wigner-Ville distribution based on [140] let us start with defining the analytical signal. A signal $z(t)$ is analytic if and only if:

$$Z(f) = 0 \text{ for } f < 0 \tag{3.21}$$

where $Z(f)$ is the Fourier transform of $z(t)$. It can be easily shown that a signal $z(t) = x(t) + jy(t)$ is analytic if and only if:

$$\begin{aligned} Y(f) &= jX(f) \quad \text{for } f < 0, \\ Y(0) &= 0 \quad \text{for } f = 0, \\ Y(f) &= -jX(f) \quad \text{for } f > 0. \end{aligned} \tag{3.22}$$

The real signal $y(t)$ is called the *Hilbert transform* of $x(t)$, meaning that "a signal is analytic with a real DC component if and only if its imaginary part is the Hilbert transform of its real part" [140]. Consequently the Hilbert transform is defined as:

$$\mathcal{H}\{x(t)\} = \hat{x}(t) = \mathcal{F}^{-1}\{-j\,\mathrm{sgn}(f)\,\mathcal{F}\{x(t)\}\}, \tag{3.23}$$

where $\mathrm{sgn}(f)$

$$\begin{aligned} \mathrm{sgn}(f) &= -1 \quad \text{for } f < 0, \\ \mathrm{sgn}(f) &= 0 \quad \text{for } f = 0, \\ \mathrm{sgn}(f) &= +1 \quad \text{for } f > 0. \end{aligned}$$

Similarly, the Hilbert transform can be defined also in the time domain using:

$$\mathcal{H}\{x(t)\} = \hat{x}(t) = \frac{1}{\pi}\int_{-\infty}^{\infty}\frac{x(\tau)}{t-\tau}\mathrm{d}\tau = x(t) * \frac{1}{\pi t}, \tag{3.24}$$

where $*$ denotes the convolution. In fact, the Hilbert transformed signal is a version of the original signal with a 90° phase shift.

Equation (3.23) is exploited for calculating the Hilbert transform by using the Fast Fourier transform. For further details the reader is referred to the work of Oppenheim *et al.* [141].

The Hilbert transform is useful for calculating instantaneous attributes of a time series because the complexed valued analytic signal $z(t) = x(t) + j\hat{x}(t)$ can be expressed,

DOI:10.15774/PPKE.ITK.2012.001

according to the Euler's formula, also in the following form:

$$z(t) = a(t)e^{j\phi(t)}, \tag{3.25}$$

where $a(t) = |z(t)|$ is the *instantaneous amplitude* and $\phi(t) = \arctan(z(t))$ is the *instantaneous phase*. The *instantaneous frequency* can be calculated by taking the derivative of $\phi(t)$:

$$f(t) = \frac{1}{2\pi}\phi'(t). \tag{3.26}$$

In this work the Hilbert transform is applied several times for calculating the envelope of the phonocardiographic signal.

The Wigner-Ville distribution

Let us now consider a simple signal $z(t) = e^{j\phi(t)}$. An optimal time-frequency representation of this monocomponent, nonstationary signal should have non-zero components only at positions defined by the instantaneous frequency $f(t)$:

$$\rho(t, f) = \delta(f - f(t)). \tag{3.27}$$

Because $\rho(t, f)$ is a kind of spectrum, it is reasonable to assume that it is the Fourier transform of a function related to the signal. Based on this assumption, by taking the inverse Fourier transform of $\rho(t, f)$ with respect to the frequency variable f we arrive at the so called *kernel function*:

$$K(t, \tau) = \mathcal{F}^{-1}_{f\to\tau}\left\{\delta(f - f(t))\right\} = e^{j2\pi f(t)\tau} = e^{j\phi'(t)\tau}. \tag{3.28}$$

By considering the approximation $\phi'(t) = \frac{1}{\tau}[\phi(t + \frac{\tau}{2}) - \phi(t - \frac{\tau}{2})]$ we find that:

$$K(t, \tau) = e^{j\phi(t+\frac{\tau}{2})}e^{-j\phi(t-\frac{\tau}{2})} = z\left(t + \frac{\tau}{2}\right) z^*\left(t + \frac{\tau}{2}\right), \tag{3.29}$$

where * denotes the complex conjugate.

By combining Eqs.(3.27)-(3.29) we conclude that the optimal time-frequency representation for the signal $z(t) = e^{j\phi(t)}$ can be calculated by taking the Fourier transform of the kernel function defined in Eq.(3.29):

$$\rho(t, f) = \mathcal{F}_{\tau\to f}\left\{z\left(t + \frac{\tau}{2}\right) z^*\left(t + \frac{\tau}{2}\right)\right\}. \tag{3.30}$$

This relation can be generally applied and leads to the definition of the *Wigner-Ville*

DOI:10.15774/PPKE.ITK.2012.001

distribution. The Wigner-Ville distribution of a signal $x(t)$ is [95, 142]:

$$\mathcal{W}_x(t,f) = \int_{-\infty}^{\infty} z(t+\tau/2)\; z^*(t-\tau/2)\; e^{-j2\pi f\tau} \mathrm{d}\tau, \tag{3.31}$$

where $z(t) = x(t) + j\mathcal{H}\{x(t)\}$ is the analytic signal associated with $x(t)$.

The $\mathcal{W}_x(t,f)$ is an optimal a quadratic energy representation of a signal in the time-frequency domain satisfying a number of desired properties, such as being always real valued. It can be shown that it produces the highest resolution among all energy distributions, however in the case of multicomponent signals, such as the heart sounds, cross terms corrupt the recognizability of the components in the time-frequency plane. Further details can be found in [140].

The transform of the Wigner-Ville distribution can also be regarded as a generalization of the Wiener-Khinchin theorem for nonstationary signals, as the Fourier-transform of the time-dependant *instantaneous autocorrelation function* $K(t,\tau) = z\left(t+\frac{\tau}{2}\right) z^*\left(t-\frac{\tau}{2}\right)$. The FFT can be applied for its efficient computation [143].

Furthermore, it can be shown that every quadratic time-frequency representation can be derived by taking the Fourier transform of the smoothed instantaneous autocorrelation function [140]. For example, in the case of the Wigner-Ville distribution the smoothing function is the $\delta(t)$ function, whereas in the case of the spectrogram one has to apply $G(t,\tau) * K(t,\tau)$, where $G(t,\tau) = g^*\left(t+\frac{\tau}{2}\right) g\left(t-\frac{\tau}{2}\right)$ and $g(t)$ being the windowing function applied in the STFT calculation. The smoothing of the instantaneous autocorrelation function reduces the effect of cross terms, but on the other hand decreases also the time-frequency resolution.

DOI:10.15774/PPKE.ITK.2012.001

Chapter 4

Phonocardiography for Fetuses

Section 1.1.2 introduced the importance of the phonocardiographic analysis of fetuses. In this chapter methods and results are described in more detail for phonocardiographic assessment of features related to the state and the wellbeing of the fetus, including the fetal heart rate (Section 4.2), the decomposition of the heart sounds (Section 4.3) and the investigation of fetal murmur (Section 4.4).

4.1 Recording of the fetal heart sound signal

Some earlier work suggested different technical solutions for recording the fetal heart sound, for example by the development of a piezopolymer pressure sensor [144], by application of compliance-matched inductive transducers [145] or by using simple electret microphones [146].

The investigations of our research group on fetal phonocardiography (PCG) began almost two decades ago[1] [147, 148]. During a project [149], supported by the National Innovation Office through the National Research and Development Program 2004, a telemetric fetal surveillance system was developed, enabling the home monitoring of the fetus (Fig. 4.1).

In the following years, in the course of high-volume cardiotocographic (CTG) measurements with the phonocardiographic CTG device type Fetaphon-2000^{TM} (Fig. 4.2), thousands of phonocardiographic records were collected. In this device, the signals are bandpass filtered (25-100 Hz) with an active filter and digitized on 8 bits with a sampling frequency of 333 Hz.

Although the special design of the recording head enables sensitive recording of the fetal heart sound, in most cases the ideal form of the heart sound signal cannot be measured due to disturbances (Fig. 4.3). One part of these disturbances stems from the fetus due to

[1] The author of this work is involved in this research group only since 2007

DOI:10.15774/PPKE.ITK.2012.001

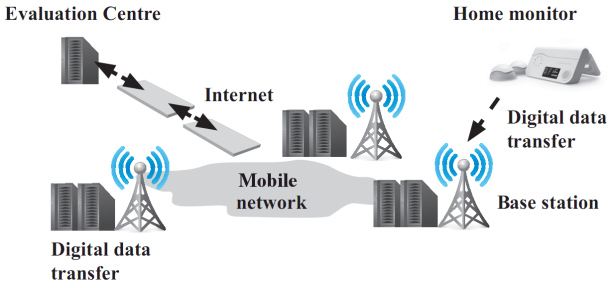

Figure 4.1: Fetal monitoring telemedicine system. The recorded heart sound signal is transferred to an information centre, where the evaluation is performed off-line.

Figure 4.2: Phonocardiographic CTG device type Fetaphon-2000™ enabling the home surveillance of the fetus.

the movement of his or her limbs or the rotation of body, or even its hiccups. Breathing movements of the fetus also produces noise, making heart sound identifications difficult. The second source of disturbances stems from the mother due to her heart sound, breathing, digestive organs and muscular movements. Furthermore, some environmental noise is always present (Fig. 4.4).

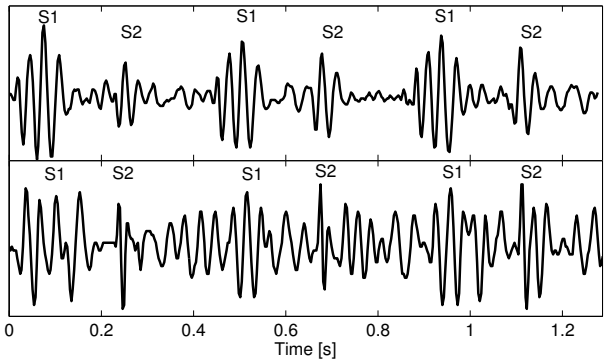

Figure 4.3: Noiseless (top) and noisy (bottom) fetal phonocardiographic signals. Note the difficulty in visually identifying the S1 and S2 heart sounds on the bottom trace.

DOI:10.15774/PPKE.ITK.2012.001

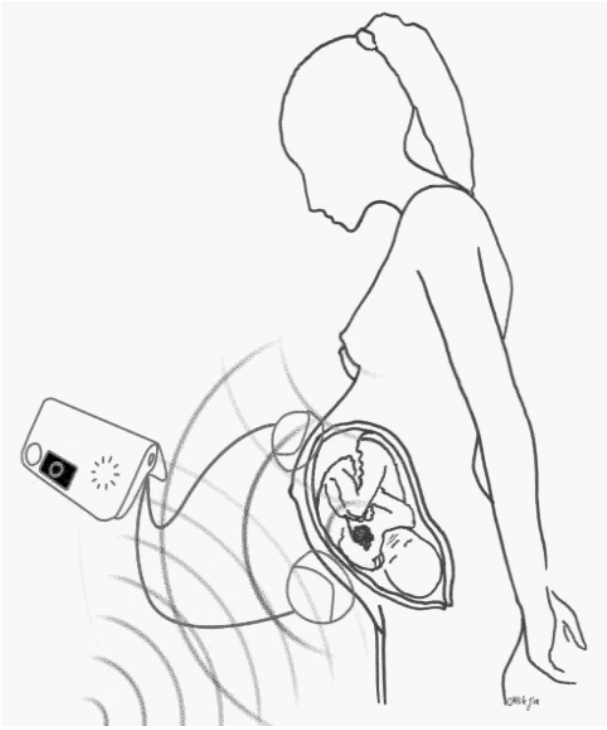

Figure 4.4: Sources of noise corrupting the low intensity fetal heart sound signal: noise from the mother (maternal heart and digestive sounds), noise from the fetus (hiccup, movements of the limbs) and noise from the environment. Courtesy of Julianna Ottlik.

DOI:10.15774/PPKE.ITK.2012.001

4.2 Fetal heart rate

4.2.1 Importance of the fetal heart rate

In everyday use, and mostly in the case of normal gestations, the evaluation of the fetal heart rate (FHR) diagram happens visually by the obstetrician observing the baseline, the number of accelerations and the variability. Nonetheless, the detailed analysis of the FHR diagram has shown that further important parameters can be assessed in addition to the usual CTG data, namely:

1. Intrauterine growth restriction (IUGR) can be identified by investigating different measures of the short-term variability (STV) [100, 150, 151].

2. The variability in the case of nonreassuring fetal status was discussed in [152, 153]. The evaluation of the low-frequency range (LF: 0.03-0.15 Hz) was improved in [154] by filtering out the accelerations and decelerations from the FHR curve. Using the frequency bands MF (0.15-0.5 Hz) and HF (0.5-1 Hz), the LF/(MF + HF) frequency band power ratio was studied to quantify the autonomic balance between the sympathetic and parasympathetic neural control. The maturation of the fetal autonomic nervous system has been assessed also based on this ratio in [99].

3. Finally, the high-frequency content of the FHR gives information on the fetal breathing [155].

Since all the fetal parameters above are basically calculated from the STV, the inaccuracy of the traditional Doppler ultrasound based CTG limits their reliability. Fetal ECG is an adequate approach, only periods of the pregnancy when the vernix caseosa corrupts the signal are difficult to monitor. In contrast, fetal phonocardiography with its enhanced accuracy offers new possibilities in this field.

All these studies imply that more features related to the fetal status can be assessed based on PCG measurements. To achieve this the very sophisticated analysis of the fetal heart sound signals and the very accurate determination of the beat-to-beat times (T_{bb}) and their variability is needed. In this way fPCG based CTG measurements do not only yield conventional fetal parameters, but also additional features can be acquired related to the well-being of the fetus.

4.2.2 Calculation of the fetal heart rate in the time domain

For calculating the FHR from cardiotocographic data usually one of the two approaches, which are described below, is applied. The first one relies on the intensity of the heart sounds and calculates the FHR from the detected heart sounds. Several methods have

DOI:10.15774/PPKE.ITK.2012.001

been utilized for robust envelope calculation and heart sound detection, such as using the Hilbert transform [156, 157], Shannon energy and homomorphic filtering [158], the Teager operator [159], and rule-based [148,160] or model based methods [27]. The Shannon energy and Teager energy functions of a fetal PCG segment are shown in Fig. 4.5.

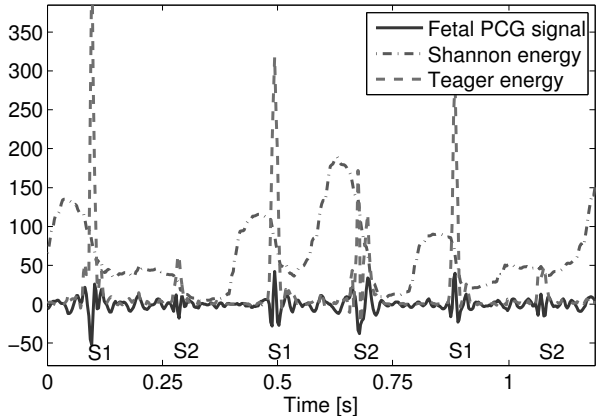

Figure 4.5: Three heart cycles of a fetal heart sound recording and the corresponding Shannon energy function (dash-dot line) and the envelope calculated using the Teager operator (dashed line). These method produce reliable results if the heart sounds are well distinguishable.

Unfortunately, in the case of fetal phonocardiographic recordings the SNR is usually low, and impulsive noise corrupts the week intensity fetal heart sound signal, thus relying on only the envelope of the data, even when using *a priori* knowledge could be misleading in identifying heart sounds and calculating the heart rate.

The second approach for FHR calculation is exploiting the cyclostationarity (Section 3.1) of the phonocardiographic signal, meaning that the estimated cyclostationary period is regarded as the actual beat-to-beat time.

The cyclostationary of heart sounds is supported by previous studies showing that consecutive heart sounds remain very similar, correlation coefficients even greater than 0.99 were consistently observed [31, 120]. Although these works have been carried out on dogs and adults, according also to our investigations, it can be applied also for fetal heart sounds (Fig. 4.6).

In practice, the heart rate calculation is performed as follows: the frequency of the autocorrelation function is equal to the heart rate when the heart rate is constant for the time window of investigation. However, the T_{bb} changes slightly from beat to beat, thus only the length of the first period of the correlation function, $C[n, k]$, is regarded as actual beat-to-beat time, and this can be determined by calculating the distance between the first two peaks of $C[n, k]$ for every n time instant. As the first peak is always at

DOI:10.15774/PPKE.ITK.2012.001

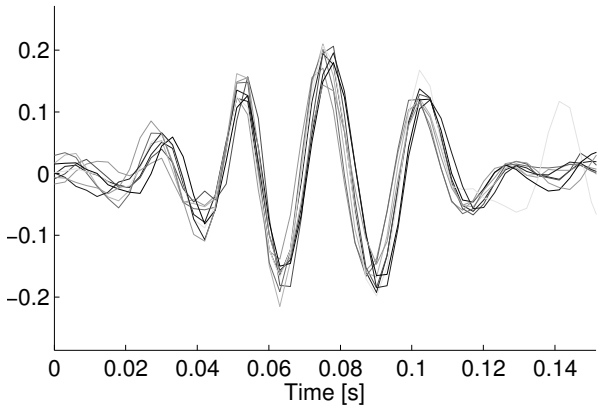

Figure 4.6: Consecutive 9 fetal S1 sounds time aligned by maximizing the cross-correlation between them which was in all cases above 0.9.

zero-lag, only the position of the next peak has to specified which can be accomplished by finding the local maximum in a given frame of $C[n,k]$, where the frame limits are calculated according to the extrema of the fetal heart rate, that is 80 and 200 beats per minute (BPM) (Fig. 4.7-4.8).

Both the autocorrelation, $C_P[n,k]$ (Eq.(3.1)), and the modulus difference, $C_\Delta[n,k]$ (Eq.(3.4)), can be reliable applied to fPCG signals, as shown in Figs. 4.7-4.8, thus for the sake of simplicity the lower index $_\Delta$ and $_P$ is omitted in this chapter where both measures perform similarly.

The determination of the length of the time window, N, for calculating $C[n,k]$ is of crucial importance. A shorter window, with the length of at least one heart sound or one heart cycle would be optimal for determining the exact T_{bb}, on the other hand a longer window, such as one covering several heart cycles is more robust against noise bursts that may be mistaken for a heart sound. Based on empirical observations by investigating a large number of fetal PCG records, a window length of 3 heart cycles proved to be a good trade-off (Fig. 4.9). In certain cases, further methods can be applied for refining these values.

The T_{bb} has to be determined only once for each heart cycle thus it is unnecessary to calculate the correlation function for every sample. We developed an adaptive predictive method, where the next position for calculating $C[n,k]$ is estimated according to the

DOI:10.15774/PPKE.ITK.2012.001

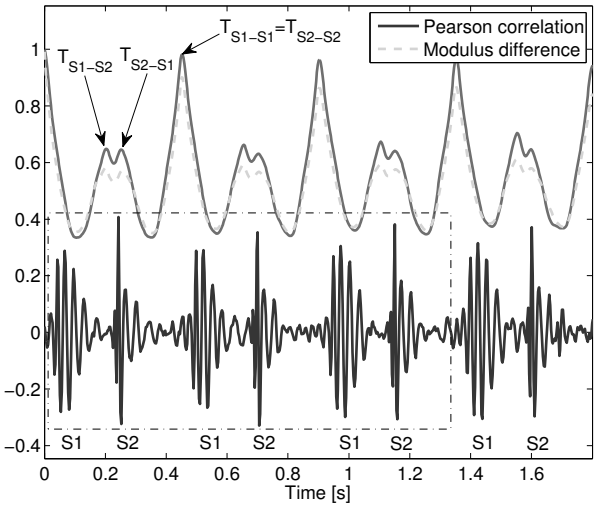

Figure 4.7: A noiseless fetal PCG segment and the corresponding Pearson correlation (solid line) and modulus difference (dashed line) values calculated by correlating the segment marked by the dash-dotted rectangle with the following heart cycles. Note the local maxima of the correlation data corresponding to length of multiple heart cycles, i.e. harmonics.

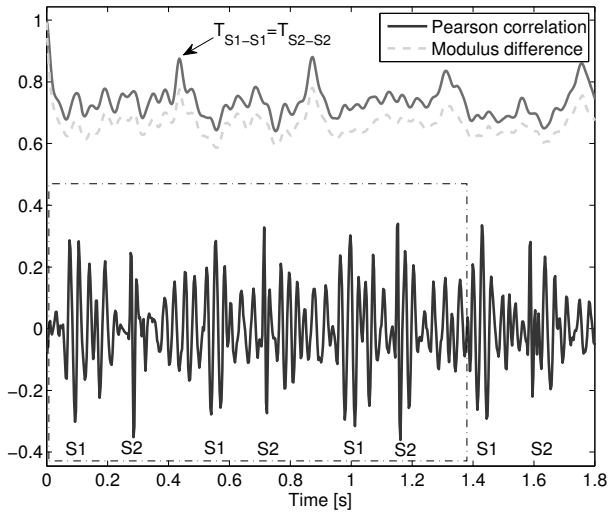

Figure 4.8: A noisy fetal PCG segment and the corresponding Pearson correlation (solid line) and modulus difference (dashed line) values calculated by correlating the segment marked by the dash-dotted rectangle with the following heart cycles. Note that although local maxima mark the beginning of the heart cycles, the S1-S2 or S2-S1 distances cannot be calculated from the correlation data contrary to Fig. 4.7.

DOI:10.15774/PPKE.ITK.2012.001

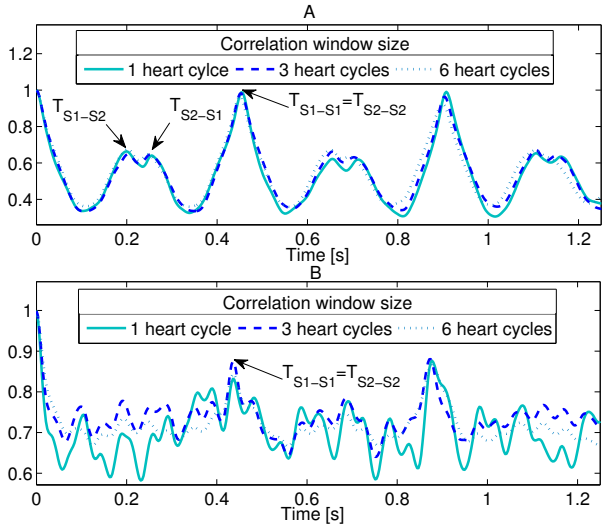

Figure 4.9: The correlation data (A) of the noiseless segment shown in Fig. 4.7 and (B) of the noisy segment shown in Fig. 4.8, in both cases calculated with correlation window sizes of 1, 3 and 6 heart cycles, respectively. Note that while in the case of the noiseless segment different window sizes result in very similar results, for the noisy segment the 3 heart cycles long correlation window produces the highest peak at time-lag of the S1-S1 time delay.

weighted average of previous K beat-to-beat times:

$$\mathrm{T}_{\mathrm{bb}}^{exp}[n] = \frac{\sum_{k=0}^{K-1} w[n-k] \cdot \mathrm{T}_{\mathrm{bb}}[n-k]}{\sum_{k=0}^{K-1} w[n-k]} \tag{4.1}$$

where $w[n]$ is the $C[n,k]$ value at that lag k from which the actual T_{bb} was determined. In Figs. 4.7-4.8 this is the value of the local maximum labelled $\mathrm{T}_{\mathrm{S1\text{-}S1}}$.

To increase the reliability of the prediction we introduced a confidence factor (CF), which is calculated from previous heart cycles:

$$\mathrm{CF}[n] = \frac{2}{3} w[n] + \frac{1}{3}\left(\frac{\mathrm{CF}[n-1] + \mathrm{CF}[n-2]}{2}\right). \tag{4.2}$$

Prediction for the next heart cycle is allowed based on whether the CF value is above a given threshold, usually 0.7. If it is not, then the next position for calculating $C[n,k]$ is based on the highest physiologically possible fetal heart rate.

In addition to the above, there is one more practical comment: the robustness of the methods above can be increased by relying on the envelope of the heart sound signal

DOI:10.15774/PPKE.ITK.2012.001

calculated by applying the Hilbert transform, $\mathcal{H}\{\cdot\}$ (Section 3.2.4), which is useful for calculating instantaneous attributes of a time series, such as the instantaneous amplitude.

The calculation of $C[n,k]$ performed on the envelope signal $|x[n] + i\mathcal{H}\{x[n]\}|$ is in general more robust against noise than the calculations on the heart sound signal.

Unfortunately at the time of this work we had no reference FHR signal with high resolution, for example from simultaneous fECG measurements, to compare the results of the different approaches with. This is why we had to introduce two measures:

- **Noise level (NL)**: this is calculated as the ratio of the average median-amplitude of the noise to the average median-amplitude of the heart sounds calculated only on segments where the heart rate calculation yielded CF values (Eq.(4.2)) higher than a given threshold:

$$\mathrm{NL} = \frac{\mathrm{mean}(\mathrm{N}_{\mathrm{med}}[i])}{\mathrm{mean}(\mathrm{S}_{\mathrm{med}}[i])}, \tag{4.3}$$

  where $\mathrm{N}_{\mathrm{med}}[i]$ is the median systolic-diastolic, and $\mathrm{S}_{\mathrm{med}}[i]$ is the median S1-S2 envelope value of heart cycle i.

- **Hit rate (HiR)**: this is the ratio of the number of detected heart cycles and the number of estimated heart cycles in the record. The latter estimation is performed based on the baseline. The HiR reflects the percentage of heart cycles which were identified with high reliability:

$$\mathrm{HiR} = \frac{\#\{\text{heart cycles with CF} > \text{threshold}\}}{|\text{recording}|/(60/\mathrm{BL})}, \tag{4.4}$$

  where |recording| is the length of the given recording in seconds and BL is the baseline in BPM.

Although these metrics are heuristic and they may not be accurate but they should certainly reflect the accuracy of the investigated methods. They proved to be adequate for a basic comparison and the identification of pros and cons of the different approaches. Regarding the time domain based correlations it can be shown (Fig. 4.10) that as the NL increases the achieved HiR decreases in the case of many recordings, meaning that in the case of a recording with a higher noise level the number and length of segments, where reliable FHR calculation can be achieved, decreases.

The exploitation of cyclostationarity is a very robust way of determining the fetal heart rate and the introduction of the CF value (Eq.(4.2)) is a very important way of discriminating reliably determined FHR segments from unreliable segments. Nonetheless, further methods are needed for FHR determination, especially in the case of low SNR recordings with long unreliable segments. In the next section a procedure is introduced

DOI:10.15774/PPKE.ITK.2012.001

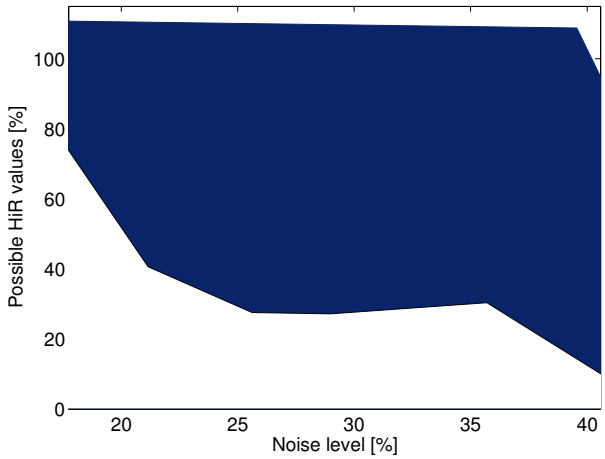

Figure 4.10: Possible range of HiR values for different level of noise in the case of the time domain based correlation calculated from analysing more than 500 recordings. Note that for an increased NL value often only a lower HiR can be achieved.

where the time-frequency distribution of the heart sounds is also considered in addition to the cyclostationarity for calculating the exact fetal heart rate.

4.2.3 Application of the wavelet transform to fetal heart rate calculation

The wavelet transform, as already mentioned in Section 3.2.2, is a highly valuable tool for the processing of nonstationary signals, especially for biomedical signals [161]. In the case of fetal PCG signals it seemed a promising approach to extend the calculations into the time-frequency domain for determining the heart rate. A motivating example is demonstrated in Fig. 4.11, where it can be observed that an approach based on the wavelet transform would clearly achieve better in identifying the heart cycles and calculate the fetal heart rate than a time domain method. It should be noted that high-pass filtering would enhance the S2 sound based heart cycle detection in the case of this segment. However, other examples could be shown where the presence of high frequency noise would have just the opposite effect. By applying a time-frequency/time-scale approach this is circumvented by considering the whole frequency scale of interest but including also temporal information in the analysis for a better differentiation between heart sounds and noise bursts.

The wavelet transform was selected among the time-frequency approaches because it can be implemented in an efficient way and it is free of the effect of cross terms, in contrast to the Wigner-Ville distribution. Moreover, because of the variable window size it produces a better resolution than the STFT. However, the selection of the mother wavelet is of importance. Several wavelets can be used as a mother wavelet, such as

DOI:10.15774/PPKE.ITK.2012.001

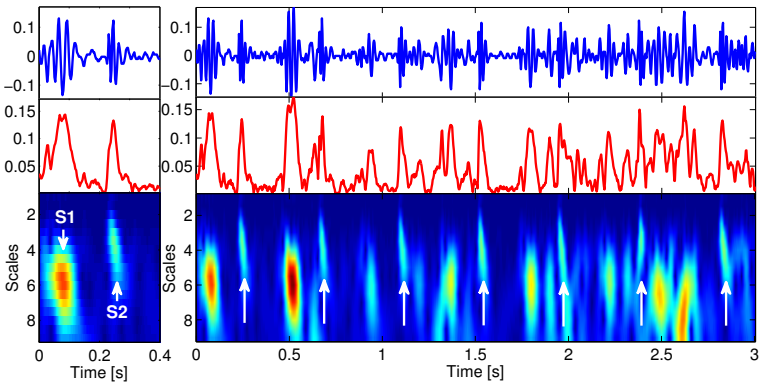

Figure 4.11: A segment of fetal PCG recording (top trace), the corresponding instantaneous amplitude (middle trace) and the same segment in the time-scale domain transformed with the wavelet transform (bottom trace). On the left the templates of the heart cycle are shown, which are correlated to the segment for determining the heart rate. Note the difficulty in identifying the heart cycles in the interval starting from 1.7 s in the top and middle trace, whereas in the case of the wavelet transformed signal the heart sounds can be clearly easier identified, especially the S2 sounds (marked with arrows).

Daubechies, Morlet or Gaussian, which show smooth oscillating behaviour similarly to the heart sounds (Fig. 4.12). On the other hand, the Daubechies wavelets show an increasing instantaneous frequency in contrast to the heart sounds. Based on empirical observations the 8^{th} order Gaussian mother wavelet, which is the 8^{th} derivative of the Gaussian exponential, produces good result in capturing the characteristics of the slower oscillating S1 sounds and the faster oscillating, short S2 sounds. An even order in the case of the Gaussian wavelet guarantees the symmetry of the wavelet and the relatively high order is needed to have a similar number of cycles than in the case of typical fetal heart sounds. In the case of the 8^{th} order Gaussian mother wavelet, there are approximately four cycles.

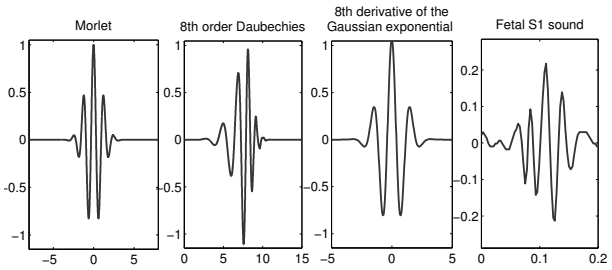

Figure 4.12: Three possible mother wavelets for fetal PCG analysis and a fetal S1 sound. Note the oscillating behaviour of these mother wavelets, resembling the heart sounds.

For calculating the fetal heart rate in the time-scale domain we introduced a similar

DOI:10.15774/PPKE.ITK.2012.001

correlation method to the multibeat autocorrelation. This extension increases the reliability of the correlation, which is extremely important in the case of unreliable segments with noise bursts.

The 2D correlation formula in the time-scale domain is defined as follows for the time instant n:

$$C_P^W[n,k] = \frac{\sum_{s=s_1}^{s_m}\sum_{u=n}^{n+N-1} W_x[u,s]\cdot W_x[u+k,s]}{\sqrt{\sum_{s=s_1}^{s_m}\sum_{u=n}^{n+N-1}(W_x[u,s])^2}\cdot\sqrt{\sum_{s=s_1}^{s_m}\sum_{u=n}^{n+N-1}(W_x[u+k,s])^2}}, \tag{4.5}$$

where $W_x[u,s]$ is the wavelet transform of the $x[n]$ fetal PCG signal and $s_1,\dots s_m$ are the selected scale bands. Once again the cyclostationarity of the heart sound signal is exploited, but here the cyclostationary period is calculated based one the time-scale distribution of the PCG signal, although the length of the first period of C_P^W is equal to the actual T_{bb}.

As already mentioned in section 3.1, the modulus difference can be similarly applied in this scenario:

$$\Delta^W[n,k] = \frac{\sum_{s=s_1}^{s_m}\sum_{u=n}^{n+N-1}|W_x[u,s]-W_x[u+k,s]|}{\sum_{s=s_1}^{s_m}\sum_{u=n}^{n+N-1}|W_x[u,s]|+\sum_{s=s_1}^{s_m}\sum_{u=n}^{n+N-1}|W_x[u+k,s]|}, \tag{4.6}$$

$$C_\Delta^W[n,k] = 1-\Delta^W[n,k]. \tag{4.7}$$

It should be noted that in the case of FHR estimation based on the wavelet transform the modulus difference yields better results in some cases than the correlation, which can be exploited. Furthermore, since each scale of the wavelet transform corresponds to a bandpass filtered version of the original signal, the Hilbert transform based enveloped calculation can be applied also in this scenario for every scale, increasing the robustness of the method (Fig. 4.13).

4.2.4 Results

Although the time domain based correlation is a fast and reliable method for FHR calculation, in some cases, especially for noisy fPCG signals with murmur, the wavelet transform based approach proves to be more robust. Some of these advantages are demonstrated on a noisy segment of a record of a fetus with grade III-IV tricuspid insufficiency producing

DOI:10.15774/PPKE.ITK.2012.001

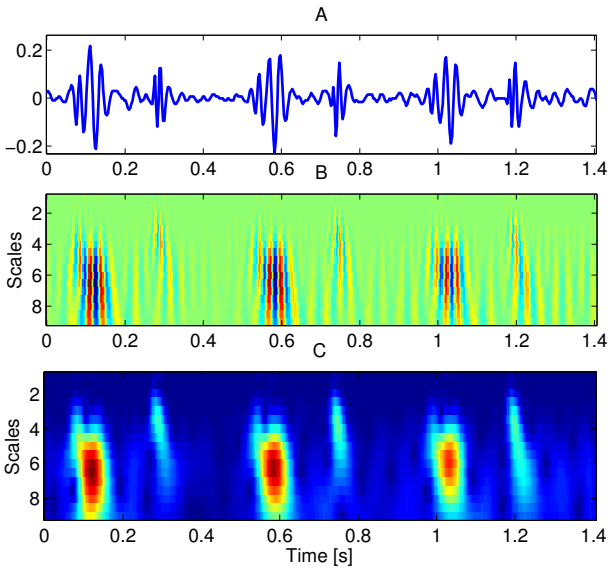

Figure 4.13: (A) A fPCG segment and the corresponding (B) time-scale representation using an 8^{th} order Gaussian mother wavelet. (C) The 2D envelope of the time-scale representation calculated using the Hilbert transform of the scales.

systolic murmur (Fig. 4.14). As shown in the exaggeration, the strong noise bursts corrupt the processing, and these noise bursts overlap with the heart sounds which makes the FHR determination extremely difficult.

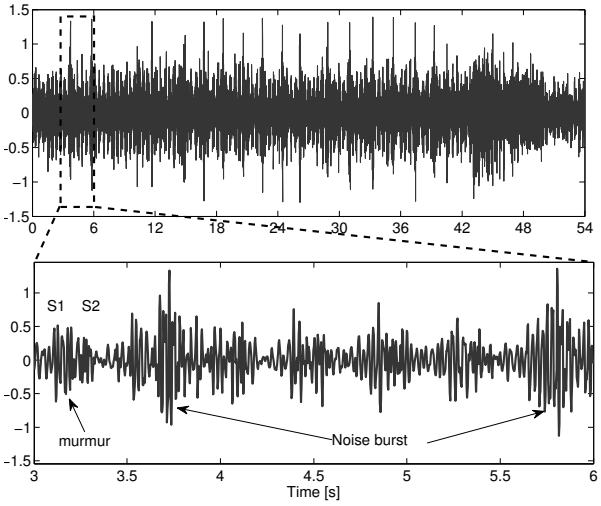

Figure 4.14: An approximately 1-minute long fPCG segment of a fetus with grade III-IV tricuspid insufficiency producing fetal heart murmur. Note the high amplitude noise burst (marked in the enlargement of the boxed area).

The segment from Fig. 4.14 is analysed using time domain and wavelet transform based

DOI:10.15774/PPKE.ITK.2012.001

correlation methods for the determination of the FHR. Comparing the two results based on a manually determined FHR the effect of the noise bursts and the murmur on the time domain autocorrelation method is apparent (Fig. 4.15(B)). In contrast, the wavelet transform based method is much less affected by these kind of disturbances (Fig. 4.15(A)).

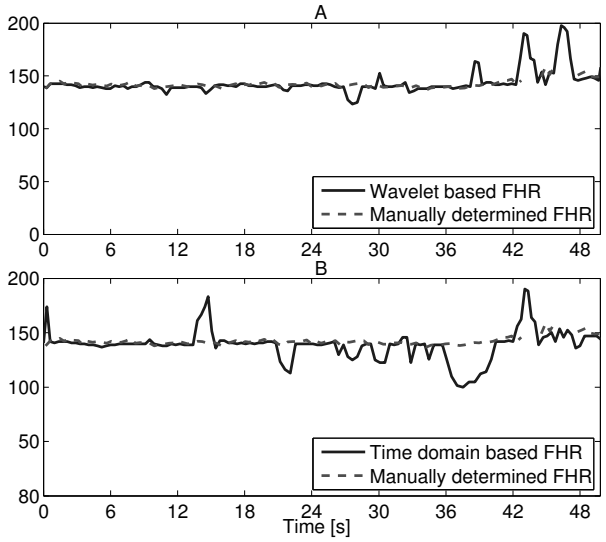

Figure 4.15: FHR calculated using (A) the wavelet transform based approach and (B) the time domain correlation. The manually determined FHR (red line) is calculated from the distances between the manually marked S1 sounds. However, due to the high noise level even the manual determination of the S1 sounds was not always possible. Note the increased occurrence of false excursions of the time domain method from the baseline (e.g. the interval after 36 s) compared to the result of the wavelet transform based approach.

For a more detailed comparison of the approaches based on time domain and the time-scale domain correlation we processed more than 500 fetal phonocardiographic recordings with different amounts of disturbances. All recordings were from the third trimester of the pregnancies and were collected during routine CTG examinations of average population. Regarding the fetal heart rate calculation the most important parameter is the amount of noise present in the recordings. Figure 4.16 shows the difference between the HiR of the wavelet transform based method and the time domain based method with respect to the noise level (NL) of the respective recording. Although the wavelet transform based method yields only a modest improvement on average, more precisely less than 5 %, the distribution of improvement values is very encouraging because improvement up to 18 % could be achieved and the amount of decrement is rarely greater than 5 %.

As also observable in Fig. 4.16, the best improvement can be achieved in the case of records with a NL between 20 and 30 %, meaning that the wavelet transform based method is more robust against the level of noise in the recording. This property is further

DOI:10.15774/PPKE.ITK.2012.001

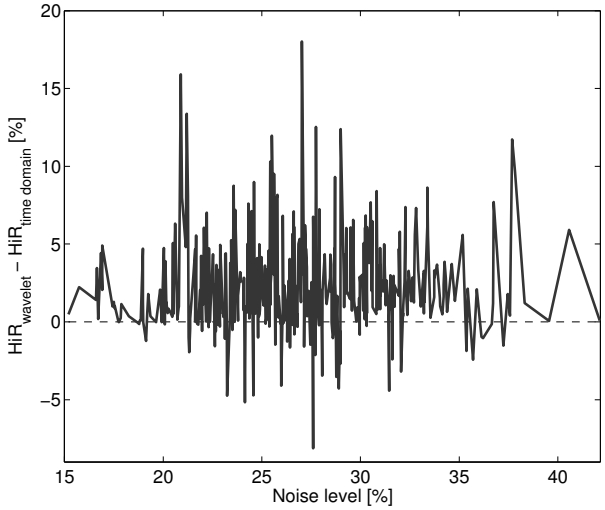

Figure 4.16: The difference between the HiR of the wavelet transform based method and the time domain based method with respect to the noise level of the given fetal PCG recording. All values above the black dashed line correspond to improvement, which is the case in 85 % of the recordings.

supported when investigating the range of possible HiR values for noise levels in the range of typical fPCG records. As shown in Fig. 4.17, for noise levels less than 20 % both methods perform fairly well. As the noise level increases the range of possible HiR values widens because in some cases the different methods achieve only lower HiRs. However, for NL in the range of 20-35 %, the time domain based method has a lower limit of possible worst HiR values than the wavelet transform based approach. In other words, the worst HiR that the wavelet transform based method can achieve in this range of NLs is always better than the worst performance of the time domain based correlation, at least in the case of these records. In the case of higher NL the performance of both methods degrades similarly.

We made also a further interesting observation: as already mentioned the modulus difference based approach performs in general similar to the autocorrelation based approach (Fig. 4.18), but in some cases it is better. Out of the 15 % of records where the wavelet based autocorrelation method achieved lower HiRs than the time domain method, in the case of nearly 40 % the 2D modulus difference based approach improved the HiR of the time domain algorithm, meaning that processing in the time-scale domain caused degradation in the case of only 9 % of the records. In practice one could use the following strategy: if the wavelet transform based autocorrelation cannot gain improvement then apply the 2D modulus difference based method.

DOI:10.15774/PPKE.ITK.2012.001

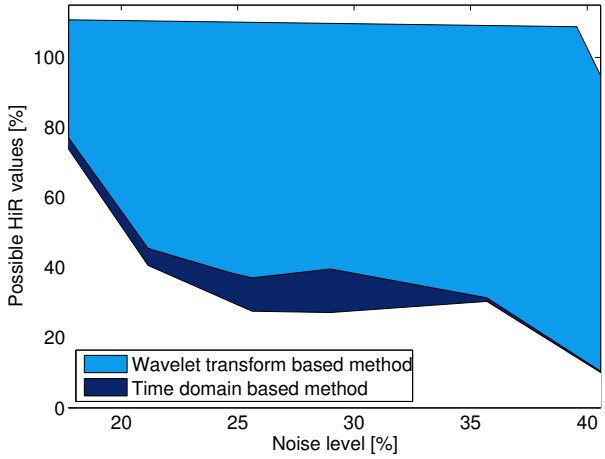

Figure 4.17: Possible range of HiR values for different level of noise in the case of the time domain based correlation and the wavelet transform based method calculated from analysing more than 500 recordings. Note that in the case of NL in the range of 20-35 % the worst performance of the wavelet transform based method is always better than the worst achievement of the time domain method.

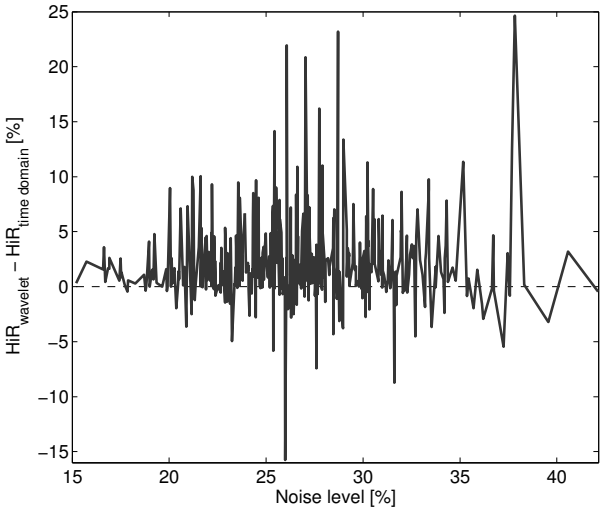

Figure 4.18: The difference between the HiR of the wavelet transform based method using 2D modulus difference and the time domain based correlation method with respect to the noise level of the given fetal PCG recording. All values above the black dashed line correspond to improvement, which is the case in 77 % of the recordings.

DOI:10.15774/PPKE.ITK.2012.001

Conclusions of fetal heart rate calculations using the wavelet transform

Since the wavelet transform based method performs better in the case of the overwhelming majority of the recordings, more precisely 85 %, and also due to the aspects highlighted in the previous paragraphs it can be used as a reliable substitute or extension of the time domain method. There is no guarantee that this time-frequency domain based approach is always better than the time domain approach, but in the vast majority of cases it will perform better. This is especially true for noisier records. Another strategy would be to apply it only on records where the time domain based approach achieved a HiR less than a given threshold. Similarly, this decision can be based also on the NL of the given record or a given segment of the record. The block diagram of a possible realization is shown in Fig. 4.19.

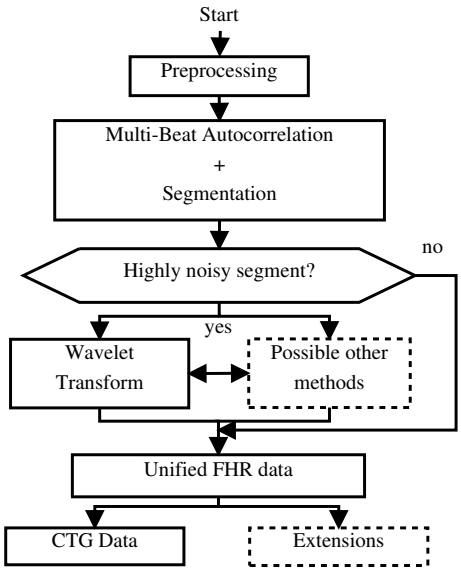

Figure 4.19: Block diagram of a possible realization of a FHR calculation algorithm including the wavelet transform based approach. Note the dashed blocks for possible extensions.

As demonstrated also in Fig. 4.15, the improved hit rate is not the only advantage of the wavelet transform based method. In that example both methods yield a similar HiR whereas the time domain based autocorrelation introduces an increased amount of error, especially important when calculating heart rate variability measures. Unfortunately the exact comparison from this aspect is not possible without, for instance, simultaneous fECG-fPCG measurements, which could not be realized at the time of this study, thus we have to rely on our empirical observation of selected segments, such as the one presented in Fig. 4.15.

A further next step of this analysis would be the calculation of different heart rate variability measures from the reliably estimated FHR segments. This could be included into the routine phonocardiographic CTG examinations, for example for the early identification of intrauterine growth restriction [100, 150, 151].

4.3 Components of the heart sounds

As already mentioned in the section 2.3.1, the S1 and S2 heart sounds consist of two major components, one due the closure of a valve on the left side, and the other due to the closure of a valve on the right side of the heart. In recent years special attention was given to the analysis and synthesis of the main heart sounds. The majority of these studies describe

DOI:10.15774/PPKE.ITK.2012.001

the decomposition of the S2 heart sound because the explanation for origin of the S2 sound is more widely accepted and the splitting of the S2 sound is a more frequent symptom of cardiovascular diseases in the case of adults [162].

Certain parameters of the S2 sound are related to important hemodynamic parameters. For instance, the resonant frequency of the P2 component is proportional to the pulmonary arterial pressure [163], as are other spectral features of the S2 sound [164], and spectral features from the beginning of the S2 sound can be related to the systematic arterial pressure [165]. These findings are based on Laplace's law which states that the tension of the blood vessel wall is proportional to the pressure inside the vessel, and the tension is related to the resonant frequency, like in the case of a drumhead. Since the splitting interval has also important implications, this has been investigated as well and it has been found that it correlates also well with the pulmonary arterial pressure [166].

The fetal circulation has some important differences compared to the developed human circulation (Section 2.1.2): the lungs are in a collapsed state thus the pulmonary circulation is not functioning and the blood from the pulmonary artery is shunted into the aorta through ductus arteriosus. This differences obviously change the meaning and significance of the S2 splitting. On the other hand, in the case of fetal PCG recordings, we observed in certain cases the splitting of the first heart sound, and assume that the assessment could contribute to the classification of congenital heart diseases.

Although several techniques have been suggested for the determination of the heart sound split, especially in the case of the S2 sound [167–169], a model based approach has several advantages:

- for the short and low bandwidth fetal heart sound signal a model based approach proved to be more reliable for the exact determination of the splitting interval,
- although the exact splitting interval is usually the most important parameter, other heart sound parameters have also discriminating value,
- model based heart sound detection can be applied for very precise T_{bb} determination.

Several heart sound models have been suggested not only for the analysis, but also for the synthesis of heart sounds, for example for educational purposes [96]. Previous attempts can be classified into three main groups [28]:

- The exponentially damped sinusoid models [170–174]: The heart sound is modelled as the sum of exponentially decaying sines associated with the constant resonant frequencies of the production and transmission system, that is the heart-thorax system. From this point of view, this signal model has a clear physical meaning, but it usually requires more than a few components to accurately model the heart sounds. Another major disadvantage is that the different valve components, e.g. A_2

DOI:10.15774/PPKE.ITK.2012.001

and P_2, cannot be separated, thus the splitting interval cannot be determined using this approach.

- Models based on Gaussian sinusoids [175,176]: In the case of this model the matching pursuit method can be applied which decomposes the heart sound signal into a set of Gaussian sinusoids, i.e. time-frequency atoms, which yields a precise time-frequency representation. Using this approach in some cases it is possible to determine the splitting interval [177], but usually more than just a few components are needed also in this scenario. True physical meaning is also lost. It can be applied effectively for denoising purposes, nonetheless [31, 32].
- The linear and nonlinear chirp model [28, 96, 97, 178]: This approach relies on the experience gained by performing time-frequency analyses of heart sounds and on the physical interpretation that the closing sound of the valve produces decaying oscillations with decreasing frequency since the blood volume in the heart changes rapidly after valve closure. Although in adults the instantaneous frequencies of S1 and S2, as well as of the components, e.g. A_2 and P_2, have generally a nonlinear relationship with time, in the case of fetuses a linear relationship is often adequate.

Although these models are mostly applied for the decomposition of the S2 heart sound, motivated by aspects mentioned above and due to the fact the S1 sound is similarly a multicomponent signal [174], we investigated the application of such models on the analysis of fetal heart sounds.

4.3.1 Fetal heart sound model and parameter estimation

By investigating the heart sounds of pigs and humans with wide S2 split Xu *et al.* suggested a dechirping method and the following nonlinear heart sound model for the second heart sound [28, 97]:

$$A(t) = c_3 \cdot \left(1 - \exp\left(\frac{-t}{c_4}\right)\right) \cdot \exp\left(\frac{-t}{c_5}\right) \cdot \sin\left(\frac{\pi t}{c_6}\right), \tag{4.8}$$

$$f(t) = c_1 + c_2(t+1)^{-0.5}, \tag{4.9}$$

$$s_{S2}(t) = A_A(t)\sin\left(\varphi_A(t)\right) + A_P(t-t_0)\sin\left(\varphi_P(t-t_0)\right), \tag{4.10}$$

where $c_1, c_2, c_3, c_4, c_5, c_6$ are constants, different for the aortic, A, and pulmonary, P, components, and t_0 is the splitting interval. $\varphi_A(t)$ and $\varphi_P(t)$ are the phase functions, calculated by integrating the different instantaneous frequency functions, that is $\varphi(t) = 2\pi \int_{-\infty}^{t} f(\tau)\mathrm{d}\tau$.

Based mainly the above model and the analysis of fetal heart sounds, we suggested the

DOI:10.15774/PPKE.ITK.2012.001

following chirp model for fetal heart sound modelling, presented here for the S1 sound:

$$s_M(t) = A_M \sin(\varphi_M(t)) \cdot e^{-t/\tau_M}, \tag{4.11}$$

$$s_T(t) = A_T \sin(\varphi_T(t - t_d)) \cdot e^{-(t-t_d)/\tau_T}, \tag{4.12}$$

$$s_{S1}(t) = s_M(t) + s_T(t), \tag{4.13}$$

where A_M and A_T are the initial amplitudes, φ_M and φ_T the phase functions, and τ_M and τ_T are the time constants of the damping of the sinusoidal mitral and tricuspid components, respectively. Finally, t_d is the delay between the above two components, that is the splitting interval.

As already noted, a linear frequency decrease often proved to be sufficient, meaning that the phase functions can be defined as follows:

$$\varphi_M(t) = 2\pi \int_{-\infty}^{t} f_M(\tau)\mathrm{d}\tau = 2\pi \int_{-\infty}^{t} F_M - \Delta f_M \cdot \tau \, \mathrm{d}\tau, \tag{4.14}$$

$$\varphi_T(t) = 2\pi \int_{-\infty}^{t} f_T(\tau)\mathrm{d}\tau = 2\pi \int_{-\infty}^{t} F_T - \Delta f_T \cdot \tau \, \mathrm{d}\tau, \tag{4.15}$$

where $f_T(t)$ and $f_M(t)$ are the instantaneous frequency functions with an initial frequency of F_M and F_T and a negative slope of Δf_M and Δf_T for the mitral and tricuspid components, respectively.

This two-component model contains altogether nine parameters ($p_1 - p_9$). It has the main advantage that it is rather simple compared to the model of Xu *et al.* but has still physical meaning. The simplicity is important because of the efficient parameter estimation from the noise-contaminated recordings. In case the beginning of the heart sound cannot be identified reliably and offset parameter can be easily included into the model. Several methods exist for the assessment of parameters of the heart sound model. In the following section a short introduction of possible approaches is presented.

Time-Frequency Approach

Xu *et al.* [28, 97] developed their heart sound model and their dechirping method based on the time-frequency analysis of the heart sounds. They applied the Wigner-Ville distribution (Section 3.2.4).

If the frequency decay of the heart sound components is great enough than the application of such a transform makes the separation of the components possible in the time-frequency plain even if they are overlapping in the time domain. Furthermore the parameter values can be estimated from the Wigner-Ville distribution.

The main disadvantage of this approach is that masking is needed in the time-frequency

DOI:10.15774/PPKE.ITK.2012.001

plane for suppressing the effect of the cross terms. This is not always possible in an automatic way, although recent results using compressed sensing could be utilized in this field [179]. However, the high level of noise and the low bandwidth of fetal heart sounds makes this approach usually not feasible.

The Monte Carlo Method

A rather brute force approach is the application of the Monte Carlo method [98]. The main idea is to apply gambling for the determination of some unknown values. Consider as an example a circle and a circumscribed square. The ratio of the area of the circle and the square is $\pi/4$, and it is reasonable to believe that if one would pick points at random from the square, the fraction $\pi/4$ would lie also inside the circle [180]. Picking points at random this way for characterising the area of the circle is also known as random sampling.

The Monte Carlo method can be applied for determining the parameters of the model by taking enough random parameters and calculating the error between the measured heart sound and the synthesized signal based on the different parameter values. It is believed that the set of parameters with the smallest error is the real solution, or at least it is near the real solution of the model-fitting problem. Obviously this presumes that i) the model is valid, ii) the intervals, i.e. the square in the case of the example above, for picking the random parameters is known, iii) the error surface is "nice", and iv) sufficient number of random parameters have been investigated.

Our suggested model is a simplified one, thus it cannot be always valid. Nature usually cannot be unveiled in such a simple way. Nonetheless according to our experiences, and based on the analysis of selected fetal heart sounds we have found that this model is capable of capturing important characteristics of the heart sound, such as splitting. The limits of the interval for valid parameters have been determined empirically based on the time-frequency analysis of selected heart sounds and the model fitting of a great number of heart sounds (Table 4.1). Regarding the error surface, unfortunately a rigorous proof is missing, and in the case of greatly overlapping components, an increased number of local minima exists often without a definitive global minimum. Fortunately heart sound parameter estimation becomes more important in the case of increased splitting which might be related to some cardiac abnormality. This increase is often still not enough for separation in the time domain, however our model-based approach becomes more reliable due to the decreased number of local minima. The number of selected random parameters is usually regarded as 10^6, on special computing architectures even more. This threshold is the result of empirical observations.

Further methods, such as simulated annealing [181, 182], or global optimization [183], have been also applied with success, however, the basic Monte Carlo method has the main

DOI:10.15774/PPKE.ITK.2012.001

Table 4.1: Parameter intervals for heart sound modelling

#	Parameter	Limits
p_1	A_M	-1-1 (normalized)
p_2	F_M	20-70 Hz
p_3	Δf_M	0.2-0.8 Hz/ms
p_4	τ_M	10-150 ms
p_5	A_T	-1-1 (normalized)
p_6	F_T	30-90 Hz
p_7	Δf_T	0.3-1 Hz/ms
p_8	τ_T	10-100 ms
p_9	t_d	0-60 ms

advantage of simplicity, although it is resource demanding. The latter can be bypassed by implementations on manycore architectures, such as GPUs. In this field preliminary results have been achieved with a running time of 300 ms for a single heart sound, which is equal to a decrease of more than two order of magnitudes [108].

The solution of the Monte Carlo method can be refined using a local optimization algorithm, which yields the local minimum near the guessed solution of the Monte Carlo process.

As an example, in Fig. 4.20 and 4.21 a fetal S1 sound is shown together with the result of the Monte Carlo based model fitting approach. With random simulation of 10^6 heart sounds and local optimization of the best fitting signal a normalized root mean square error (NRMSE) of 24 % was achieved. NRMSE is defined as

$$\text{NRMSE} = \sqrt{\frac{\sum_{i=1}^{N} e[i]^2}{\sum_{i=1}^{N} x[i]^2}}, \tag{4.16}$$

where $e[n]$ is the error between the original heart sound sound ($x[n]$) and the synthesized signal ($s[n]$). The time delay between the two components, that is the splitting interval, was found to be 12 ms. Based on the modelling of more than one hundred fetal S1 heart sounds on average a NRMSE of around 30 % was achieved (Fig. 4.22), which is possibly sufficient for reliable parameter estimation in this low SNR scenario (consider Figs. 4.20-4.21 as a point of reference).

Conclusions of fetal heart sound modelling

Using a valid fetal heart sound model it is possible to perform fetal PCG examinations in a more objective manner because the characterization of the the measurements can be accomplished from a basic level of the data, namely from the level of the heart sounds.

DOI:10.15774/PPKE.ITK.2012.001

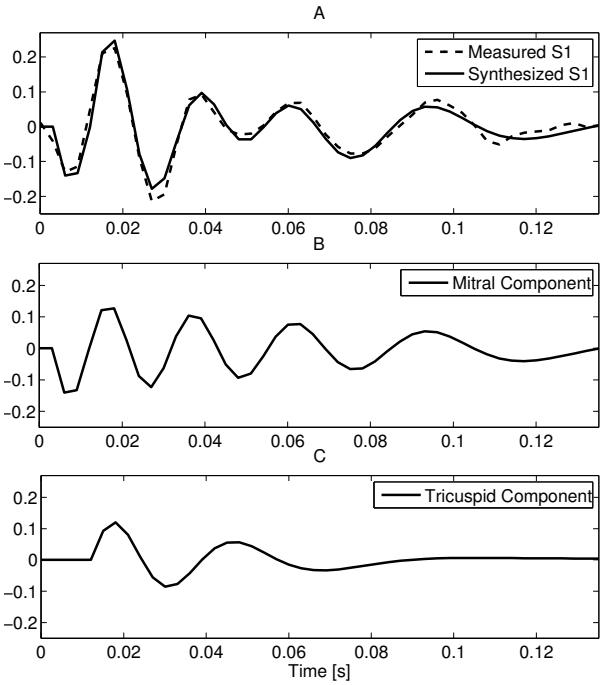

Figure 4.20: (A) A fetal S1 sound (blue) and the result of the Monte Carlo based model fitting (red). The normalized root mean square error between the measured and synthesized S1 sound is 24 %. (B) The mitral component and (C) the tricuspid component of the synthesized S1 sound.

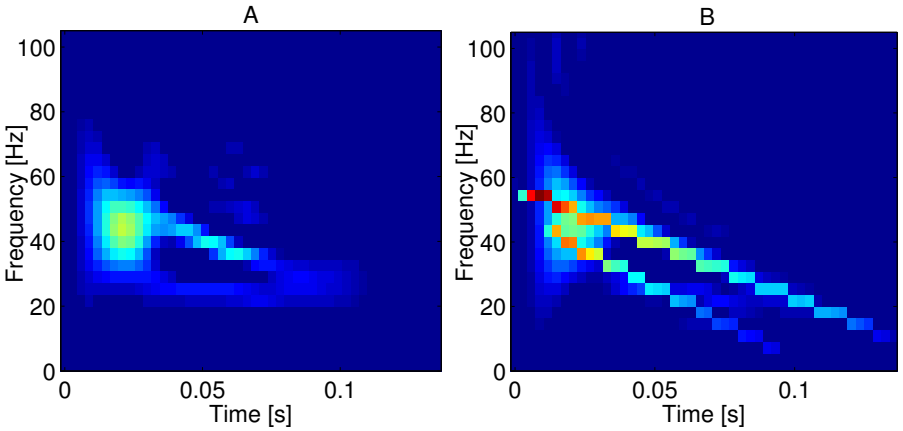

Figure 4.21: The time-frequency distribution of (A) the fetal S1 sound from Fig. 4.20 and (B) the corresponding synthesized heart sound superimposed by the instantaneous frequency function of the model (the color of the line corresponds to the instantaneous amplitude). Note the linear frequency decrease, especially observable of the component with higher frequencies. The time-frequency representations were calculated using the Wigner-Ville distribution.

DOI:10.15774/PPKE.ITK.2012.001

It has been demonstrated that heart sound parameters in the case of adults have clinical significance [163–166], this should also, at least partly, apply to fetuses. However, the validation is much more difficult in the case of fetuses. This is why the the real significance of the above presented results can only be established based on clinical investigations of a great number of fetuses with possibly echocardiographically verified diagnosis of different states and diseases.

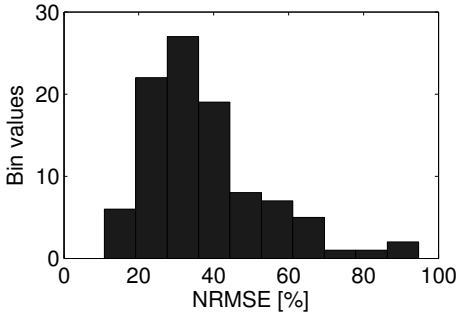

Figure 4.22: The histogram of the achieved NRMSEs of the modelling of more than one hundred fetal S1 heart sounds.

4.4 Fetal heart murmur and congenital heart diseases

The presence of murmur is a warning sign for a possible underlying heart disease. Several studies investigated murmurs related to congenital heart defects (CHD) using PCG for children and adults, for instance [167,184]. For children an automatic cardiac examination has been also suggested [20]. It should be noted that these results can be only partly adapted to fetal PCG, nonetheless, fetal murmur seems still to of significance. This is also demonstrated by preliminary results in [185].

4.4.1 Principles of fetal murmur detection

As already explained in Section 2.3.2, normally the fetal heart exhibits only two well distinguishable valve sounds (S1 and S2). In the case of certain morphological abnormalities murmurs also appear, which is the result of turbulent blood flow. The detection of murmur is often very difficult since noise from multiple sources corrupts the low intensity fetal heart sound signal. Furthermore, long records have to be processed, thus sophisticated signal processing methods are needed. The automated murmur detection method relies on the fact that if a murmur is present then it appears in nearly all heart cycles, usually with a similar envelope, duration and timing whereas noise does not correlate with the heart rate.

In recent years several methods have been investigated for heart murmur detection and classification, such as artificial neural networks [186], detection based on dynamic parameters of different time-frequency representations [187, 188] or detection based on fractal features [189–191]. All these studies deal with PCG recordings form children and adults. Although these techniques might be at least partly applicable for fetal heart sound data, major differences between fetal and postnatal PCG signals introduce some

DOI:10.15774/PPKE.ITK.2012.001

limitations. Among these dissimilarities are the much lower bandwidth of the fetal PCG signal due to the attenuation caused by the maternal tissues and the lower signal-to-noise ratio with more sources of noise (e.g. maternal heart and digestive sounds). There is also an important empirical observation, namely dominant low-frequency components of fetal heart murmur can be recorded on the maternal abdomen. In contrast, the murmur of children and adults has usually higher dominant frequency components than the main heart sounds (Fig. 4.23). In addition, it might be the corollary of the previous phenomenon that the recorded fetal heart murmurs exhibit in some cases a rather cyclostationary property despite the certainly turbulent origin of the murmur signal (Fig 4.26). Ongoing investigations are trying to find a confirmed explanation for this observation.

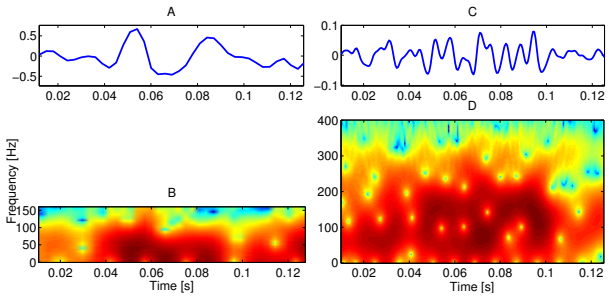

Figure 4.23: Heart murmur of an infant with pulmonary atresia before birth (left) and after birth (right). Although similar dominant frequency components are present in the low frequency range (<100 Hz), the postnatal segment exhibits strong high frequency components, which are filtered out by the different maternal tissue in the fetal recording.

The aforementioned aspects are one of the main reasons why we apply other techniques for murmur detection compared to studies on children and adults. For example a higher heart rate, the increased level of noise and the only low-frequency components of the murmur pose constraints on the mentioned approaches which are based on a time-frequency representation. Likewise, the rather cyclostationary nature of the murmur limits the possibility of fractal feature based classification. Our suggested method tries to exploit these differences and exploits the cyclostationarity of the signal by calculating a characteristic heart sound for a given record.

4.4.2 Characteristic heart sounds by improved ensemble averaging

The techniques of ensemble averaging was introduced in Section 3.1, which is a useful method for investigating also cyclostationary signals, such as PCG signals. In this scenario the different heart cycles are regarded as the elements of the ensemble. However, some limitations have to be taken into account. First, different level of noise is present in

DOI:10.15774/PPKE.ITK.2012.001

different heart cycles and the noise is often non-Gaussian. Second, the heart sound signal might not remain the same over all the heart cycles, due to factors such as variable splitting. Third, there is no compensation for the misalignment of the window containing the heart sound or heart cycle caused by heart rate variability and the inaccuracy of the heart sound detection method.

The first two obstacles are tackled by defining weights for the averaging and introducing the concept of element specific ensemble averaging. The weights are defined in the following way: we start with a segment $x_i[n]$. Because we want to enhance the heart sound signal underlying this segment, we need to take into account those other segments with great weights which are similar to and those segments with lower weight which differ from the selected i^{th} segment. A simple similarity measure, which proved to be useful in this scenario, is the normalized correlation value. Ensemble averaging even in a weighted manner is a linear technique and, as such, performs well only if the noise is Gaussian. However, noise bursts with large amplitudes will decrease the performance of this averaging method, thus a similarity condition is included into the calculation: if the normalized correlation coefficient is less than a given threshold, the corresponding heart cycle is rejected from the ensemble taking advantage of the great number of available heart cycles. This way the calculated ensemble average will be specific for the selected initial i^{th} segment.

The last difficulty is resolved by calculating the Pearson correlation coefficients (Eq.(3.1)) between the segments, and define the offset parameter as the time-lag with maximal normalized correlation value, which latter is regarded as the actual weight for the averaging. In summary, the improved ensemble average $\hat{s}_i$ is calculated from the different heart cycles x_j as weighted sum in the following way:

$$\hat{s}_i[n] = \frac{1}{\sum_j w_{ij}} \sum_j w_{ij} \cdot x_j[n - o_{ij}], \tag{4.17}$$

where $\hat{s}_i$ is the ensemble average for segment i and w_{ij} is the maximal normalized correlation coefficient between segment i and j, producing the offset o_{ij}.

In order to increase robustness against noise bursts a selection criterion can be included meaning that only those segments are involved in the averaging which have a normalized correlation coefficient greater than a given threshold $\mathrm{r}_{\mathrm{thres}}$.

After performing the calculations described above we end up with a set of heart cycle segments for every heart cycle segment, denoted as *correlation groups*. Each of this groups contains segments which are similar to the initial segment of the group with a correlation coefficient greater than the given threshold $\mathrm{r}_{\mathrm{thres}}$. A natural question arising is which group to choose for characterizing the given record. A trivial answer is to select the group containing the largest number of segments. This approach is in most cases appropriate

DOI:10.15774/PPKE.ITK.2012.001

since the heart sound dynamics usually do not change significantly during a 20-minute record. Yet in some cases some major differences can be observed, for example between the heart sounds in the first and second half of the record. In such a case obviously further analysis should be carried out on correlation groups from both parts of the recording. The number of analysed correlation groups can be controlled by investigating the temporal distribution of the segments of the groups in the given recording. This, however, is a field of possible further work.

It should be noted that this algorithm is a brute force approach, and compares every heart cycle, which means a complexity of $\mathcal{O}(n!)$. In practice, however, this is not a crucial disadvantage because due to the low-frequency content a low sampling frequency can be used and the length of the recordings is limited, enabling the presentation of results after a couple of minutes after the end of the PCG recordings in the present realization. However, in the case of other applications, such as continuous monitoring, central evaluation of many recordings in a telemetric system or analysis of other biomedical signals, with increased data length and sampling frequency run time improvement could be realized by dividing the data of interest into multiple parts and applying kilocore computing architectures, for instance FPGAs or GPUs, for parallel processing.

Some examples for fetal heart sound enhancement using ensemble averaging are presented in the following section. In this scenario, the resulting ensemble averaged heart sound from the greatest correlation group is denoted as the *characteristic heart sound* or *cycle* for the given record. The block diagram of the characteristic heart sound calculation algorithm is shown in Fig. 4.24.

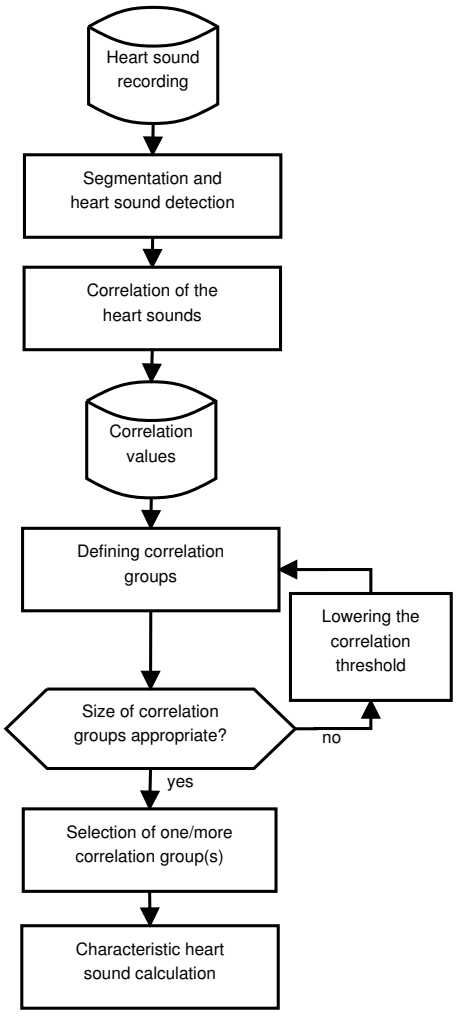

Figure 4.24: Block diagram of the characteristic heart sound calculation algorithm.

4.4.3 Characteristic heart sound calculation for murmur detection

The technique introduced in the previous section is not only interesting for the analysis of the first and second fetal heart sounds. As already remarked fetal heart murmurs exhibit

DOI:10.15774/PPKE.ITK.2012.001

surprisingly cyclostationary properties enabling the calculation of a "characteristic heart murmur" (Fig. 4.25). Based on this observation a straightforward idea arises: apply the characteristic heart sound calculation technique on the systolic or diastolic segments and if a correlation group of acceptable size and a characteristic sound of acceptable average energy can be determined then the record can be marked as possibly containing murmur. In practice, however, usually the characteristic heart cycle is calculated based on correlating only the first heart sound, or the S1 sound and the systolic segment in order to increase robustness. The acceptable size of a correlation group is regarded as around 5% of the number of detected heart cycles in the record, depending on the quality of the signal. Because in a 20-minute recording usually around 2000 heart cycles of acceptable quality are present, the aforementioned threshold leaves us still with around 100 cycles, which is in most of the cases sufficient to decide whether a systematic extra component, i.e. a murmur, is present or not.

Examples for characteristic heart cycles in the case of recordings with and without murmur are shown in Fig. 4.26 and Fig. 4.27, respectively.

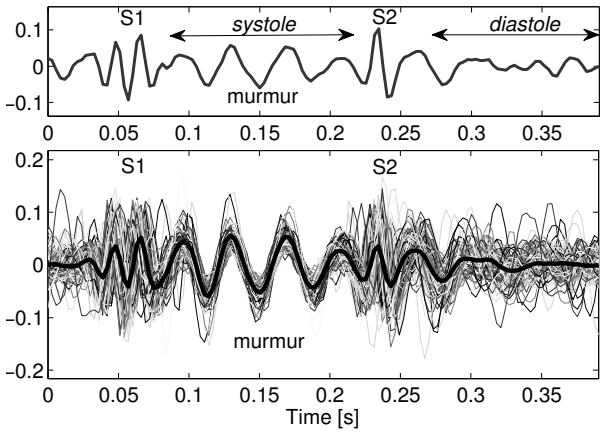

Figure 4.25: The characteristic murmur (thick line in bottom trace) of a record from a fetus with Tetralogy of Fallot calculated from 127 heart cycles (thin lines in bottom trace) and one heart cycle from the ensemble (top trace). A component of around 30 Hz is present in the systole. The systolic timing of this murmur component varies from cycle to cycle.

Decision about the presence of murmur can be performed by visual examination of the characteristic heart cycle because it is a comprehensive form of the typical heart sound dynamics in the given recording. On the other hand automatic algorithms can also be applied. We have developed a heuristic method which calculates an envelope of the systolic segment based on the local extrema. By analysing certain properties of the envelope (maximal and average value, maximal and average rate of change, ...) a murmur is suspected and localized [12, 109].

DOI:10.15774/PPKE.ITK.2012.001

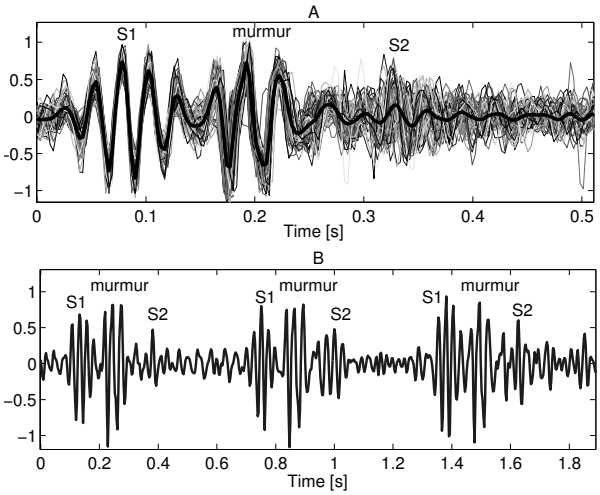

Figure 4.26: (A) The characteristic heart cycle (thick line) of a fetus with a ventricular septal defect and the corresponding 84 heart cycles (thin lines). Note the cyclostationary nature of the heart murmur with a very similar waveform from cycle to cycle observable also on a segment of the record (B) showing three consecutive heart cycles.

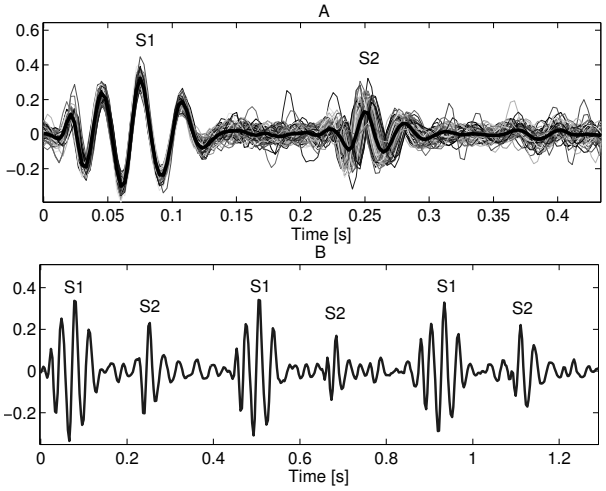

Figure 4.27: (A) The characteristic heart cycle (thick line) of a healthy fetus and the corresponding 89 heart cycles (thin lines). Note the low variability of the length of the systole. (B) A segment showing three consecutive heart cycles of the same recording.

DOI:10.15774/PPKE.ITK.2012.001

Parameters of the fetal heart murmur

In cardiac auscultation heart murmur is usually characterized by five properties as already explained in Section 2.3.2. In the case of fetal heart murmur not all of them can be determined (e.g. point of maximal intensity or radiation). However, in order to be be consistent with the aforementioned medical murmur parameters, and in this way facilitate the acceptance of fetal murmur analysis in the medical community we defined the following parameters:

- **Length**: is calculated as the length of the time window containing the murmur relative to the length of the cardiac cycle.
- **Timing**: at present we discriminate between systolic, diastolic and murmur with components in the systole and diastole.
- **Intensity**: is the average ratio of the maximal murmur intensity to the maximal S1 sound intensity.
- **Dominant frequency**: is determined based on the average zero-crossing rate or frequency of the maximal spectral component.
- **Shape of the envelope**: is classified into crescendo (positive derivative above a given threshold during the whole murmur), decrescendo (negative derivative above a given threshold during the whole murmur), band-type (absolute value of the derivative below a threshold) or crescendo-decrescendo (positive derivative at the beginning and negative at the end of the murmur).

It is important to note that during our investigations we found that these parameters can be calculated in an automatic way and have possible high discriminative value.

4.4.4 Significance of fetal murmur detection

For demonstrating the clinical significance of fetal murmur detection we present selected cases because at the time of this work sufficient amount of records with verified clinical diagnosis was still not available.

Table 4.2 summarizes the cases where the clinical diagnosis was established based on detailed echocardiographic examinations. As observable also in this table, serious congenital heart diseases produce often detectable fetal heart murmur. However, in some cases no murmur can be detected although a congenital heart disease can be diagnosed. It should be noted that these results are based on single phonocardiographic measurements whereas some malformation might produce murmur only at a later stage of pregnancy because of the increase in the fetal blood pressure during pregnancy [192]. Since fetal phonocardiographic measurements can be used for routine CTG examinations even on a daily basis in home environment, CHDs which produce heart murmur only at a later stage

DOI:10.15774/PPKE.ITK.2012.001

Table 4.2: Fetuses with verified clinical diagnosis and the parameters of detected fetal heart murmur

ID	Diagnosis*	Murmur	Length	Timing	Intensity	Dominant Frequency [Hz]	Shape of the Envelope
P1	ASD	✓	24%	systolic	46%	36	band-type
P2	TI, Ebstein's anomaly	✓	23%	systolic	76%	45	crescendo-decrescendo
P3	VSD	✓	17%	systolic	120%	41	crescendo-decrescendo
P4	VSD	✓	21%	systolic	107%	26	decrescendo
P5	VSD	✓	15%	systolic	60%	30	crescendo-decrescendo
P6	VSD	–	–	–	–	–	–
P7	VSD	✓	13%	systolic	22%	27	crescendo-decrescendo
P8	TOF, MAPCA	✓	55%	systolic-diastolic	38%	30	band-type
P9	PA, MAPCA	✓	25%	systolic	125%	27	crescendo-decrescendo
P10	–	✓	29%	systolic	39%	32	crescendo-decrescendo

*ASD - Atrial septum defect, TI - Tricuspid insufficiency, VSD - Ventricular septum defect, TOF - Tetralogy of Fallott, MAPCA - Major aorto-pulmonary collateral arteries, PA - Pulmonary atresia

DOI:10.15774/PPKE.ITK.2012.001

of the pregnancy might be still assessable. On the other hand, there are also cases where a fetal murmur can be detected but no underlying cardiac abnormality can identified. The cause of these so called *innocent* murmurs is also a turbulent blood flow but with no associated hemodynamically significant malformation. Innocent murmur often even disappears over time or during childhood. The discrimination of innocent murmurs is still an important open question, even in the case of children and adults. Here again, the possibility of daily fetal measurements could be advantageous.

In Appendix A two selected cases with serious congenital heart diseases are presented with detailed clinical descriptions, where in the first case prospective and in the second case retrospective analysis of the fetal phonocardiographic records revealed fetal heart murmur. The latter case is an important example because the CHD of that fetus became evident only after birth, whereas it might have been already indicated earlier based on the fetal heart murmur. However, the automatic murmur detection method is not yet included into the routine CTG examination thus the fetal murmur analysis was performed only after birth. Although in this way the significance of fetal murmur detection is not fully established we believe that these results support the feasibility of our new method, which could contribute to the prenatal detection of CHDs, as a pre-screening method for a comprehensive echocardiographic examination, especially in the low risk population.

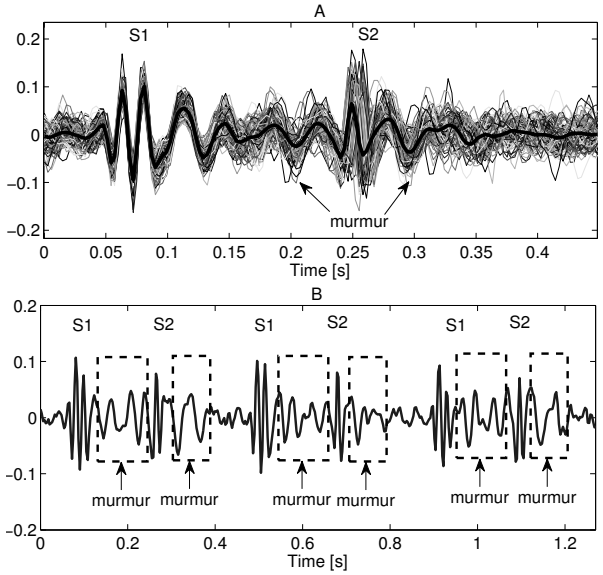

Figure 4.28: (A) The characteristic heart cycle (thick line) and the corresponding heart cycles (thin lines) of the fetus with Tetralogy of Fallot, pulmonary insufficiency and and aorta-pulmonary vessels producing fetal heart murmur (Case I). (B) Three consecutive heart cycles from the same recording.

DOI:10.15774/PPKE.ITK.2012.001

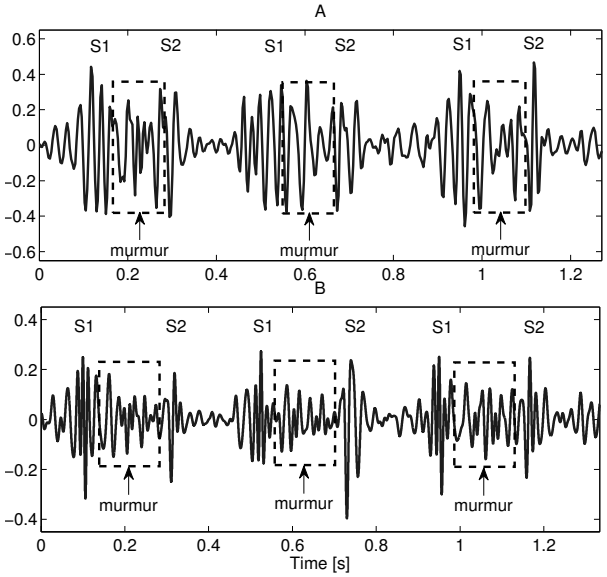

Figure 4.29: Segments of the phonocardiographic recordings of a fetus with pulmonary atresia combined with a ventricular septal defect and major aorto-pulmonary collateral arteries producing heart murmur (Case II). (A) Fetal and (B) postnatal heart sound recordings are both filtered to the frequency band of 30-100 Hz.

The detection of fetal heart murmur is of great importance because it might open new possibilities for prenatal screening of CHDs. The required equipment for fetal phonocardiography is of low cost and automatic methods help in the analysis. In this way fetal PCG could assist the prenatal detection of CHDs as a pre-screening method for a comprehensive echocardiographic examination, especially in the low risk population. Although it can be applied at the earliest in the second half of the second trimester, it could contribute to an appropriately prepared delivery and early postnatal treatment. There are also other factors, such as allowing parents time to adjust to their unborn child's diagnosis, blunting postnatal psychological stress [193]. Further research is needed for quantitative verification of the sensitivity and specificity of the suggested method.

A possible expert system

One could go a step even further, if the significance of fetal heart murmur is more supported, by trying to differentiate between different CHDs. Automated murmur classification is a difficult task, although in the case of children and adults promising results can be found, e.g. [194]. Because of the differences of the fetal circulation and the low intensity and bandwidth of the fPCG signal not all knowledge of adult murmur classification can

DOI:10.15774/PPKE.ITK.2012.001

be adapted. Nevertheless, our observations so far support the possibility of finding adequate features for discriminating different CHDs. This, on the other hand would also help in separating innocent murmurs from murmurs related to severe cardiac abnormalities. Unfortunately, at present, we have not enough data available for verifying parameters for reliable classification thus only some preliminary results can be demonstrated.

As an example a record of detected fetal heart murmur originating from a tricuspid valve insufficiency (TI) related to the Ebstein syndrome is shown in Fig. 4.30. This murmur exhibits fairly high frequency components, which has, for instance, a surely discriminative value.

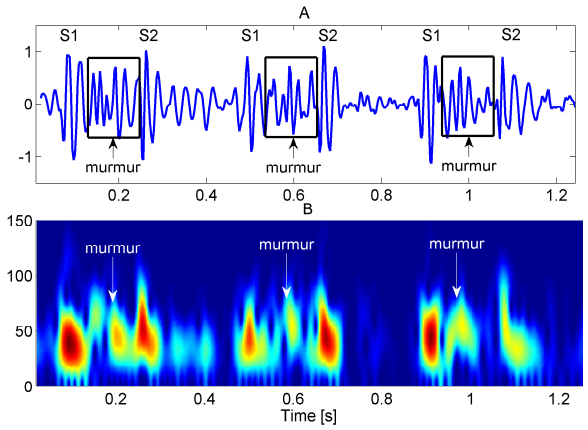

Figure 4.30: (A) A segment of the phonocardiographic recording of the fetus with tricuspid insufficiency related to Ebstein syndrome. (B) The time-frequency distribution of the segment above. Note the high frequency components of the murmur.

Analysis of ten records from fetuses with four different CHDs and an innocent murmur substantiate also the possibility of murmur classification. For each record we extracted parameters from six heart cycles taking into account the deviations of the dynamics, producing altogether more than 50 points in the feature space. As observable in Fig. 4.31, although there is some overlap, different domains that correspond to different CHDs can possibly be defined. Note also that not all parameters have been used because of limitation of the visualisation. A quantitative classification method has not been applied on this data because of the low number of cases.

Fortunately, using the telemetric system there is hope to collect sufficient amount of data for verification of an appropriate classification method, such as different types of clustering, or application of a naive Bayes classifier or a support vector machine. This way it would be possible to build-up a knowledge base for the development of a fetal phonocardiographic expert system, which could serve the increased safety of the fetus during the pregnancy and the birth.

DOI:10.15774/PPKE.ITK.2012.001

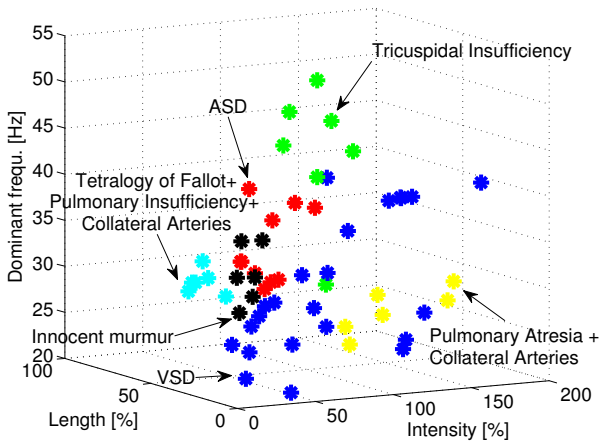

Figure 4.31: The distribution of three murmur parameters (length, intensity, dominant frequency). Each data point represents a murmur extracted from fPCG recordings of fetuses with different CHDs. The different colors represent the related CHD to the murmur. Black dots denote innocent murmur. Although there is some overlap, different domains that correspond to different CHDs can be defined.

DOI:10.15774/PPKE.ITK.2012.001

DOI:10.15774/PPKE.ITK.2012.001

Chapter 5

Phonocardiography for Preterm Infants with Patent Ductus Arteriosus

A persistent patent ductus arteriosus (PDA) may have serious complications, such as pulmonary hypertension, heart failure, an infection of the heart (endocarditis) or irregular heartbeat (arrhythmia) [76]. The prevalence of PDA is especially high in the case of low-birth-weight premature neonates, however the rate of spontaneous closure during the first two years is also high in the case of these patients. Furthermore, the role of PDA in causing associated morbidities in the case of preterms is still in question [195]. Due to these factors the major question a pediatrician faces when a patent ductus arteriosus is diagnosed is whether the infant needs treatment and if yes, then which treatment should be administered. The diagnosis is usually based on an echocardiographic examination which is a snapshot of the infant's current cardiovascular status, but there are no tools for continuous monitoring of any parameter of the PDA which could help in decision making and better understanding of the closure process.

Phonocardiography might open new possibilities for assessing and monitoring the PDA. There are two main features which are in relation with the PDA and can be investigated: heart murmur and the splitting of the S2 heart sound. Some related biological and theoretical background is presented in the following section.

DOI:10.15774/PPKE.ITK.2012.001

5.1 Biophysical background

5.1.1 Short theoretical summary on the generation of murmurs

In order to deeper understand the relation of certain parameters of the murmur and important clinical parameters in the following short excursion some of the physical laws governing the generation of vibrations by a fluid flows are presented.

Normally the blood flow in the blood vessels remains laminar, meaning that the blood flows in parallel layers, with no disruption between the layers. The flow rate in such a scenario was described by Jean Louis Marie Poiseuille in the 19^{th} century and is defined through the Hagen-Poiseuille equation [196]:

$$Q = \frac{\Delta P \pi r^4}{8 \mu L}, \tag{5.1}$$

where Q is the volumetric flow rate of a Newtonian fluid with dynamic viscosity μ, ΔP is the pressure drop over the distance L in a cylindrical tube of diameter r. This means that to maintain a particular flow rate on a narrowed (i.e. stenosed) segment, where r is decreased, the pressure drop will increase. As the pressure gradient increases, the flow velocity will also increase because blood is an incompressible fluid. However, at some point the rate of flow will not increase further with increasing pressure and the blood flow becomes turbulent, meaning that the flow becomes irregular. When laminar flow transitions to turbulent flow depends on the Reynolds number defined as

$$Re = \frac{\rho u L}{\mu}, \tag{5.2}$$

where ρ is the density of the fluid, u is the fluid velocity, L is the characteristic length (i.e. the diameter of the vessel) and μ is the dynamic viscosity. The geometry of the vessel also affects the transition to turbulence.

Figure 5.1 shows a schematic illustration of a vessel segment with stenosis, where D denotes the vessel diameter and d the diameter of the stenosis. At low rates corresponding to a very low Reynolds number the flow will be completely laminar and the blood will follow the boundaries of the obstruction. At flow velocities corresponding to $Re \approx 20$ a jet will be formed at the orifice of the stenosis due to separation of the layers and introducing eddies just behind the stenosis, as shown in the figure. As the flow, and equivalently the Re increases even more, the generated vortices start to detach and the post stenotic flow becomes more and more irregular and chaotic, that is turbulent [197].

Turbulent blood flow causes pressure fluctuations which causes vibration of the post

DOI:10.15774/PPKE.ITK.2012.001

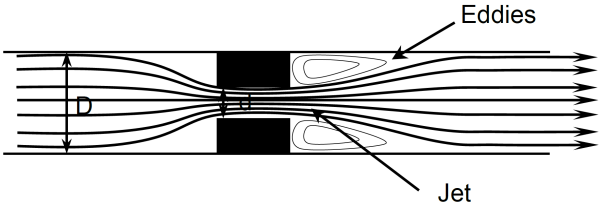

Figure 5.1: Schematic illustration of the flow through a stenosed segment. Taken from Schmidt *et al.* [196].

stenotic vessel wall. Some of these vibrations can be sensed as murmur, although the frequency dependant damping of the surrounding tissues has to be taken into account [198] and the post stenotic segment can behave as a resonant chamber introducing frequency peaks in the spectrum of the recorded murmur [199, 200].

Nonetheless, the genesis of murmurs is still not completely understood. The mathematical theory behind this question is described by the laws of fluid dynamics, namely by the Navier-Stokes equations [197]. Although these equations were written down in the 19^{th} century, the understanding of the mathematics behind them is still minimal. For instance, it is still not proven that in three dimensions solutions always exist, or if they exist, then they do not contain any singularity. It was also recognized as one of seven most important mathematical problems by the Clay Mathematics Institute in 2000, known as Millennium Prize Problems [201].

Turbulence is a time dependent chaotic behaviour of fluid flow, and it is believed that the Navier–Stokes equations describe turbulence properly. Numerical simulation of the Navier-Stokes equations for turbulent flow is extremely difficult, since for a stable solution a very fine mesh is required which makes the computations often infeasible. These attempts are referred as *direct numerical simulations* (DNS), and with the growth of solutions on kilocore processor architectures these approaches might produce simulations of increased accuracy. In the case of computational fluid dynamics (CFD) simulations of lower computational need time-averaging of the equations is applied based on statistical assumptions and a turbulence model (e.g. k-ϵ) is used to close the equations. The large eddy simulation (LES) is another, computationally demanding but more accurate approach. Further details can be found in the rich literature of CFD, e.g. [202].

Several works have been published in the recent decades on experimentally validated, model based calculations [199, 203, 204] and blood flow simulations [122, 205, 206]. Unfortunately nearly all of them deal only with investigating the effect of a stenosed artery on the blood flow, which is probably the simplest turbulence producing scenario in the circulatory system. Even in this situation not all questions are answered (for example the effect of surrounding human tissues). Another important topic of blood flow simulations

DOI:10.15774/PPKE.ITK.2012.001

are studies on the effect of a prosthetic heart valve [207–209], but also here the geometries are different than in the case of the ductus arteriosus. These aspects also underline the difficulty of investigating a more complicated situation of turbulent blood flow, such as in the case of the ductus arteriosus where scientists have to deal with interconnected vessels with flows coming from different directions.

Some results of these studies can be adapted. For example several of them suggest a wide band spectrum of the acoustic energy radiated by the turbulence [199, 200, 204]. In particular, Yazicioglu *et al.* [203] defined, based on the work of Tobin and Chang [210], an explicit formula for calculating the power spectral density of the wall pressure fluctuations of a steady flow of water in a straight, compliant, cylindrical tube with a constricted region of various diameters:

$$\begin{aligned} \mathrm{PSD}(f) &= \rho^2 D u^3 \left(\frac{d}{D}\right)^2 F_{n2}\left(\frac{fD}{u}\right), \\ F_{n2}\left(\frac{fD}{u}\right) &= \frac{0.00208}{1+20\cdot(fD/u)^{5.3}}. \end{aligned} \tag{5.3}$$

The wideband spectrum estimated by using the Eq.(5.3) is depicted in Fig. 5.2. The independent variables have been set to match parameters typical for a preterm with PDA. Note the relatively high power of frequencies below approximately 200 Hz, where the power rolls of. This point is regarded as the break frequency and studies have shown that is related to the rate of vortex shedding [211].

The measured spectrum of the murmur of PDA is also of a wideband nature, as observable in Fig. 5.3, although the transfer function of the vessels and tissues is unknown.

Some of these works investigate also the propagation of the pressure fluctuations through the surrounding tissues [200, 203, 204, 212, 213]. For instance the study by Wang et al. [199] describes the wideband wall pressure fluctuations as an input signal for the stenotic or poststenotic vessel segment, which is regarded as a resonator in the case of coronary artery stenosis. They also suggested a lumped model for the segments and found good agreement between theoretic and measured data. As already mentioned, in the case of the PDA the vessel structure is much more complex compared to a single vessel and a stenosis, consequently such a simple model is surely not valid. However, the estimation of an appropriate model is beyond the scope of this work.

Studying the noise generated by a turbulent blood flow for diagnostic purposes, as already mentioned, is also referred as phonoangiography [91, 214], and has been regarded as a possible tool for noninvasive diagnostic examination of coronary artery disease (CAD). As already described above, the extraction of parameters from the acoustic signal which

DOI:10.15774/PPKE.ITK.2012.001

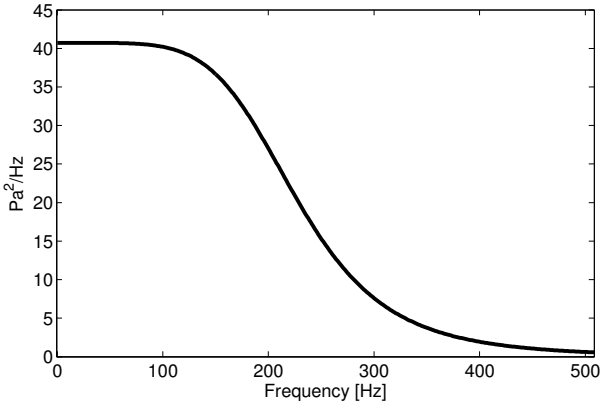

Figure 5.2: Theoretical wideband spectrum of the wall pressure fluctuations generated by stenosis with a diameter of 3.3 mm in a tube with a diameter of 5 mm. The flow velocity in the constriction zone was set to 2 m/s. These parameters correspond to a $Re = 1749$ in the constriction zone in the case of blood ($\rho = 1060\,\mathrm{kg/m^3}$, $\mu = 4 \cdot 10^{-3}\,\mathrm{Pa{\cdot}s}$). Based on the work of Yazicioglu *et al.* [203].

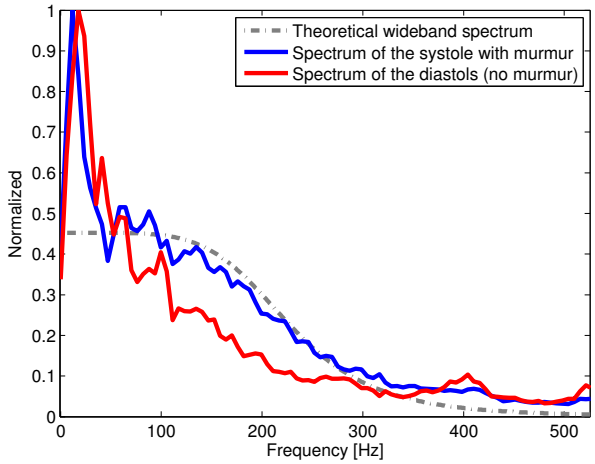

Figure 5.3: Average spectrum of the systolic (blue) and diastolic (red) segments of a preterm infant with PDA. The diameter of the PDA was estimated to be 3.3 mm, and the maximal blood flow was measured to be 2 m/s. The gray dotted line is the scaled theoretical wideband spectrum of Fig. 5.2.

DOI:10.15774/PPKE.ITK.2012.001

can be related to important medical parameters is extremely difficult, although promising results have been achieved [215], also for aortic valve stenosis [34] and for urinary bladder outlet obstruction [216]. However, it should be noted that until a deep understanding of turbulent flows, acoustic sound generation and propagation through human body tissues is not achieved, the correlation of sound parameters and important medical parameters is of rather phenomenological nature, which is also one weakness of this work...

5.1.2 Splitting of the S2 heart sound in the case of PDA

The splitting of the S2 sound in the case of preterms was first observed during the visual examination of the recordings (Fig. 5.4) but there are biological factors which support this concept: normally the two main arteries are not connected directly. In contrast, when the ductus arteriosus is patent, there is a direct linkage between them not very far away from the aorto-pulmonary valves (Fig. 5.5). This will obviously affect the closure of these valves and hence the splitting of the second heart sound [217]. If the overload on the left ventricle is large then even a reversed split can develop, meaning that the pulmonary component precedes the aortic component. Based on the observations and this reasoning it seemed a promising idea to investigate this feature in a more rigorous manner.

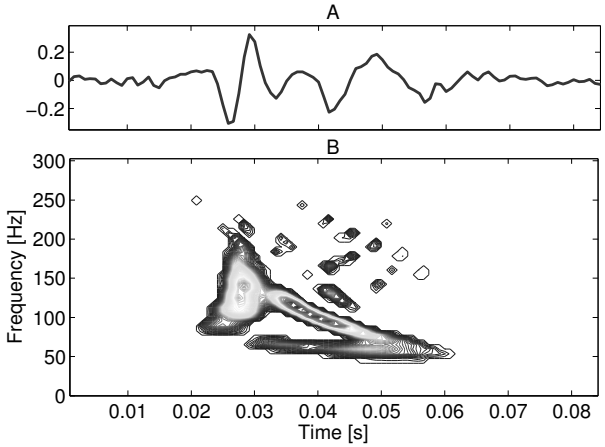

Figure 5.4: A split S2 sound of preterm treated pharmacologically in the time (A) and in the time-frequency (B) domain. The time-frequency representation was calculated using the Wigner-Ville distribution. Note that the nonlinearly decreasing frequency components.

5.2 Measurements

In this study 25 preterm newborns have been examined (Table 5.1), with an average of 3 measurements per infant, but with large deviations: only those newborns were examined

DOI:10.15774/PPKE.ITK.2012.001

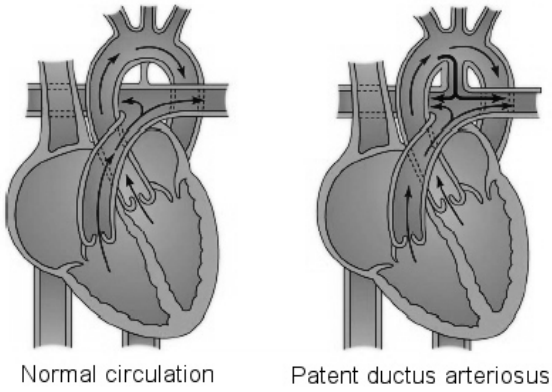

Figure 5.5: The direct connection between the main arteries via the ductus arteriosus. This has a direct effect on the aortic and pulmonary pressures which govern the closure of the aorto-pulmonary valves. Figure reprinted from [218].

several times which were diagnosed with PDA, those without PDA or with other cardiac malformation only once. Preterms without PDA were measured as a control group. Hemodynamically significant PDA was verified by echocardiography in the case of 15 infants but only 8 of those were examined over several days because the others had either also some other malformation or some other circumstances made further measurements not possible. The diagnostic parameters of the PDA acquired with echocardiography (diameter of the ductus, maximal velocity through the ductus, the left atrial to aortic root ratio) were all collected for later comparison with phonocardiographic parameters. In the case of the 8 newborns mentioned above, the PDA was closed by means of pharmacological treatment (4 infants) or surgical intervention (4 infants).

These infants, except one, all weighed less than 2300 g at birth, with an average weight of 1400 g. Except one, all of them were less than 33 weeks of gestation, with an average of 29. They were examined on average on their 6^{th} day after birth and those with PDA then every day until the closure of the PDA, which was verified by echocardiography (the maximum was 9 measurements on one infant). Three measurements had to be posteriorly excluded from the study because of the poor quality of the records due to the fact that the measuring equipment was also developed during the study.

Each measurement consisted of about three 30 seconds long phonocardiographic records which were recorded at 48 kHz, with a resolution of 16 bits. The components of the heart sounds lie in the low frequency range (<1000 Hz), thus after prefiltering the data was resampled at 3000 Hz and only the useful part of the record (at least 10 secs) was kept for further analysis.

DOI:10.15774/PPKE.ITK.2012.001

Table 5.1: Parameters of the examined preterm neonates

ID	Diagnosis*	Treatment	Number of Measure-ments	Weeks of Gesta-tions	Birth weight [g]
P1			2	28	990
P2			1	27	1050
P3			1	27	1000
P4			2	26,5	1100
P5	PDA, PS		1	35	2400
P6	PDA		1	26	500
P7	PDA	Surgical	2	32	1830
P8	PDA		1	33	1800
P9			1	33	1340
P10			1	34	1800
P11			2	31	2230
P12	PDA, TI	Pharmacological	5	31	1490
P13	PDA, TI, ASD		1	40	3380
P14			3	29	1240
P15			2	26	1500
P16			1	31	1290
P17	PDA	Pharmacological	4	27	985
P18	PDA	Pharmacological	7	28	1150
P19	PDA	Pharmacological	4	27	1200
P20	PDA	Surgical	9	27	600
P21	ASD		1	28	970
P22			2	27	1120
P23	PDA	Surgical	8	27	990
P24	PDA	Surgical	2	24	700
P25	PDA	Surgical	2	29	1530

*PDA - Patent ductus arteriosus, TI - Tricuspid insufficiency, ASD - Atrial septum defect

DOI:10.15774/PPKE.ITK.2012.001

5.2.1 Recording equipment

The measurements were made with a self-made electronic stethoscope: an electret microphone cartridge (MCE-4000, Panasonic), connected to a laptop, was joined together with a commercial stethoscope head for neonates, see Fig. 5.6. The applied microphone had a flat frequency response between $20 - 20\ 000$ Hz. Some further improvement could be achieved by designing a stethoscope head where the microphone is fitted inside the head piece (Fig. 5.7).

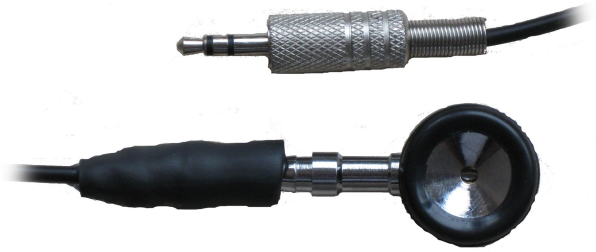

Figure 5.6: The self assembled electronic stethoscope for neonates with an electret microphone connected to the outlet of the stethoscope head.

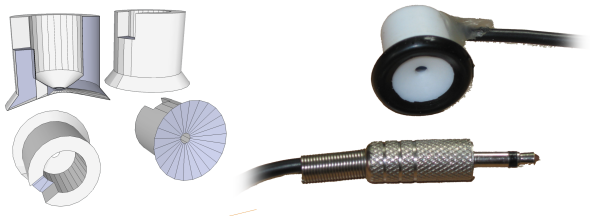

Figure 5.7: The design of the stethoscope head with space for the microphone to fit inside the head (left) and the manufactured stethoscope (right).

Figure 5.8 shows some comparison of the equipments. The frequency characteristics are very similar but the self-designed head produces an increased sensitivity which can be attributed to the fact that the microphone is fitted inside the head piece. Nonetheless, the quality of the recordings performed with the commercial head piece were usually also of appropriate quality. The self-designed head weighed only 10 g because it was manufactured of plastic compared to the metal commercial head with a weight of 40 g. The lighter weight has the advantage that it is less disturbing for the infants because the neonates are in a lying position.

It should be noted that the clinical environment introduces a lot of noise in the recordings, such as alarm sound of monitoring equipment, friction noise in the case of body movement, the crying and the babble of the newborn and the sound of the ventilator (Fig. 5.9).

DOI:10.15774/PPKE.ITK.2012.001

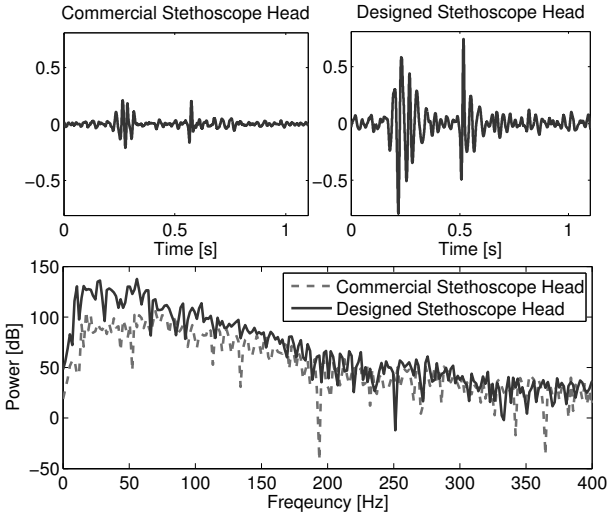

Figure 5.8: Two heart cycles recorded with the commercial stethoscope head (Fig. 5.6) and the designed stethoscope head (Fig. 5.7), and the corresponding power spectral densities. Note the increased sensitivity in the case of the self-designed head resulting from the microphone to be located inside the head piece in contrast to the commercial stethoscope head.

Many of the disturbances can be filtered out by simple bandpass filtering. The most serious problem is the noise coming from the breathing machine because this noise lies in the same frequency bands than the heart sounds. Furthermore it comes from inside of the chest similarly to the heart sounds, and because of that it cannot be filter out even with a specially designed stethoscope head. Unfortunately practically all of the preterms need breathing aid.

5.3 Methods

One of the main goals was to investigate certain parameters of the heart sounds and, if present, of murmurs which could be related to some attributes of the ductus arteriosus (for example diameter, velocity of blood flowing through it, etc.). Although there are differences between fetal and preterm PCG recordings, the high level of noise introduces similar problems. A 1-min preterm phonocardiographic record contains around 140 heart cycles, some of them disturbed by impulsive noise, thus it might be misleading to analyse the heart cycles separately. This is why the technique of improved ensemble averaging (section 4.4.2) was applied also in this scenario, assuming the following:

- preterm heart sounds exhibit cyclostationary properties,
- murmur caused by PDA will appear in most of the heart cycles with similar envelope,

DOI:10.15774/PPKE.ITK.2012.001

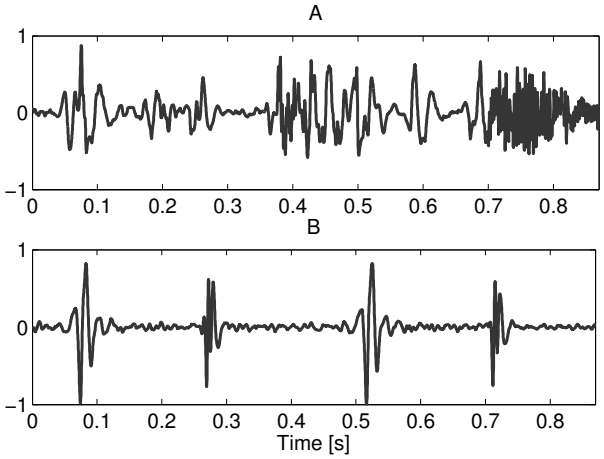

Figure 5.9: Segments of two recordings of a preterm neonate with breathing aid before (A) and after (B) the condense water was emptied form the breathing tube. Note that in the upper trace the heart sounds are barely identifiable, unfortunately valid for the complete recording.

- according to these measurements averaging will suppress the usually occurring noise (e.g. from breathing machines) since their periodicity does not correlate with the heart rate.

The basic steps of the method are outlined in Fig. 5.10.

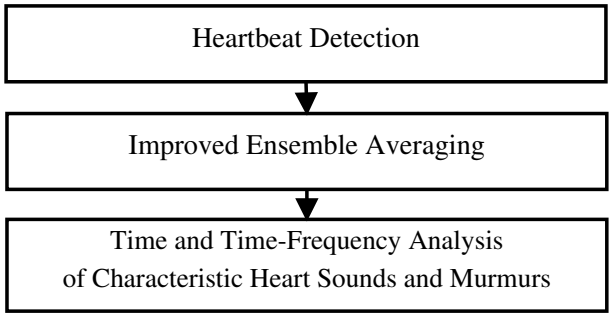

Figure 5.10: General scheme of the analysing method.

5.3.1 Heartbeat detection

In Section 4.2 a robust method was introduced for fetal heart rate estimation and the confidence factor (CF) for identifying reliable segments. These results can be also applied in the case of preterm PCG recordings because of the similarly low signal-to-noise ratio. However, for identifying the PDA related heart murmur not only the heart rate has to be

DOI:10.15774/PPKE.ITK.2012.001

determined but also the heart sounds have to be detected. For this reason and because of the much shorter length of the recordings compared to the fetal ones, the detection of the heart cycles and heartbeats was done with a heuristic decomposition method with a very good timing accuracy and robustness against noisy bursts, such as the one produced by the breathing machine [9]. The outline of this heartbeat detection algorithm is as follows:

For a given phonocardiographic signal $x[n]$ lets define a kind of contrast enhancement by summing up the signal on a short time window of length N_1 and taking the difference of neighbouring windows:

$$I_1[n] = \sum_{i=n}^{n+N_1} x[i] - \sum_{j=n-N_1}^{n} x[j]. \tag{5.4}$$

Preprocessing with high-pass filtering slightly improves the performance of the method, but this is not essential. Contrast enhancement is achieved by adding this local intensity difference $I_1[n]$ to the phonocardiographic signal $x[n]$, and a secondary local intensity difference is calculated based on this result, like in Eq.(5.4) but with a greater time window of length N_2:

$$I_2[n] = \sum_{i=n}^{n+N_2} (x[i] + I_1[i]) - \sum_{j=n-N_2}^{n} (x[j] + I_1[j]). \tag{5.5}$$

Finally, the differences of the signal $I_2[n]$ have to be computed in a similar way once more as in Eq.(5.4), with the slight extension that the whole expression has to be negated and the negative values set to zero:

$$V[n] = \begin{cases} -(\sum_{i=n}^{n+N_2} I_2[i] - \sum_{j=n-N_2}^{n} I_2[j]) & \text{if} > 0, \\ 0 & \text{otherwise} \end{cases}. \tag{5.6}$$

Based on the values N_1 and N_2, the local maxima of the signal $V[n]$ show the heart sounds or the cardiac cycles.

5.3.2 Improved ensemble averaging revisited

In this scenario, because the murmur of PDA is late systolic, cross-correlation of the S2 sound was most often applied to compare the different heart cycles. According to our measurements this was calculated with a 50 ms window for S2 heart sounds, and if needed – because the murmur overlapped the S2 sound – with a 100 ms long time window for S1 heart sounds (Fig. 5.11). A threshold for the normalized cross-correlation coefficient of 0.9 (in case of poorer quality data 0.8 or 0.85) was used for the selection of the most

DOI:10.15774/PPKE.ITK.2012.001

typical heartbeat for the given record: the heart sound was selected which had normalized correlation coefficients greater than the mentioned threshold with the greatest number of other heart sounds. From these heart sounds a characteristic heart sound was calculated using Eq.(4.17) of improved ensemble averaging. The thresholds have been determined empirically based on the records.

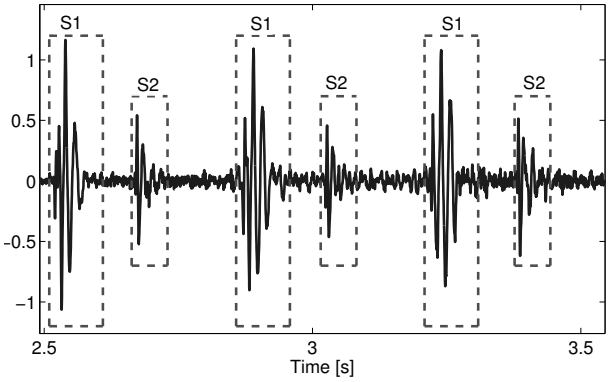

Figure 5.11: Time windows used for extracting heart sounds for cross-correlation.

The analysis of the characteristic heartbeats for a given record was done in the time and in the time-frequency domain due to the nonstationary nature of heart sounds. The Short time Fourier transform with a 27 ms long Hamming window was used to compute the time-frequency representation. Window shifting was 1 ms.

For the investigation in the time domain linear filtering was applied with different bandwidths. To avoid the phase distortion of IIR filters zero phase filtering was used: after filtering the data in the forward direction, the data was reversed and run back through the filter [219].

The analysis focused on looking for components which could be related to some attributes of the PDA. This means that the length, the envelope and the frequency components of the heartbeats, and the splitting of the S2 heart sounds, and the presence of murmurs and their frequency relationship were investigated.

5.3.3 Detection of murmur related to PDA

The characteristic heart sound calculation revealed that even in case of short and noisy (breathing machine) records, the improved ensemble averaging achieves the a extraction of heart sound waveforms. As an example average S1 and S2 sounds are shown in Fig. 5.12.

By observing not only the selected heart sound but also the complete heart cycle murmurs can be identified (Fig. 5.13). Because murmurs lie usually in higher frequency

DOI:10.15774/PPKE.ITK.2012.001

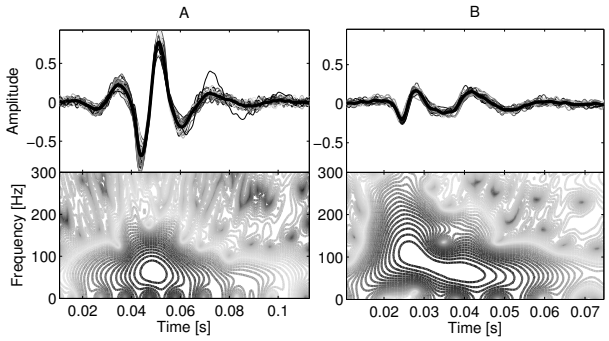

Figure 5.12: (A) Characteristic S1 sound and (B) characteristic S2 sound of a preterm after the closure of PDA. The average S1 sound (thick line) was calculated from 43 consecutive S1 sounds (thin lines). In case of the average S2 sound 25 sounds were used. The records were bandpass filtered (bandwidth from 30 to 400 Hz).

bands than the main components of the heart sounds we applied high-pass filtering.

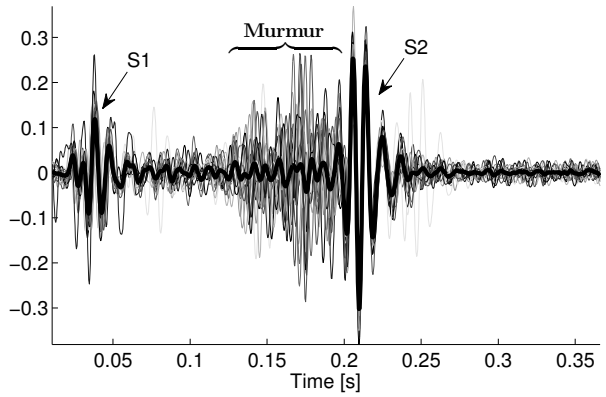

Figure 5.13: Characteristic S2 sound of a preterm with PDA. The murmur can be identified by plotting on each other the complete heart cycles (in this case 17 heart cycles). The records were bandpass filtered (bandwidth from 75 to 250 Hz).

Heart murmur of preterms displays chaotic behaviour, cyclostationary components are usually not present. This is a major difference compared to fetal murmurs which affects also the detection of murmurs.

We used the average maximal late systolic envelope value (LSEV_{max}) as a simple parameter for the assessment of murmur:

$$\mathrm{LSEV}_{max} = \sum_{i=1}^{K} \max\{l_i[n]\} \; / \; K, \tag{5.7}$$

DOI:10.15774/PPKE.ITK.2012.001

$$l_i[n] = \begin{cases} |x[n] + j\hat{x}[n]| & \text{if } P_{S2}[i] - \frac{sys}{3} \leq n \leq P_{S2}[i] - \frac{sys}{10} \\ 0 & \text{otherwise} \end{cases},$$

where $x[n]$ is the heart sound signal, $\hat{x}[n]$ is the Hilbert transform of $x[n]$ (Section 3.2.4), K is the number of S2 heart sounds and $l_i[n]$ is the windowed late systolic envelope function for the heart cycle i, which is defined according to the position of the i^{th} S2 heart sound, $P_{S2}[i]$, and the average length of the systoles in the recording, sys.

Due to the continuous noise coming from the breathing machine the envelope had a positive baseline shift (Fig. 5.14-A). This was corrected by estimating the baseline for each heart cycle based on the histogram of the envelope values (Fig. 5.14-B). Those envelope values were set to zero which were smaller than a scalar times the baseline value. In the case of records with murmur the average envelope had still non-zero values in the systolic segment after the baseline correction (Fig. 5.14-C). In this way the murmur was detected using adaptive thresholding of the systolic segment. It is based also on the observation that PDA related murmur in the case of preterms was found to be always late systolic, meaning that the end of the murmur was regarded as the beginning of the S2 sound. The beginning of the murmur was regarded as the beginning of the interval with non-zero corrected envelope starting after the S1 sound. Simple rules, such as looking for intermediate segments with zero envelope value or using the morphological closing operation help in avoiding noise bursts to be regarded as murmur (Fig. 5.14-D).

.

5.3.4 Parameter extraction of the murmur

As mentioned in Section 5.1.1, certain parameters of the acoustic vibrations caused by a turbulent fluid can be related to the underlying geometry or fluid dynamics in some cases [34, 91, 215, 216]. Because in the case of the patent ductus arteriosus the vessel geometry is more difficult compared to a single stenosed vessel, we applied a sort of "top-down" or data-based approach and investigated parameters of the recorded murmur for finding any relationship with the underlying cardiac disease.

Using the time window for extracting the murmur mentioned in the previous section the murmur was analysed in all heart cycles from which the characteristic heart sound was calculated. During the analysis the following parameters were extracted:

1. *Length of the murmur*: length relatively to the length of the heart cycle
2. *Average maximal murmur amplitude*: this is equal to the LSEV_{max} parameter
3. *Average maximal S2 amplitude*: the average over the record

DOI:10.15774/PPKE.ITK.2012.001

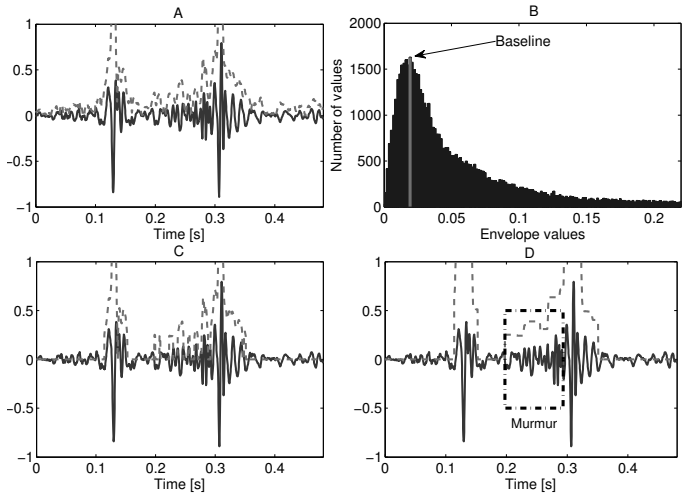

Figure 5.14: Steps of murmur detection using adaptive thresholding of the envelope of the systolic segment. (A) One heart cycle with late systolic murmur related to PDA and the envelope (dashed line). (B) The histogram of the envelope values where the maximum corresponds to the baseline. (C) The thresholded envelope of this heart cycle where the threshold is calculated based on the baseline. (D) Closing of intermediate segments with zero envelope values and the detection of the murmur.

4. *Average ratio of the maximal murmur to the maximal S2 amplitude*: the average over the record
5. *Average instantaneous frequency of the murmur*
6. *Maximal instantaneous frequency of the murmur*
7. *Minimal instantaneous frequency of the murmur*
8. *Frequency limits of the murmur*: maximal and minimal frequencies of the thresholded spectrogram

The amplitude parameters were investigated because according to Eq.(5.3) for a certain frequency range the amplitude of the power spectral density of the murmur is related to the third power of the flow velocity in the constriction and to the second power of the degree of the constriction.

The spectrum was analysed because several frequency parameters showed good correlation with important medical parameters in aforementioned studies, for example [199, 216]. The instantaneous frequency for a given time instance was estimated by calculating the first moment of the Fourier transform in a 20 ms time window as follows:

$$IF[n] = \sum_{f=F_1}^{F_2} (S[f])^2 \cdot f \;\; / \;\; \sum_{f=F_1}^{F_2} (S[f])^2, \tag{5.8}$$

DOI:10.15774/PPKE.ITK.2012.001

where $IF[n]$ is the instantaneous frequency at the time instance n, $S[f]$ is the Fourier transform of the 20 ms long heart sound signal segment at the frequency f, and F_1 and F_2 are the limits of the investigated frequency interval. In [216] this is called weighted average frequency and was found to be related to the degree of the obstruction in the case of urinary bladder obstruction.

Frequency limits are estimated by finding the maximal and minimal frequencies of the thresholded spectrogram, in this study a threshold of -50 dB was employed. This parameter is related to the break frequency (Section 5.1.1) and to the standard deviation of the instantaneous frequency [216].

5.3.5 Heuristic method for estimating the S2 splitting

Although several methods have been introduced for the estimation of splitting interval (SI) this problem is not solved for very short ones and for noisy signals like in case of recordings from preterm infants in clinical environment [28, 97, 169]. The solution for fetal heart sounds which is based on Monte Carlo simulation (Section 4.3.1) presumes a valid heart sound model which was unknown for preterm infants. Even though it was possible to adapt a previously suggested heart sound model [28], it contains significantly more parameters than the model valid for fetuses which introduces many more local minima on the error surface and increased computing time. This makes the selection of the real parameters in most cases infeasible. Thus we had to suggest other ways of SI estimation. One of them is the application of the heuristic method described in section 5.3.1. The estimation of the split was achieved by using this heuristic method on S2 signals and by decreasing the length of the time windows N_1 and N_2. In this manner a heuristic decomposition of the heart sounds is performed into an estimate of the aortic and pulmonary components.

Because the estimated SI cannot be verified in case of most of the records, a model-based validation was performed. In some of the measurements the splitting of the S2 sound could be assessed by visual inspection and the two components of the S2 sound could be separated in the time-frequency domain (Fig. 5.15). These records were selected and the method similar to a study of Xu *et al.* [28] was applied for obtaining a S2 sound model valid for preterm neonates. This involved the following steps:

1. Estimation of the instantaneous frequency function of the aortic component (A_2) of the S2 sound.
2. Estimation of the instantaneous amplitude function of the aortic component of the S2 sound.
3. Subtraction of the synthesized aortic component from the original S2 sound. The synthesized aortic sound is computed form the above two estimates.

DOI:10.15774/PPKE.ITK.2012.001

4. Estimation of the instantaneous frequency function of the pulmonary component (P_2) of the S2 sound.
5. Estimation of the instantaneous amplitude function of the pulmonary component of the S2 sound.

All estimation of the time-frequency characteristics was performed based on the Wigner-Ville distribution of the selected S2 signals.

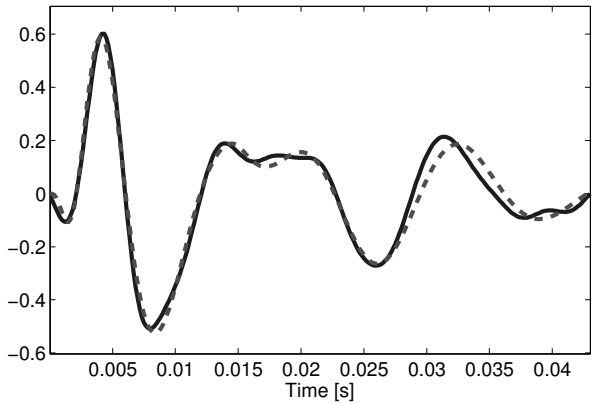

Figure 5.15: Original S2 sound (solid line) of a preterm and the synthesized S2 sound based on a model described in this work (dashed line). Normalized root means square error is 16 %.

The analysis revealed that a slightly different model should be used than in the study of Xu *et al.* (Section 4.3.1), which might be explained by the smaller size of the preterm heart, great vessels and thorax. We made two modifications to the aforementioned model. First of all, the instantaneous frequency ($f[n]$) was found to be an exponentially decreasing function for both the aortic and the pulmonary component. The second modification was the k_1 and k_2 exponents in the instantaneous amplitude functions ($A[n]$) of both of the components:

$$f[n] = F_1 \cdot \exp\left(-\frac{n}{\tau_1 \cdot \mathrm{f}_s}\right) + F_2, \tag{5.9}$$

$$A[n] = a \cdot \left(1 - \exp\left(-\frac{n^{k_1}}{\tau_2 \cdot \mathrm{f}_s}\right)\right) \cdot \sin\left(\frac{\pi n}{\tau_3 \cdot \mathrm{f}_s}\right) \cdot \exp\left(-\frac{n^{k_2}}{\tau_4 \cdot \mathrm{f}_s}\right), \tag{5.10}$$

where F_1, F_2 are frequencies, τ_1, τ_2, τ_3, τ_4, a, k_1 and k_2 are free parameters and f_s is the sampling frequency.

The final parametric signal model is:

$$S_2[n] = A_A[n] \cdot \sin(\varphi_A[n]) + A_P[n - n_s] \cdot, \sin(\varphi_P[n - n_s]), \tag{5.11}$$

DOI:10.15774/PPKE.ITK.2012.001

where $A_A[n]$, $\varphi_A[n]$ and $A_P[n]$, $\varphi_P[n]$ are the instantaneous envelope and the phase functions of the aortic and the pulmonary component of the second heart sound, respectively. The SI is defined by n_s.

The calculation of the phase functions, i.e. $\varphi(t) = 2\pi \int f(\tau) d\tau$, was achieved by using trapezoidal numerical integration:

$$\varphi_A[n] = \frac{2\pi}{\mathrm{f}_s} \cdot \left(\frac{1}{2} f_A[1] + \sum_{i=2}^{n-1} f_A[i] + \frac{1}{2} f_A[n] \right), \tag{5.12}$$

$$\varphi_P[n] = \frac{2\pi}{\mathrm{f}_s} \cdot \left(\frac{1}{2} f_P[1] + \sum_{i=2}^{n-1} f_P[i] + \frac{1}{2} f_P[n] \right), \tag{5.13}$$

where $f_A[i]$ and $f_P[i]$ are the instantaneous frequency functions of the aortic and the pulmonary components, respectively, and f_s is the sampling frequency.

Using this model original S2 sounds could be approximated even with 16 % normalized root mean square error, see Fig. 5.15.

Motivated by the fact that at the start of the A_2 and the P_2 components their frequency is the greatest we investigated also the high-pass filtered version of the original signal. Since the initial instantaneous frequency of the components is unknown, and its value can vary greatly, filtering was performed with low order FIR filters (Fig. 5.16).

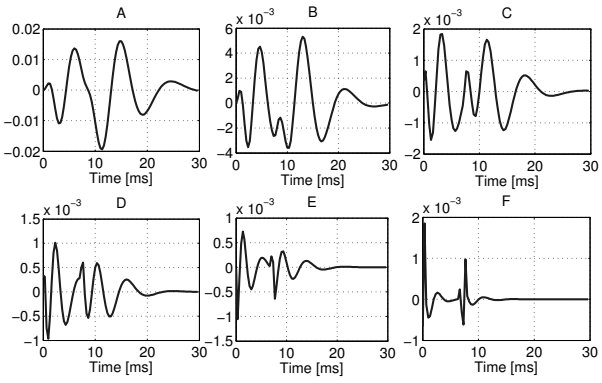

Figure 5.16: (A) A synthesized S2 sound and (B-F) its high-passed filtered versions, filtered with FIR filters of order one to five. The cutoff frequencies were 345, 414, 455, 476 and 488 Hz, respectively. High-pass filtering emphasizes the beginning of the aortic and pulmonary components.

Although with high-pass filtering the model data, the beginning of the components can be emphasized, the assessment of these beginnings could also be achieved with the presented heuristic decomposition applied even to the unfiltered S2 sound (Fig. 5.17). This is important because by high-pass filtering real, clinical data, the usually high frequency noise is also accentuated.

DOI:10.15774/PPKE.ITK.2012.001

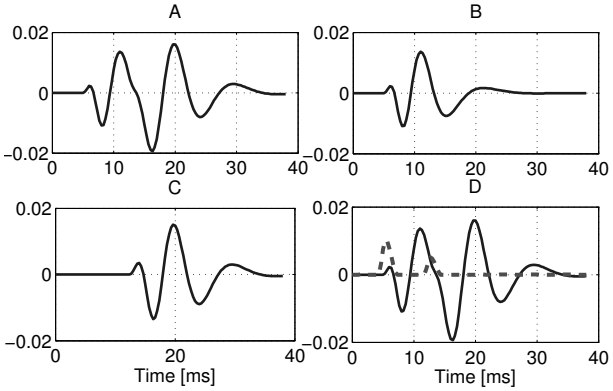

Figure 5.17: (A) A synthesized S2 sound with an SI of 7 ms, (B) the aortic and (C) pulmonary components and (D) $V[n]$ (dashed). $V[n]$ was calculated by applying the heuristic method to synthesized S2 signal. The local maxima of $V[n]$ correlate well with the beginnings of the components.

5.4 Results

5.4.1 Heart sound detection

Using the method introduced in Section 5.3.1 the detection of the heart sounds was achieved reliably even in the presence of clinical noise and murmur (Fig. 5.18). Due to the short length of the recordings this could be manually verified in the many cases. Furthermore, the improved ensemble averaging method (Section 5.3.2) was another filtering step, because it selected only those heart cycles which where characteristic for the recording.

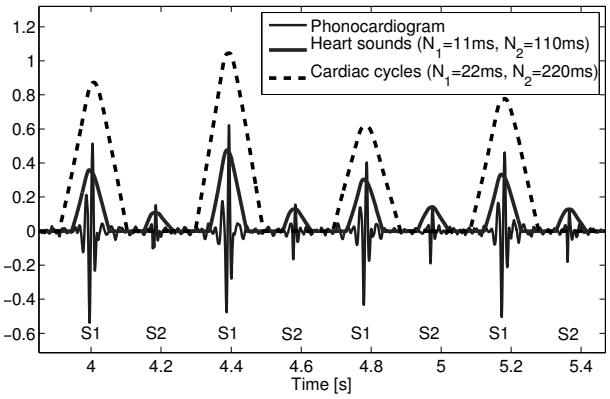

Figure 5.18: Results of the heuristic heartbeat detection method with different resolutions.

Classification of S1 and S2 sounds was based on the observation that S2 heart sounds have higher frequency components than S1 heart sounds, the systole is usually shorter than

DOI:10.15774/PPKE.ITK.2012.001

the diastole and that these heart sounds alternate. Because the S1 and S2 heart sounds differ also in their waveform, the application of improved ensemble averaging guaranteed also that indeed only one type of heart sound was analysed.

5.4.2 Detected murmur related to PDA

The presence of murmur could be justified even by investigating its amplitude: the LSEV_{max} to average maximal S2 envelope value ratio was significantly greater in the case of preterm infants with PDA ($p < 0.05$).

Further investigations have been carried out regarding the length of time window containing the detected murmur. Figure 5.19 shows a detected murmur related to PDA with the time window of the detection. Using a threshold of 7 % of the length of the systole for classification based on the length of the detection window, 90 % sensitivity and 60 % specificity could be achieved. Although the specificity is quite low, these are promising results, since the major goal is not a diagnosing but a monitoring application. In that case obviously the sensitivity is more important because in order to extract parameters of the murmur first it has to be identified. The low specificity means that a low intensity late systolic component can be detected in the case of many preterms without PDA as well. Due to adaptive thresholding all late systolic components with significantly greater amplitude than the baseline will be included in the detection window. Nonetheless, a high intensity late systolic component is specific for preterms with PDA as has been shown earlier based on the LSEV_{max} parameter. Thus the specificity might be increased by including a fix threshold into the adaptive thresholding procedure ensuring that very low intensity components, which are still significantly greater than the baseline, are rejected from the detection window. This, however, would certainly decrease the sensitivity, which would not be beneficial in the case of a monitoring application.

The low specificity also means that some other CHDs produce systolic murmur as well. Preterm neonates with other malformations producing systolic murmur could be classified based on other modalities. However, neonates with PDA and another cardiac disease producing systolic murmur at the same time could be a major problem. These cases obviously need not only a more complex treatment but also a more complex monitoring approach. Fortunately this is not very frequent (Table 5.1).

5.4.3 Relation of murmur parameters and parameters of the PDA

All the measured parameters, enumerated in Section 5.3.4, were correlated with the medical parameters of the PDA, that is with the diameter of the PDA ($\mathrm{D_{PDA}}$), the maximal blood velocity through the PDA ($\mathrm{v_{max}}$) and the left atrial to aortic root ratio (LA/Ao). A regression curve was fitted to each of the investigated data point sets.

DOI:10.15774/PPKE.ITK.2012.001

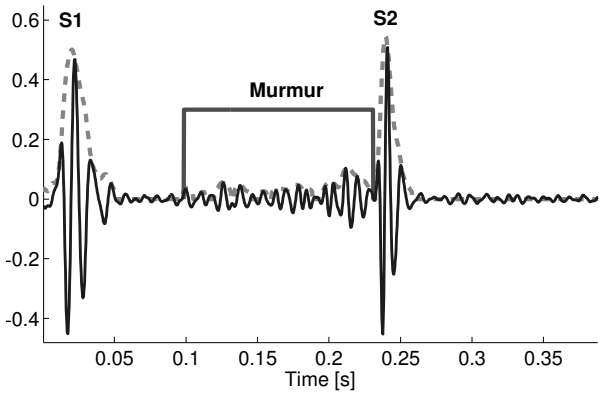

Figure 5.19: Detected heart murmur related to PDA of a preterm infant. Detection was accomplished based on nonzero envelope (dashed line) values after baseline correction

Based on the NRMSE of the fitted regression curves the average mean, maximal and minimal instantaneous frequency parameters correlate the most with the medical parameters. These relationships are shown in Fig. 5.20.

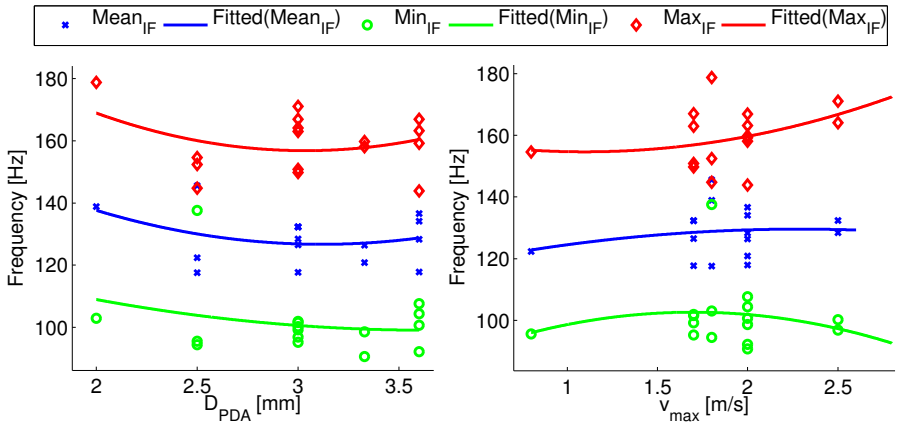

Figure 5.20: Extracted murmur parameters vs. medical parameters of the PDA: diameter of the PDA (top) and maximal blood flow velocity through the PDA (bottom). The frequency parameters are calculated from the instantaneous frequency of the murmur. The fitted regression curves are quadratic functions. As observable the frequency parameters of the murmur decrease substantially with D_{PDA} and increase with v_{max}.

Although these results are promising it should be noted that much improvement is still necessary since the fitted regression curves have a NRMSE > 20 %. Unfortunately the medical parameters assessed with echocardiography were not measured simultaneously with the PCG examination. This may account for one part of the error, because the parameters of the PDA change rather dynamically. In further studies this should be also

DOI:10.15774/PPKE.ITK.2012.001

taken into account. A further possibility is to develop a PDA model and apply CFD simulations for a better understanding of the blood dynamics.

5.4.4 Analysis of the S2 split of preterms with PDA

The application the heuristic method described in Section 5.3.5 showed promising results. Based on the derived model (Eqs.(5.9)-(5.11)) 1000 simulated S2 sounds were generated with random parameter values in the range of real S2 sound parameters. Average error was 4.46 ms, with a standard deviation of 3.82 for unfiltered S2 signals. With high-pass filtering the average error could decreased to 3.06 ms, standard deviation was 3.01. The error was significantly higher for small SI values, and the method showed to be reliable for SI values greater than 7 ms.

The heuristic decomposition method was applied to phonocardiographic records of preterm newborns with PDA to estimate the S2 splitting. Due to the inherent noise in real, clinical data, high-pass filtering not always improved the recognizability of the splitting. Even though promising results were achieved (Fig. 5.21).

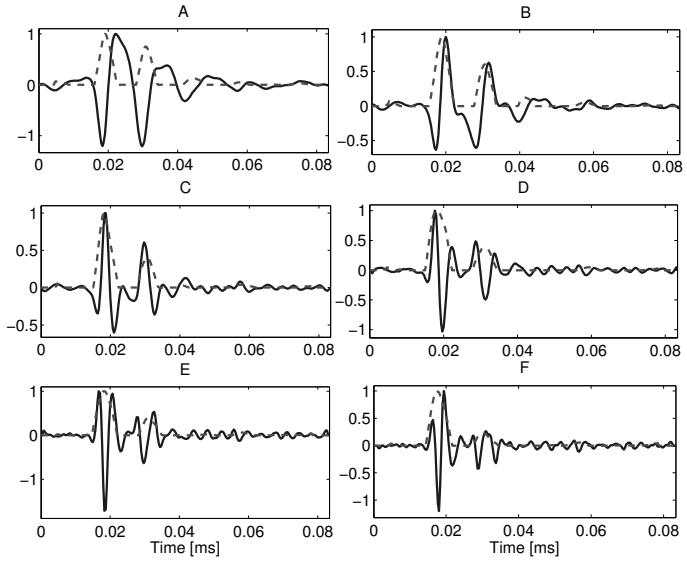

Figure 5.21: (A) The S2 sound of a preterm infant recorded after the closure of the PDA (solid line) and the result of the heuristic method, $V[n]$ (dashed line). The estimated SI is the time difference between the local maxima of $V[n]$. (B-F) The high-passed filtered versions of the signal (solid lines), filtered with FIR filters of order one to five, and the the calculated $V[n]$ signals (dashed lines), respectively.

An SI estimate for a given S2 sound was assumed to be the time difference between the two greatest local maxima of $V[n]$ in a 33 ms long time window fitted to the S2 sound. Only those maxima were taken into consideration which were greater than a given

DOI:10.15774/PPKE.ITK.2012.001

threshold (in this study 10 % of the maximum of $V[n]$ in the recording was used). If only one maximum was found in the time window, then the split was regarded as zero. $V[n]$ was calculated with $N_1 = 1$ ms and $N_2 = 5$ ms.

For a given record the SI estimates were computed for each S2 sound belonging to the set from which the characteristic heart sound was calculated. From these values the mean value ($m(n_s)$) and the standard deviation ($std(n_s)$) was calculated. Those values were rejected, which were outside the interval of $[m(n_s) - std(n_s), m(n_s) + std(n_s)]$. The mean, the standard deviation and the median was computed from the remaining values. The median value was regarded as an estimated SI value for a given record. The standard deviation was used as a simple measure of the reliability of the estimated SI for the given record.

In Fig. 5.23 the estimated splitting times of the infants can be observed who were treated pharmacologically. In the case of those neonates who needed surgical intervention the splitting time estimation proved not to be reliable enough because the amplitude of their S2 sounds decreased greatly after the ligature (Fig. 5.22). Surgical intervention is needed in the case of those preterms whose ductus arteriosus is too wide, and the shunt through it too great for a possibly successful pharmacological closure. It follows that the operation causes a significant change in the hemodynamical system: the blood load on the left ventricle will be significantly decreased, which affects the pressure ratios between the two sides of the valves. This directly influences the amplitude of the closure sounds.

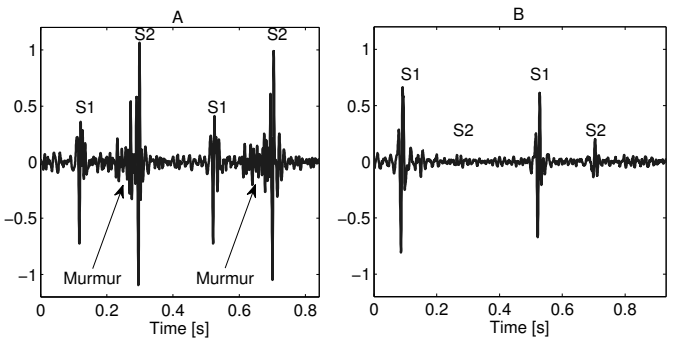

Figure 5.22: Two cardiac cycles of a preterm with PDA before the surgical intervention (A) and after the surgical intervention (B). As observable, the murmur disappeared since it was related to the turbulent blood flow through the PDA, and the amplitude of the S2 sound decreased in a great manner making the SI estimation not reliable.

In the case of the pharmacologically treated infants, the median of the estimated SI values always increased around the time of the closure of the ductus arteriosus, except in one case. In that case it was unfortunately not possible to make measurements earlier than one day before the closure and four days after the closure. Consequently earlier

DOI:10.15774/PPKE.ITK.2012.001

changes and possible changes one or two days after the closure could not be assessed. The estimated SI increased in average with 11 ms in case of the other three preterms, which is an average change of 85 %. This was computed by calculating the average relative difference between the first estimated SI value after the closure and the local minimum estimated SI before the closure (one or at most two days before the closure). Regarding all measurements this means an average increase of 30 %. In the case of one infant the estimated SI increased already one day before the clinically verified closure. This might be explained with the dynamical nature of the closing process. The estimated SI decreased after the closure in three cases, in average after 3.7 days (Fig. 5.23).

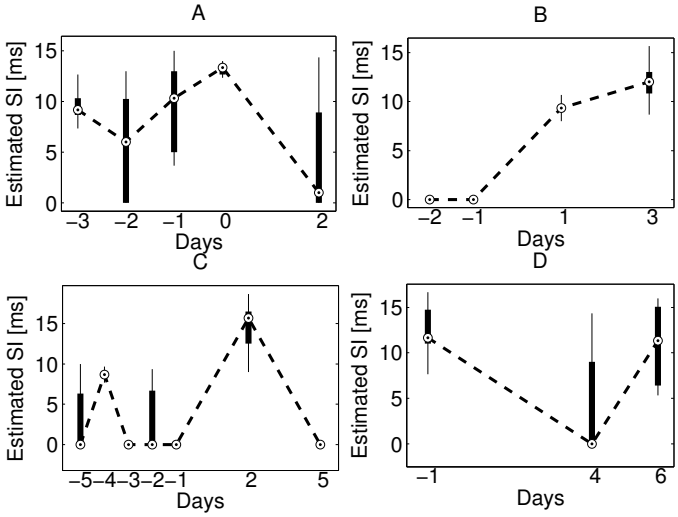

Figure 5.23: Box plot of the estimated SI over several days of four preterm infant with PDA treated pharmacologically. All four figures are drawn in a way that the closure of the PDA lies on Day 0. The dashed line shows the change of the median. An increase of the estimated SI around the time of the closure is observable.

5.5 Conclusions of the phonocardiographic investigations of preterms with PDA

Nevertheless preterms with PDA develop murmur usually only from the third day after birth [220], decision to treat PDA should be based also on clinical signs [77]. Thus a robust and sensitive heart sound and murmur inspection method would be of great importance since there is an extremely noisy auscultation environment in the clinical set-up. Furthermore, continuous monitoring of the PDA is not possible currently. A PCG based approach might open new possibilities in this respect.

Characteristic heart sound calculation showed promising results for sensitive identifi-

DOI:10.15774/PPKE.ITK.2012.001

cation of murmurs even in case of noisy records. This is important, because the detection of murmur is crucial in the assessment and possible monitoring of the blood flow through the PDA. Furthermore, we have found that the relative maximal envelope value of the systolic period and the length of the murmur detection window are significant features for automated murmur detection. By simple parameter extraction of the murmur related to the PDA some relations to medical parameters could be revealed. Although these results are promising further improvement is needed for clinical application. Reliable estimation of PDA related parameters would be of great importance.

Another interesting approach of preterm neonates with PDA was the investigation of S2 splitting. As described earlier, the SI depends on the pressure relations between the left and the right side of the heart and great arteries. These are obviously affected by the state of the PDA but other factors influence also these circumstances, thus for using the estimated SI for diagnostic purposes it is reasonable to take into account also other easily measurable parameters, such as the systolic-diastolic pressure ratio, the presence and some parameters of murmur, etc. Nevertheless, it is worth mentioning that the proposed SI estimation method could be applied also in other fields of phonocardiography.

DOI:10.15774/PPKE.ITK.2012.001

Chapter 6

Conclusions

The starting question of the dissertation was in what way clinically important information can be gained by using an old examination technique combined with present information technology. It has been shown that different signal processing techniques can be successfully applied, which are especially important in dealing with the low signal-to-noise ratio and in the detection of abnormal signals, such as murmur. A remaining open question is whether using certain nonlinear techniques, for example [25, 35], can result in further improvement because the level of noise and the low bandwidth might pose limitations to their successful application.

The investigation of heart sound models is surely a possible way to arrive at more quantitative results. I suppose that the presented fetal heart sound model can be further improved resulting in even more parameters, which would necessitate more sophisticated methods for nonlinear parameter estimation. The deep understanding of heart sound generation and propagation, especially important in the case of the fetal heart sounds, should be more involved in this analysis.

Methods for parameter extraction are especially important in diagnosing and monitoring cardiac diseases, the presented results support this concept. Developments in computational fluid dynamics could aid this analysis. With a sufficiently accurate model important clinical parameters, for instance the amount of blood flowing through the PDA, could be assessed by reverse engineering the generated murmur. Although this approach needs hard work, possibly this one could result in identifying the real potential of phonocardiography.

DOI:10.15774/PPKE.ITK.2012.001

Summary

6.1 New scientific results

The results of this dissertation can be summarized in two main parts: the first one dealing with the results on fetal phonocardiography and the second one describing achievements in investigating preterm neonates with patent ductus arteriosus.

Thesis I: *Analysis of fetal heart sounds and murmurs*

> **I.1. Based on the analysis of fetal phonocardiographic records I have found that different levels of accuracy are needed for the determination of T_{bb} beat-to-beat times in the case of conventional obstetrician fetal heart rate (FHR) analysis (e.g. NST) than in the case of profound FHR analysis for the assessment of fetal wellbeing (IUGR, fetal breathing, ...), where the starting point is the variability of the T_{bb}, thus, by introducing NL, as a metric for the level of noise, and HiR, as a metric for the rate of beat detection, I have shown that the HiR of FHR calculation based on conventional time-domain autocorrelation can be improved by applying a wavelet transform based, time-frequency domain autocorrelation, where prediction based on preceding beat-to-beat times further improves the reliability.**
>
> Related publications: [1]

In the case of conventional FHR calculation of CTG data often the autocorrelation of the time-domain signal or envelogram is used. However, with noisy signals, such as fPCG, noise bursts and in some cases even murmur corrupts the determination of the cyclostationary period, i.e. the heart rate. I introduced a method which exploits the specific time-frequency signature of the heart sounds, thus not only the periodicity of high intensity pulses, that is heart sounds, is taken into account for determining the heart rate, but also the time varying spectra of the heart sounds.

For comparison with conventional time-domain autocorrelation more than 500 fetal phonocardiographic records with different amounts of disturbances were processed. Although the wavelet transform based method yields only a modest improvement on average,

DOI:10.15774/PPKE.ITK.2012.001

more precisely less than 5 %, the distribution of improvement values is very encouraging because improvement up to 18 % could be achieved and the amount of decrement is rarely greater than 5 %.

Further analysis revealed that for noise levels less than 20 % both methods perform fairly well. As the noise level increases the range of possible HiR values widens because in some cases the different methods achieve only lower HiR-s. However, for NL in the range of 20-35 %, the time domain based method has a lower limit of possible worst HiR values than the wavelet transform based approach. In other words, the worst HiR that the wavelet transform based method can achieve for increased level of noise is always better than the worst performance of the time domain based correlation, at least in the case of these records. In the case of higher NL the performance of both methods degrades similarly.

I.2. I have shown that by modifying the amplitude and frequency characteristics of an existing heart sound model – which assumes the heart sounds as the superposition of two components, one from each side of the heart – it can be applied for modelling fetal first heart sounds; furthermore, the nine parameters of this model can be in general estimated using Monte Carlo simulation.

Related publications: [1]

Based mainly on the work of Xu *et al.* on S2 sound modelling of adults [28, 97], the following chirp model has been adapted for fetal heart sound modelling, presented here for the S1 sound:

$$s_M(t) = A_M \sin(\varphi_M(t)) \cdot e^{-t/\tau_M}, \tag{6.1}$$

$$s_T(t) = A_T \sin(\varphi_T(t - t_d)) \cdot e^{-(t-t_d)/\tau_T}, \tag{6.2}$$

$$s_{S1}(t) = s_M(t) + s_T(t), \tag{6.3}$$

where A_M and A_T are the initial amplitudes, φ_M and φ_T the phase functions, and τ_M and τ_T are the time constants of the damping of the sinusoidal mitral and tricuspid components, respectively. Finally, t_d is the delay between the above two components, that is the splitting interval.

A linear frequency decrease often proved to be sufficient, meaning that the phase functions can be defined as follows:

$$\varphi_M(t) = 2\pi \int_{-\infty}^{t} f_M(\tau) \mathrm{d}\tau = 2\pi \int_{-\infty}^{t} F_M - \Delta f_M \cdot \tau \, \mathrm{d}\tau, \tag{6.4}$$

DOI:10.15774/PPKE.ITK.2012.001

$$\varphi_T(t) \quad = \quad 2\pi \int_{-\infty}^{t} f_T(\tau)\mathrm{d}\tau = 2\pi \int_{-\infty}^{t} F_T - \Delta f_T \cdot \tau \ \mathrm{d}\tau, \tag{6.5}$$

where $f_T(t)$ and $f_M(t)$ are the instantaneous frequency functions with an initial frequency of F_M and F_T and a negative slope of Δf_M and Δf_T for the mitral and tricuspid components, respectively.

This two-component model contains altogether nine parameters. The estimation of these parameters can be performed by using the Monte Carlo method [98]. In the case of this analysis the number of random simulated heart sounds was in the order of 10^6. Although the error surface of this optimization contains a great number of local minima, which may result in false parameter values, in the case of increased splitting – which may be a symptom of a cardiac anomaly – the method becomes more reliable. Furthermore, preliminary results achieved with an implementation on manycore computing architectures, namely GPUs, show a running time improvement of more than two orders of magnitude. This makes an increased number of simulations possible, resulting in increased reliability.

As an example, one fetal S1 sound and the corresponding synthesized signal is presented in Figs. 4.20 and 4.21 together with the time-frequency representations of both signals.

I.3. Based on the analysis of a great number of fetal PCG recordings I have revealed that certain congenital heart diseases can be suspected based on the presence of fetal heart murmur, and that five parameters characterising fetal heart murmur are the length, the intensity, the timing, the dominant frequency and the shape of the envelope. Furthermore, the determination of these parameters is crucial for finding a possible relationship between heart murmurs and different heart defects.

Related publications: [2, 8, 12]

The detection of fetal murmurs is extremely difficult due to the attenuation caused by the maternal tissues and the low signal-to-noise ratio with many sources of noise (for example maternal heart and digestive sounds). There is also an important empirical observation, namely dominant low-frequency components of fetal heart murmur can be recorded on the maternal abdomen. In contrast, the murmur of children and adults has usually higher dominant frequency components than the main heart sounds. In addition, the recorded fetal heart murmurs exhibit in some cases a rather cyclostationary property despite the certainly turbulent origin of the murmur signal.

The suggested method tries to exploit these differences and applies an improved version of ensemble averaging for heart sound signal enhancement and heart cycle comparison.

DOI:10.15774/PPKE.ITK.2012.001

In order to be be consistent with medical murmur parameters, and in this way facilitate the acceptance of fetal murmur analysis in the medical community we defined the following aforementioned five parameters. It is important to note that during the investigations it has been found that these five parameters can be calculated in an automatic way and have possible high discriminative value. For demonstrating the clinical significance of fetal murmur detection a case of congenital heart disease is presented hereunder where fetal phonocardiographic records revealed fetal heart murmur (Fig. 4.28). Although this is not a verified clinical trial these results support the feasibility of this new method, which could contribute to the prenatal detection of CHDs, as a pre-screening method for a comprehensive echocardiographic examination, especially in the low risk populatio

— • —

DOI:10.15774/PPKE.ITK.2012.001

Thesis II: *Phonocardiographic analysis of preterm neonates with patent ductus arteriosus (PDA) with special attention on the detection of heart murmur related to PDA and the relationship between parameters of the heart sounds and murmur and clinical parameters.*

II.1. I have worked out a method for the detection of murmur originating from the turbulent blood flow through the ductus arteriosus that achieves 90 % reliability, hereby opening possibilities for monitoring the disease through murmur analysis. This was confirmed by preliminary results from the correlation of certain murmur parameters with important medical parameters, in particular the diameter of the PDA and the maximal blood flow velocity through the PDA.

Related publications: [3, 6, 7]

The first step towards a PCG based PDA monitoring framework is the detection of the murmur related to the turbulent blood flow through the ductus arteriosus. Although methods have been suggested for murmur detection [188, 191], it is an especially difficult task for preterm neonates due to the high level of noise (e.g. breathing machine) and the low intensity of the murmur.

The introduced characteristic heart sound calculation method provides a way for observing typical heart cycle dynamics. Furthermore, the set of heart cycles used for the characteristic sound calculation can be used for automated processing, applied also for murmur detection. Due to the presence of wide band noise I introduced a signal envelope based detection algorithm using baseline correction, which can be regarded as a form of adaptive thresholding. Heuristic rules based on *a priori* knowledge are also incorporated in the method for increased robustness.

When classifying preterms with and without PDA based on the length of detected late systolic sound components, and using a threshold of 7 % of the length of the systole, 90 % sensitivity and 60 % specificity could be achieved. Although the specificity is quite low, these are promising results, since the major goal is not a diagnosing but a monitoring application.

A second step of the development of a possible PDA monitor is to select appropriate parameters and find the relationship with important medical parameters. This is an even more challenging problem because the generation of murmur in such a complex scenario is still not completely understood. Nonetheless results exist on the relationship between frequency parameters of the murmur and important parameters of a stenosis producing heart murmur [199, 203]. During my investigations I also performed measurements analysing this aspect. I found a weak relationship between the frequency parameters of

DOI:10.15774/PPKE.ITK.2012.001

the murmur and the diameter of the PDA (D_{PDA}) and the maximal blood flow though the PDA (v_{max}), shown in Fig. 5.20. Unfortunately, due to the lack of reference data with sufficient accuracy, these results are of a preliminary nature.

II.2. I have observed the temporal separation (split) of the aortic and pulmonary components of the second heart sound (S2) of preterm neonates with PDA, and I have introduced a heuristic method for estimating the splitting interval (SI) making the quantitative analysis possible and finding a 30 % average increase of the SI around the time of the closure of the PDA in the case of preterms under pharmacological treatment.

Related publications: [3]

The closure of the patent ductus arteriosus is a dynamic process that is still not completely understood. Clearly, this process also affects the pressure ratios between the left and right side of the heart which can be assessed based on the splitting of the S2 sound. This phenomenon was also visually observed in the case of some of the recordings. Unfortunately the two components of the S2 sound usually overlap even in the time-frequency domain in a great manner, making separation very difficult. I introduced a solution for estimating the SI by applying a heuristic method which exploits the fact that the aortic and pulmonary components have an exponentially decreasing instantaneous frequency function resulting in high frequency oscillations only at the beginning of the components.

Since the exact accuracy of this method could not be verified because invasive measurements would have been needed, I applied a model-based approach. I adapted an existing heart sound model [28] to the characteristics of S2 sounds of preterm neonates, and verified the suggested SI estimation method on synthesised S2 sounds. This analysis revealed that reliable splitting interval estimation can be performed in the case of SI > 7 ms.

I applied the introduced algorithm on the PCG data from preterm infants with PDA and found that in the case of pharmacologically treated infants the SI increased significantly around the time of the closure of the ductus arteriosus with respect to the period before the closure (Fig. 5.23). This result could also contribute to a possible PDA monitor although long term measurements on more patients are needed for better investigation of the SI dynamics.

DOI:10.15774/PPKE.ITK.2012.001

6.2 Possible Applications

Most of the application possibilities of the presented results are rather evident because in most of the cases practical motivations were behind the investigations. The results of Thesis I are mostly specific to the analysis of fetal heart sounds, however the improved ensemble averaging could be utilized also for the heart sound analysis of preterm neonates, because a low signal to noise ratio was present also in that scenario. Improved fetal heart rate determination is an important step towards extending monitoring capabilities of the fetal wellbeing, namely based on heart rate variability analysis. This would be especially beneficial in the case of the telemetric system where surveillance is possible on a daily basis. Regarding the fetal heart sound model there is a possibility for further parameter extraction. For instance, it might be possible to track the blood pressure changes of the fetus in a throughout the pregnancy because some heart sound parameters correlate with certain blood pressure values. This is not possible with any other present technology. One of the most important findings is the observation of fetal heart murmurs in the case of certain congenital heart diseases (CHD). Although the significance of this result depends on the incidence of innocent murmurs and "silent" CHDs, having obtained the preliminary results it may be established that murmur detection and analysis can contribute to the widespread screening of cardiac abnormalities, especially in the low risk population. Furthermore, all these findings could assist in the development of a fetal expert system for automated surveillance or clinical decision support (Fig. 4.31).

The major motivation behind the analysis of the heart sounds of preterm infants with patent ductus arteriosus (PDA) was the investigation of a possible PCG-based PDA monitor, which is also the most important possible application. It should be mentioned that continuous monitoring of important medical parameters of the PDA is not possible at present. Although a difficult step is still ahead, namely to relate extracted heart murmur parameters reliably with medical parameters, the presented results support this concept. The method for splitting interval estimation serves the same issue, but it could be also applied in other fields of phonocardiography because the separation of the heart sound components is an important symptom in the case of other cardiovascular diseases as well. It should be noted, however, that in order to achieve the accurate and reliable tracking of important parameters of the ductus arteriosus, a multimodal approach is needed, since the hemodynamic significance of the PDA also depends on several parameters. These multimodal measurements could consist of the analysis of the murmur, estimation of the SI, analysis of the pulse wave, and monitoring of the blood oxygen level as well as some further parameters. The above envisaged system would improve the monitoring of patients with heart diseases such as PDA as well as lead to an increased understanding of the process of the PDA closing and its response to medication.

DOI:10.15774/PPKE.ITK.2012.001

Appendix A

Significance of Fetal Heart Murmur Detection

In order to estimate the contribution of fetal heart murmur detection to the screening for congenital heart diseases a large number of fetuses with and without congenital heart diseases (CHD) have to be examined. This is left for further work. However, in order to give some quantitative support to this concept we present two cases of serious CHDs where in the first case prospective and in the second case retrospective analysis of the fetal phonocardiographic records revealed fetal heart murmur.

A.1 Case reports

Case I A 28-year woman presented for echocardiographic screening in the 21 weeks' gestation at the Institute of Cardiology because of history of complex pulmonary atresia in the case of a previous pregnancy. The 2D and color Doppler examination revealed Tetralogy of Fallot with systemic-to-pulmonary collateral shunting and pulmonary insufficiency. The mother decided to continue her pregnancy, thus a control examination was recommended for the 27 weeks' of gestation when also the fetal phonocardiographic data was recorded. Cesarean delivery of a neonate weighing 3620 g occurred at 39 weeks and 4 days. The Apgar score[1] was 8/8, and the infant showed moderate cyanosis, thus prostin infusion was performed for several hours until satisfactory antegrade pulmonary blood flow. Postnatal echocardiographic examination verified Tetralogy of Fallot, aorta-pulmonary vessels and pulmonary valve agenesis[2] producing a grade III pulmonary insufficiency. Cardiac catheterization also confirmed these findings. Due to balanced pulmonary circulation sur-

[1] The Apgar score is the result of a simple and repeatable examination method to quickly and summarily assess the health of newborn children immediately after birth. A low score is a sign of a critical status

[2] Insufficient development of the pulmonary valve

DOI:10.15774/PPKE.ITK.2012.001

gical intervention was performed at the age of two. The reconstructive surgical procedure closed the ventricular septal defect using patch and reconstructed the pulmonary outflow with homograft[1] valve replacement. Control examination at an age of 3 years showed normal development and good postoperative results.

Case II A 4 days old neonate delivered at 38 weeks' of gestation with cesarean section (Apgar score was 9/10) was admitted to the Institute of Cardiology due to diagnosis of pulmonary atresia[2] indicated by mild cyanosis observed on the second day of life. Echocardiographic examination verified pulmonary atresia combined with a ventricular septal defect and Major Aorto-Pulmonary Collateral Arteries. Cardiac catheterization revealed 4 collateral arteries. The collateral circulation ensured satisfactory pulmonary flow. The infant was discharged until the next control examination. Fetal phonocardiographic measurements were performed daily from the 35 weeks' gestation until birth, and postnatal heart sound was also recorded one week after birth. At the time of the fetal phonocardiographic measurements only conventional CTG examination was performed. The analysis of murmur detection is not yet included in the routine examination thus it was carried out only after birth when the CHD was already evident.

Despite the different congenital heart diseases described above the development of aorto-pulmonary collateral arteries is a common point in these two cases. In both cases the fetal phonocardiogram showed well identifiable murmur (Fig. 4.28-4.29). Murmur originating from collateral arteries is usually continuous, but it should be noted that the flow dynamics in fetuses and neonates is different, thus turbulent blood flow causing murmur might evolve only during the systole when the blood pressure is greater. The murmur in case I has also an early diastolic component, whereas in case II it is only systolic. A possible reason is that the diastolic component of case I originates from the pulmonary valve insufficiency, which is not present in case II and the collateral arteries produce the systolic murmur component. In case II the murmur was also verified after birth. It should be mentioned that in this case the fetal and neonatal circulation remained very similar, which is also reflected by the similar parameters of the detected murmur.

[1] A tissue graft obtained from an organism of the same species as the recipient

[2] Pulmonary atresia is a serious congenital malformation of the pulmonary valve in which the valve orifice fails to develop, thus there is no outflow from the right ventricle to the lungs at all

DOI:10.15774/PPKE.ITK.2012.001

Bibliography

Journal publications by the author

[1] F. Kovács, C. Horváth, A. T. Balogh, and G. Hosszú, "Extended noninvasive fetal monitoring by detailed analysis of data measured with phonocardiography," *IEEE Transactions on Biomedical Engineering*, vol. 58, no. 1, pp. 64–70, 2011. 102, 103

[2] A. T. Balogh, K. Kádár, A. Nagy, Z. Varga, and F. Kovács, "Detection of fetal heart murmur related to congenital heart diseases," *prepared for submission*, 2012. 104

[3] A. T. Balogh and F. Kovács, "Application of phonocardiography on preterm infants with patent ductus arteriosus," *Biomedical Signal Processing and Control*, vol. 6, no. 4, pp. 337–345, 2011. 106, 107

International conference publications by the author

[4] A. T. Balogh and F. Kovács, "Application of heart sound analysis in preterm neonates with patent ductus arteriosus," in *Applied Sciences in Biomedical and Communication Technologies, 2009. ISABEL 2009. 2nd International Symposium on*, Bratislava, 2009, pp. 1–2.

[5] A. T. Balogh, F. Kovács, and Z. Molnár, "Phonocardiography in preterm newborns with patent ductus arteriosus," in *Biomedical Engineering 2010,The 7th IASTED International Conference on*, vol. 1, Innsbruck, 2010.

[6] A. T. Balogh and F. Kovács, "Parameter extraction for diagnosing patent ductus arteriosus in preterm neonates using phonocardiography," in *2010 3rd International Symposium on Applied Sciences in Biomedical and Communication Technologies (ISABEL)*, Rome, Nov. 2010, pp. 1–2. 106

[7] A. T. Balogh and F. Kovács, "Detection of heart murmur related to patent ductus arteriosus using phonocardiography," in *5th European Conference of the International Federation for Medical and Biological Engineering (IFMBE)*, A. Jobbágy, Ed., vol. 37, Budapest, 2011, p. 438–441. 106

[8] G. Fodor, A. T. Balogh, G. Hosszú, and F. Kovács, "Screening for congenital heart diseases by murmurs using telemedical phonocardiography," in *2012 Annual International Conference of the IEEE Engineering in Medicine and Biology Society (EMBC)*, San Diego, 2012, accepted. 104

DOI:10.15774/PPKE.ITK.2012.001

Other publications by the author

[9] E. Kósa, A. T. Balogh, B. Üveges, and F. Kovács, "Heuristic method for heartbeat detection in fetal phonocardiographic signals," in *Signals and Electronic Systems, 2008. ICSES '08. International Conference on*, 2008, pp. 231–234. 86

[10] F. Kovács, M. Török, C. Horváth, A. T. Balogh, T. Zsedrovits, A. Nagy, and G. Hosszú, "A new, Phonocardiography-Based telemetric fetal home monitoring system," *Telemedicine and e-Health*, vol. 16, no. 8, pp. 878–882, Oct. 2010. 2

[11] F. Kovács, C. Horváth, A. T. Balogh, and G. Hosszú, "Fetal phonocardiography-Past and future possibilities," *Computer Methods and Programs in Biomedicine*, vol. 104, no. 1, pp. 19–25, 2011.

Patent

[12] F. Kovács, G. Hosszú, A. T. Balogh, N. Kersner, A. Nagy, and T. Zsedrovits, "Eljárás és rendszer magzati szívműködésre jellemző phonokardiográfiás jel kiértékelésére," Hungarian Patent P1 100 254, May 17, 2011. 66, 104

Publications connected to the dissertation

[13] H. Vermarien, "Phonocardiography," in *Encyclopedia of Medical Devices and Instrumentation*, J. G. Webster, Ed. Hoboken, New Jersey: John Wiley & Sons, 2006, vol. 5, pp. 278–290. 1, 2, 18

[14] P. Findlen and R. Bence. The history of the heart. Accessed: 5/06/2012. [Online]. Available: http://www.stanford.edu/class/history13/earlysciencelab/body/heartpages/heart.html 1

[15] V. A. McKusick, *Cardiovascular sound in health and disease.* Williams & Wilkins, 1958. 2

[16] F. Yu, A. Bilberg, and F. Voss, "The development of an intelligent electronic stethoscope," in *IEEE/ASME International Conference on Mechtronic and Embedded Systems and Applications, 2008. MESA 2008*, Oct. 2008, pp. 612–617. 2

[17] N. Celik, J. Baker, H. Youn, and M. Iskander, "An internet based interactive telemedicine system for remote healthcare," in *2010 IEEE Antennas and Propagation Society International Symposium (APSURSI)*, Jul. 2010, pp. 1–4. 2

[18] J. Iwamoto, H. Ogawa, H. Maki, Y. Yonezawa, A. W. Hahn, and W. M. Caldwell, "A mobile phone-based ecg and heart sound monitoring system," *Biomedical Sciences Instrumentation*, vol. 47, pp. 160–164, 2011. 2

DOI:10.15774/PPKE.ITK.2012.001

[19] L. B. Dahl, P. Hasvold, E. Arild, and T. Hasvold, "Heart murmurs recorded by a sensor based electronic stethoscope and e-mailed for remote assessment," *Archives of Disease in Childhood*, vol. 87, no. 4, pp. 297–301, Jan. 2002. 2

[20] J. de Vos and M. Blanckenberg, "Automated pediatric cardiac auscultation," *Biomedical Engineering, IEEE Transactions on*, vol. 54, no. 2, pp. 244–252, 2007. 2, 62

[21] I. Germanakis, S. Dittrich, R. Perakaki, and M. Kalmanti, "Digital phonocardiography as a screening tool for heart disease in childhood," *Acta Pædiatrica*, vol. 97, no. 4, p. 470–473, 2008. 2

[22] S. Lukkarinen, "Phonocardiography: Development of a clinical system and its application to screening for paediatric heart murmurs," Ph.D. dissertation, Aalto University, Department of Electronics, 2012. 2

[23] R. R. Sarbandi, J. D. Doyle, M. Navidbakhsh, K. Hassani, H. Torabiyan *et al.*, "A color spectrographic phonocardiography (CSP) applied to the detection and characterization of heart murmurs: preliminary results," *Biomedical engineering online*, vol. 10, no. 1, p. 1–10, 2011. 2

[24] J. Shin, S. Lim, Y. Kim, S. Kim, E. Cha, and T. Lee, "Portable digital esophageal stethoscope system," in *2010 Annual International Conference of the IEEE Engineering in Medicine and Biology Society (EMBC)*, Sep. 2010, pp. 1844–1847. 2

[25] Y. Tseng, P. Ko, and F. Jaw, "Detection of the third and fourth heart sounds using Hilbert-Huang transform," *BioMedical Engineering OnLine*, vol. 11, no. 1, p. 8, Feb. 2012. 2, 101

[26] Z. Yan, Z. Jiang, A. Miyamoto, and Y. Wei, "The moment segmentation analysis of heart sound pattern," *Computer Methods and Programs in Biomedicine*, vol. 98, no. 2, pp. 140–150, May 2010. 2

[27] S. Choi and Z. Jiang, "Comparison of envelope extraction algorithms for cardiac sound signal segmentation," *Expert Systems with Applications*, vol. 34, no. 2, pp. 1056–1069, Feb. 2008. 2, 43

[28] J. Xu, L.-G. Durand, and P. Pibarot, "Nonlinear transient chirp signal modeling of the aortic and pulmonary components of the second heart sound," *IEEE Trans. Biomed. Eng.*, vol. 47, no. 10, pp. 1328–1335, 2000. 2, 11, 56, 57, 58, 91, 103, 107

[29] A. Voss, A. Mix, and T. Hübner, "Diagnosing aortic valve stenosis by parameter extraction of heart sound signals," *Annals of Biomedical Engineering*, vol. 33, no. 9, pp. 1167–1174, 2005. 2

[30] S. Debbal and F. Bereksi-Reguig, "Computerized heart sounds analysis," *Computers in Biology and Medicine*, vol. 38, no. 2, pp. 263–280, 2008. 2

[31] H. Tang, T. Li, and T. Qiu, "Noise and disturbance reduction for heart sounds in cycle-frequency domain based on nonlinear time scaling," *IEEE Trans. Biomed. Eng.*, vol. 57, no. 2, pp. 325–333, Feb. 2010. 2, 43, 57

DOI:10.15774/PPKE.ITK.2012.001

[32] H. Tang, T. Li, Y. Park, and T. Qiu, "Separation of heart sound signal from noise in joint cycle Frequency–Time–Frequency domains based on fuzzy detection," *Biomedical Engineering, IEEE Transactions on*, vol. 57, no. 10, pp. 2438–2447, 2010. 2, 57

[33] S. A. Tapidou and L. J. Hadjileontiadis, "Nonlinear analysis of heart murmurs using wavelet-based higher-order spectral parameters," in *28th Ann. Int. Conf. IEEE Eng. Med. Biol. Soc.*, New York, USA, 2006, pp. 4502–4505. 2

[34] C. Ahlstrom, K. Hoglund, P. Hult, J. Haggstrom, C. Kvart, and P. Ask, "Assessing aortic stenosis using sample entropy of the phonocardiographic signal in dogs," *IEEE Transactions on Biomedical Engineering*, vol. 55, no. 8, pp. 2107–2109, 2008. 2, 80, 89

[35] C. Ahlstrom, "Nonlinear phonocardiographic signal processing," Ph.D. dissertation, Linköping University, Deptartment of Biomedical Engineering, 2008. 2, 19, 101

[36] S. Schmidt, C. Holst-Hansen, C. Graff, E. Toft, and J. Struijk, "Detection of coronary artery disease with an electronic stethoscope," in *Computers in Cardiology, 2007*, Oct. 2007, pp. 757–760. 2

[37] M. Akay, Y. Akay, D. Gauthier, R. Paden, W. Pavlicek, F. Fortuin, J. Sweeney, and R. Lee, "Dynamics of diastolic sounds caused by partially occluded coronary arteries," *IEEE Transactions on Biomedical Engineering*, vol. 56, no. 2, pp. 513–517, Feb. 2009. 2

[38] A. Bagno, F. Anzil, V. Tarzia, V. Pengo, A. Ruggeri, and G. Gerosa, "Application of wavelet analysis to the phonocardiographic signal of mechanical heart valve closing sounds," *The International journal of artificial organs*, vol. 32, no. 3, pp. 166–172, Mar. 2009. 2

[39] M. Schlömicher, A. Brensing, and A. Laczkovics, "Detection of valve malfunction after mechanical MVR using digital phonocardiography," *The Thoracic and cardiovascular surgeon*, vol. 59, no. 8, pp. 493–495, Dec. 2011. 2

[40] A. Leatham, *Auscultation of the heart and phonocardiography.* Churchill Livingstone, 1975. 3

[41] E. Kennedy, *Observations on obstetric auscultation: with an analysis of the evidences of pregnancy and an inquiry into the proofs of the life and death of the foetus in utero.* Dublin: Hodges and Smith, 1833. 4

[42] R. K. Freeman, T. J. Garite, and M. P. Nageotte, *Fetal heart rate monitoring.* Lippincott Williams & Wilkins, Apr. 2003. 4, 5

[43] L. Hatle and B. Angelsen, *Doppler ultrasound in cardiology.* Lea and Febiger Philadelphia, 1985. 5

[44] "Electronic fetal heart rate monitoring: research guidelines for interpretation. national institute of child health and human development research planning workshop,"

DOI:10.15774/PPKE.ITK.2012.001

American Journal of Obstetrics and Gynecology, vol. 177, no. 6, pp. 1385–1390, Dec. 1997. 5

[45] E. S. B. C. Ang, V. Gluncic, A. Duque, M. E. Schafer, and P. Rakic, "Prenatal exposure to ultrasound waves impacts neuronal migration in mice," *Proceedings of the National Academy of Sciences*, vol. 103, no. 34, pp. 12 903–12 910, Aug. 2006. 6

[46] M. Fatemi, J. Ogburn, P L, and J. F. Greenleaf, "Fetal stimulation by pulsed diagnostic ultrasound," *Journal of Ultrasound in Medicine*, vol. 20, no. 8, pp. 883–889, Aug. 2001. 6

[47] D. Francis A., "Hazards, risks and safety of diagnostic ultrasound," *Medical Engineering & Physics*, vol. 30, no. 10, pp. 1338–1348, Dec. 2008. 6

[48] M. Stanton, R. Ettarh, D. Arango, M. Tonra, and P. Brennan, "Diagnostic ultrasound induces change within numbers of cryptal mitotic and apoptotic cells in small intestine," *Life Sciences*, vol. 68, no. 13, pp. 1471–1475, Feb. 2001. 6

[49] J. Jezewski, J. Wrobel, and K. Horoba, "Comparison of doppler ultrasound and direct electrocardiography acquisition techniques for quantification of fetal heart rate variability," *Biomedical Engineering, IEEE Transactions on*, vol. 53, no. 5, pp. 855–864, 2006. 6, 8

[50] R. Sameni and G. D. Clifford, "A review of fetal ECG signal processing; issues and promising directions," *The Open Pacing, Electrophysiology & Therapy Journal*, vol. 3, pp. 4–20, Jan. 2010. 6

[51] C. Peters, R. Vullings, J. Bergmans, G. Oei, and P. Wijn, "The effect of artifact correction on spectral estimates of heart rate variability," in *Engineering in Medicine and Biology Society, 2008. EMBS 2008. 30th Annual International Conference of the IEEE*, Aug. 2008, pp. 2669–2672. 6

[52] T. F. Oostendorp, A. van Oosterom, and H. W. Jongsma, "The effect of changes in the conductive medium on the fetal ECG throughout gestation," *Clinical Physics and Physiological Measurement*, vol. 10 Suppl B, pp. 11–20, 1989. 6

[53] M. Peters, J. Crowe, J. Piéri, H. Quartero, B. Hayes-Gill, D. James, J. Stinstra, and S. Shakespeare, "Monitoring the fetal heart non-invasively: a review of methods," *J. Perinat. Med.*, vol. 29, no. 5, pp. 408–416, 2001. 6

[54] J. G. Stinstra and M. J. Peters, "The influence of fetoabdominal tissues on fetal ECGs and MCGs," *Archives of Physiology and Biochemistry*, vol. 110, no. 3, pp. 165–176, Jul. 2002. 6

[55] R. T. Wakai, J. M. Lengle, and A. C. Leuthold, "Transmission of electric and magnetic foetal cardiac signals in a case of ectopia cordis: the dominant role of the vernix. caseosa," *Physics in Medicine and Biology*, vol. 45, no. 7, pp. 1989–1995, Jul. 2000. 6

DOI:10.15774/PPKE.ITK.2012.001

[56] M. Peters, J. Stinstra, and S. Uzunbajakau, "Fetal magnetocardiography," in *Advances in electromagnetic fields in living systems*. Springer, Aug. 2005, pp. 1–40, editor: James C. Lin. 6

[57] J. Crowe, A. Harrison, and B. Hayes-Gill, "The feasibility of long-term fetal heart rate monitoring in the home environment using maternal abdominal electrodes," *Physiological Measurement*, vol. 16, no. 3, pp. 195–202, 1995. 6

[58] P. Olofsson, "Current status of intrapartum fetal monitoring: cardiotocography versus cardiotocography + ST analysis of the fetal ECG," *European Journal of Obstetrics & Gynecology and Reproductive Biology*, vol. 110, Supplement, no. 0, pp. S113–S118, 2003. 6

[59] P. Van Leeuwen, D. Geue, S. Lange, D. Cysarz, H. Bettermann, and D. Grönemeyer, "Is there evidence of fetal-maternal heart rate synchronization?" *BMC Physiology*, vol. 3, no. 1, pp. 1–11, 2003. 6

[60] P. Van Leeuwen, D. Geue, S. Lange, W. Hatzmann, and D. Grönemeyer, "Changes in the frequency power spectrum of fetal heart rate in the course of pregnancy," *Prenatal Diagnosis*, vol. 23, no. 11, pp. 909–916, Nov. 2003. 6

[61] N. Colley, D. G. Talbert, N. G. Abraham, W. L. Davies, P. Fayers, and D. P. Southall, "The fetal phonogram: a measure of fetal activity," *Lancet*, vol. 1, no. 8487, pp. 931–935, Apr. 1986. 7

[62] Y. Song, W. Xie, . Chen, and K. Phua, "Passive acoustic maternal abdominal fetal heart rate monitoring using wavelet transform," *Computers in Cardiology*, pp. 581–584, 2006. 7

[63] A. Mittra, A. Shukla, and A. Zadgaonkar, "System simulation and comparative analysis of foetal heart sound de-noising techniques for advanced phonocardiography," *International Journal of Biomedical Engineering and Technology*, vol. 1, no. 1, pp. 73–85, 2007. 7

[64] R. Ortiz, R. González, M. Pena, S. Carrasco, M. Gaitán, and C. Vargas, "Differences in foetal heart rate variability from phonocardiography and abdominal electrocardiography," *Journal of Medical Engineering & Technology*, vol. 26, no. 1, pp. 39–45, 2002. 7

[65] M. Abdel Raheem and W. Mohamed, "Impact of congenital heart disease on brain development in newborn infants," *Annals of Pediatric Cardiology*, vol. 5, no. 1, pp. 21–26, 2012. 7

[66] S. Yagel, A. Weissman, Z. Rotstein, M. Manor, J. Hegesh, E. Anteby, S. Lipitz, and R. Achiron, "Congenital heart defects: Natural course and in utero development," *Circulation*, vol. 96, no. 2, pp. 550–555, Jul. 1997. 7

[67] V. L. Roger *et al.*, "Heart disease and stroke statistics—2012 update a report from the american heart association," *Circulation*, vol. 125, no. 1, pp. e2–e220, Mar. 2012. 7, 24

DOI:10.15774/PPKE.ITK.2012.001

[68] E. Tegnander, W. Williams, O. J. Johansen, H. K. Blaas, and S. H. Eik-Nes, "Prenatal detection of heart defects in a non-selected population of 30,149 fetuses–detection rates and outcome," *Ultrasound in Obstetrics & Gynecology*, vol. 27, no. 3, pp. 252–265, Mar. 2006. 8

[69] U. Gembruch and A. Geipel, "Indications for fetal echocardiography: screening in low-and high-risk populations," in *Fetal cardiology: Embryology, Genetics, Physiology, Echocardiographic Evaluation, Diagnosis and Perinatal Management of Cardiac Diseases*, 2nd ed., S. Yagel *et al.*, Eds. New York, USA: Informa HealthCare, 2008, pp. 111–129. 8

[70] T. Perri, B. Cohen-Sacher, M. Hod, M. Berant, I. Meizner, and J. Bar, "Risk factors for cardiac malformations detected by fetal echocardiography in a tertiary center," *The Journal of Maternal-Fetal & Neonatal Medicine*, vol. 17, no. 2, pp. 123–128, Feb. 2005. 8

[71] R. J. Acherman, W. N. Evans, C. F. Luna, R. Rollins, K. T. Kip, J. C. Collazos, H. Restrepo, J. Adasheck, B. K. Iriye, D. Roberts, and A. J. Sacks, "Prenatal detection of congenital heart disease in southern Nevada: the need for universal fetal cardiac evaluation," *Journal of Ultrasound in Medicine*, vol. 26, no. 12, pp. 1715–1719; quiz 1720–1721, Dec. 2007. 8

[72] K. Ueda, T. Ikeda, N. Iwanaga, S. Katsuragi, K. Yamanaka, R. Neki, J. Yoshimatsu, and I. Shiraishi, "Intrapartum fetal heart rate monitoring in cases of congenital heart disease," *American Journal of Obstetrics and Gynecology*, vol. 201, no. 1, pp. 64.e1–6, Jul. 2009. 8

[73] D. Bonnet, A. Coltri, G. Butera, L. Fermont, J. Le Bidois, J. Kachaner, and D. Sidi, "Detection of transposition of the great arteries in fetuses reduces neonatal morbidity and mortality," *Circulation*, vol. 99, no. 7, pp. 916–918, Feb. 1999. 8

[74] W. Tworetzky, D. B. McElhinney, V. M. Reddy, M. M. Brook, F. L. Hanley, and N. H. Silverman, "Improved surgical outcome after fetal diagnosis of hypoplastic left heart syndrome," *Circulation*, vol. 103, no. 9, pp. 1269–1273, Mar. 2001. 8

[75] Nucleus Medical Media. Patent ductus arteriosus. Accessed: 16 Aug 2012. [Online]. Available: http://demo.smartimagebase.com/patent-ductus-arteriosus/view-item?ItemID=4551 9

[76] D. J. Schneider and J. W. Moore, "Patent ductus arteriosus," *Circulation*, vol. 114, pp. 1873–1882, 2006. 9, 75

[77] A. Chiruvolu, P. Punjwani, and C. Ramaciotti, "Clinical and echocardiographic diagnosis of patent ductus arteriosus in premature neonates," *Early Human Development*, vol. 85, no. 3, pp. 147–149, 2009. 9, 99

[78] J. Koch, G. Hensley, L. Roy, S. Brown, C. Ramaciotti, and C. R. Rosenfeld, "Prevalence of spontaneous closure of the ductus arteriosus in neonates at a birth weight of 1000 grams or less," *Pediatrics*, vol. 117, no. 4, pp. 1113–1121, 2006. 9

DOI:10.15774/PPKE.ITK.2012.001

[79] J. Skinner, "Diagnosis of patent ductus arteriosus," *Seminars in Neonatology*, vol. 6, no. 1, pp. 49–31, 2001. 9

[80] P. Kwinta, A. Rudzinski, P. Kruczek, Z. Kordon, and J. J. Pietrzyk, "Can early echocardiographic findings predict patent ductus arteriosus?" *Neonatology*, vol. 95, no. 2, pp. 141–148, 2009. 9

[81] D. Little, T. Pratt, S. Blalock, D. Krauss, D. Cooney, and M. Custer, "Patent ductus arteriosus in micropreemies and full-term infants: The relative merits of surgical ligation versus indomethacin treatment," *Journal of Pediatric Surgery*, vol. 38, no. 3, pp. 492–496, 2003. 9

[82] S. Bouwstra, L. Fejis, C. Wei, and S. Oetomo, "Smart jacket design for neonatal monitoring with wearable sensors," in *Sixth International Workshop on Wearable and Implantable Body Sensor Networks, BSN 2009*, Berkley,CA, 2009, pp. 162–167. 9

[83] O. Ciani, L. Piccini, S. Parini, A. Rullo, F. Bagnoli, P. Marti, and G. Andreoni, "Pervasive technology in neonatal intensive care unit: a prototype for newborns unobtrusive monitoring," in *Engineering in Medicine and Biology Society, EMBS 2008, 30th Annual International Conference of the IEEE*, Vancouver, BC, 2008, pp. 1292–1295. 9

[84] Felice *et al.*, "Skin reflectance changes in preterm infants with patent ductus arteriosus," *Early Human Development*, vol. 78, no. 1, pp. 45–51, 2004. 9

[85] B. P. Lundell, "Pulse wave patterns in patent ductus arteriosus." *Archives of Disease in Childhood*, vol. 58, no. 9, pp. 682–685, Sep. 1983. 9

[86] M. Gevers, K. van der Mooren, N. Stergiopulos, H. R. Van Genderingen, H. N. Lafeber, W. W. Hack, and N. Westerhof, "Bisferiens peaks in the radial artery pressure wave during patent ductus arteriosus in newborn infants: relationship with ascending aortic flow," *Pediatric Research*, vol. 40, no. 1, pp. 163–168, Jul. 1996. 9

[87] K. A. Hallidie-Smith, "Murmur of persistent ductus arteriosus in premature infants," *Archives of Disease in Childhood*, vol. 47, pp. 725–730, 1972. 10

[88] H. Holmström, C. Hall, and E. Thaulow, "Plasma levels of natriuretic peptides and hemodynamic assessment of patent ductus arteriosus in preterm infants," *Acta Paediatrica (Oslo, Norway: 1992)*, vol. 90, no. 2, pp. 184–191, Feb. 2001. 10

[89] N. Evans, "Diagnosis of the preterm patent ductus arteriosus: Clinical signs, biomarkers, or ultrasound?" *Seminars in Perinatology*, vol. 36, no. 2, pp. 114–122, Apr. 2012. 10

[90] ——, "Assessment and support of the preterm circulation," *Early Human Development*, vol. 82, no. 12, pp. 803–810, 2006. 10

[91] R. S. Lees and C. F. Dewey, "Phonoangiography: A new noninvasive diagnostic method for studying arterial disease," *Proceedings of the National Academy of Sciences*, vol. 67, no. 2, pp. 935–942, Jan. 1970. 10, 78, 89

DOI:10.15774/PPKE.ITK.2012.001

[92] L. Sörnmo and P. Laguna, "Noise reduction by ensemble averaging," in *Bioelectrical signal processing in cardiac and neurological applications*. Elsevier Academic Press, 2005, pp. 192–241. 11, 31

[93] D. Gabor, "Theory of communication. part 1: The analysis of information," *Journal of the Institution of Electrical Engineers*, vol. 93, no. 26, pp. 429–441, Nov. 1946. 11, 32

[94] S. Mallat, *A Wavelet Tour of Signal Processing, Third Edition: The Sparse Way*, 3rd ed. Burlington, MA: Academic Press, Dec. 2008. 11, 32, 33, 34

[95] Ville, "Théorie et application de la notion de signal analytique," *Cables et Transmission*, vol. 1, no. 1, pp. 61–74, 1948. 11, 38

[96] T. Tran, N. Jones, and J. Fothergill, "Heart sound simulator," *Medical and Biological Engineering and Computing*, vol. 33, no. 3, pp. 357–359, 1995. 11, 56, 57

[97] J. Xu, L. Durand, and P. Pibarot, "Extraction of the aortic and pulmonary components of the second heart sound using a nonlinear transient chirp signal model," *IEEE Trans. Biomed. Eng.*, vol. 48, no. 3, pp. 277–283, 2001. 11, 57, 58, 91, 103

[98] N. Metropolis and S. Ulam, "The Monte Carlo Method," *Journal of the American Statistical Association*, vol. 44, no. 247, pp. 335–341, 1949. 11, 59, 104

[99] M. David, M. Hirsch, J. Karin, E. Toledo, and S. Akselrod, "An estimate of fetal autonomic state by Time-Frequency analysis of fetal heart rate variability," *Journal of Applied Physiology*, vol. 102, no. 3, pp. 1057–1064, Jan. 2007. 11, 42

[100] M. Ferrario, M. G. Signorini, and G. Magenes, "Complexity analysis of the fetal heart rate variability: early identification of severe intrauterine growth-restricted fetuses," *Medical & Biological Engineering & Computing*, vol. 47, pp. 911–919, Jun. 2009. 11, 42, 55

[101] "Part VII - congenital cardiovascular malformations," in *Moss and Adams' Heart Disease in Infants, Children, and Adolescents: Including the Fetus and Young Adults*, 7th ed., H. Allen *et al.*, Eds. Philadelphia: Lippincott Williams & Wilkins, 2008, vol. 1–2, pp. 632–1170. 11, 24

[102] J. Joósz, "Magzati szívzörejek vizsgálata phonocardiográfiás módszerrel," MSc thesis, Pázmány Péter Catholic University, Faculty of Information Technology, 2009. 12

[103] N. Kersner, "Magzati szívzörejek és extraszisztolék azonosítására szolgáló számítógépes program kidolgozása," MSc thesis, Pázmány Péter Catholic University, Faculty of Information Technology, 2009. 12

[104] K. Gőcze, "Magzatok phonocardiográfiás vizsgálata során kapott jelek elemzése a billentyűhangoknál jelentkező split-effektusok meghatározására," MSc thesis, Pázmány Péter Catholic University, Faculty of Information Technology, 2009. 12

DOI:10.15774/PPKE.ITK.2012.001

[105] T. Zsedrovits, "Magzatok phonokardiográfiás vizsgálata során kapott billentyűhangok analízise, akusztikus jellemzőinek és azok szórásának meghatározására," MSc thesis, Pázmány Péter Catholic University, Faculty of Information Technology, 2009. 12

[106] Z. Nagy, K. Gőcze, and T. Zsedrovits, "A magzati szívműködés vizsgálata phonocardiográfiás módszerrel, különös tekintettel a split-effektusra," TDK dolgozat, Pázmány Péter Catholic University, Faculty of Information Technology, 2007. 12

[107] B. Üveges, "Magzati phonocardiografikus jelek vizsgálata az ütések azonosítására a zajjal erősen terhelt időszakaszokban," MSc thesis, Pázmány Péter Catholic University, Faculty of Information Technology, 2009. 12

[108] B. Gera, "Magzati szívhangok paramétereloszlásainak statisztikai becslése sokprocesszoros architektúrával," Mernöki tervezés, Pázmány Péter Catholic University, Faculty of Information Technology, 2012. 12, 60

[109] A. Nagy, "Magzati szívhangokban jelentkező, veleszületett szívbetegségekre utaló zörejek felderítése és jellemzése," Master's thesis, Pázmány Péter Catholic University, Faculty of Information Technology, 2012. 12, 66

[110] Yale Medical Group. Normal heart. Accessed: 16 Aug 2012. [Online]. Available: http://www.yalemedicalgroup.org/stw/images/125864.jpg 14

[111] A. M. Katz, *Physiology of the Heart*, 4th ed. Lippincott Williams & Wilkins, Nov. 2005. 14

[112] Dummies.com. Heart valves. Accessed: 16 Aug 2012. [Online]. Available: http://www.dummies.com/how-to/content/figuring-out-cardiac-anatomy-your-heart.html 15

[113] A. C. Gittenberger-de Groot and R. E. Poelmann, "Cardiac morphogenesis," in *Fetal cardiology: Embryology, Genetics, Physiology, Echocardiographic Evaluation, Diagnosis and Perinatal Management of Cardiac Diseases*, 2nd ed., S. Yagel *et al.*, Eds. New York, USA: Informa HealthCare, 2008, pp. 9–17. 15

[114] T. W. Sadler, "Cardiovascular system," in *Langman's Medical Embryology*, 10th ed. Lippincott Williams & Wilkins, 2006, pp. 159–194. 16

[115] M. N. Levy, B. M. Koeppen, and B. A. Stanton, "Chapter 23," in *Berne & Levy Principles of Physiology*, 4th ed. Mosby, 2005. 17

[116] Columbia Center for New Media Teaching and Learning. Pressure-volume loop of the heart. Accessed: 16 Aug 2012. [Online]. Available: http://ccnmtl.columbia.edu/projects/heart/exercises/MechPropHeart/lecture.html 17

[117] A. G. Tilkian and M. B. Conover, *Understanding heart sounds and murmurs: with an introduction to lung sounds.* Saunders, 2001. 18, 22

[118] R. F. Rushmer, *Cardiovascular dynamics.* Saunders, 1976. 18

DOI:10.15774/PPKE.ITK.2012.001

[119] D. Smith and E. Craige, "Heart sounds: toward a consensus regarding their origin," *American journal of noninvasive cardiology*, vol. 2, no. 3, pp. 169–179, 1988. 18

[120] J. Wood, A. Buda, and D. Barry, "Time-frequency transforms: a new approach to first heart sound frequency dynamics," *Biomedical Engineering, IEEE Transactions on*, vol. 39, no. 7, pp. 730–740, 1992. 20, 43

[121] L. G. Durand and P. Pibarot, "Digital signal processing of the phonocardiogram: review of the most recent advancements," *Critical Reviews in Biomedical Engineering*, vol. 23, no. 3-4, pp. 163–219, 1995. 20

[122] S. S. Varghese, S. H. Frankel, and P. F. Fischer, "Direct numerical simulation of stenotic flows. part 2. pulsatile flow," *Journal of Fluid Mechanics*, vol. 582, p. 281, Jun. 2007. 21, 77

[123] B. Karnath and W. Thornton, "Auscultation of the heart," *Hosp. Physician*, vol. 38, no. 9, pp. 39–43, 2002. 22

[124] B. Phibbs, "The heart valves," in *The Human Heart: A Basic Guide to Heart Disease*. Lippincott Williams & Wilkins, 2007, pp. 65–76. 23

[125] ——, "Congenital heart disease," in *The Human Heart: A Basic Guide to Heart Disease*. Lippincott Williams & Wilkins, 2007, pp. 120–131. 24

[126] M. Gewillig, S. C. Brown, L. De Catte, A. Debeer, B. Eyskens, V. Cossey, D. Van Schoubroeck, C. Van Hole, and R. Devlieger, "Premature foetal closure of the arterial duct: Clinical presentations and outcome," *European Heart Journal*, vol. 30, no. 12, pp. 1530–1536, Jan. 2009. 26

[127] P. Moore, M. M. Brook, and M. A. Heymann, "Chapter 33: Patent ductus arteriosus and aortopulmonary window," in *Moss and Adams' Heart Disease in Infants, Children, and Adolescents: Including the Fetus and Young Adults*, 7th ed., H. Allen, D. Discoll, R. Shaddy, and T. Feltes, Eds. Philadelphia: Lippincott Williams & Wilkins, 2008, vol. 1, pp. 683–702. 26

[128] R. I. Clyman, "Mechanisms regulating the ductus arteriosus," *Biology of the Neonate*, vol. 89, no. 4, pp. 330–335, 2006. 26

[129] M. Tynan, "The ductus arteriosus and its closure," *The New England Journal of Medicine*, vol. 329, pp. 1570–1572, 1993. 26

[130] F. Coceani and B. Baragatti, "Mechanisms for ductus arteriosus closure," *Seminars in Perinatology*, vol. 36, no. 2, pp. 92–97, Apr. 2012. 26

[131] D. B. Knight, "The treatment of patent ductus arteriosus in preterm infants: a review and overview of randomized trials," *Seminars in Neonatology*, vol. 6, no. 1, pp. 63–73, 2001. 26

[132] G. Jamous, L.-G. Durand, Y. E. Langlois, T. Lanthier, P. Pibarot, and S. Carioto, "Optimal Time-Window duration for computing time frequency representations of

DOI:10.15774/PPKE.ITK.2012.001

normal phonocardiograms in dogs," *Med. Biol. Eng. Comput.*, vol. 30, no. 5, pp. 503–508, 1992. 29, 33

[133] G. Giannakis, "Cyclostationary signal analysis," in *Digital Signal Processing Handbook*, 3rd ed. FL, USA: CRC Press, Inc., 1999, p. 17–1. 29

[134] J. G. Proakis and D. G. Manolakis, "Power spectrum estimation," in *Digital signal processing*. Pearson Prentice Hall, 2007, pp. 896–968. 30

[135] G. Manning and J. Dripps, "Comparison of correlation and modulus difference processing algorithms for the determination of foetal heart rate from ultrasonic doppler signals," *Medical and Biological Engineering and Computing*, vol. 24, no. 2, pp. 121–129, 1986. 30

[136] I. Daubechies, *Ten Lectures on Wavelets*. SIAM, Jun. 1992. 33

[137] S. Mallat, "Time meets frequency," in *A Wavelet Tour of Signal Processing, Third Edition: The Sparse Way*, 3rd ed. Burlington, MA: Academic Press, Dec. 2008, pp. 89–115. 34

[138] S. S. Chen, "Basis pursuit," Ph.D. dissertation, Stanford University, Department of Statistics, 1995. 35

[139] D. Donoho, "Compressed sensing," *IEEE Transactions on Information Theory*, vol. 52, no. 4, pp. 1289–1306, Apr. 2006. 35

[140] B. Boashash, "Introduction to the concepts of TFSAP," in *Time frequency signal analysis and processing: A comprehensive reference*. Oxford, UK: Elsevier, 2003, pp. 1–82. 36, 38

[141] A. V. Oppenheim, R. W. Schafer, and J. R. Buck, "Discrete Hilbert Transform," in *Discrete-Time Signal Processing*, 2nd ed. NJ: Prentice Hall, Jan. 1999. 36

[142] E. Wigner, "On the quantum correction for thermodynamic equilibrium," *Physical Review*, vol. 40, no. 5, pp. 749–759, 1932. 38

[143] F. Auger, P. Flandrin, P. Gonçalves, and O. Lemoine, "TFTB– Time-Frequency toolbox," 1996. [Online]. Available: http://tftb.nongnu.org/tutorial.pdf 38

[144] A. Zuckerwar, R. Pretlow, J. Stoughton, and D. Baker, "Development of a piezopolymer pressure sensor for a portable fetal heart rate monitor," *Biomedical Engineering, IEEE Transactions on*, vol. 40, no. 9, pp. 963–969, 1993. 39

[145] H. Goovaerts, O. Rompelman, and H. van Geijn, "A transducer for detection of fetal breathing movements," *IEEE Transactions on Bio-Medical Engineering*, vol. 36, no. 4, pp. 471–478, Apr. 1989. 39

[146] P. Várady, L. Wildt, Z. Benyó, and A. Hein, "An advanced method in fetal phonocardiography," *Computer Methods and Programs in Biomedicine*, vol. 71, no. 3, pp. 283–296, Jul. 2003. 39

DOI:10.15774/PPKE.ITK.2012.001

[147] F. Kovács and M. Török, "An instrument using parallel filtering of acoustic signals to record fetal heart rate," *Biomedical Instrumentation & Technology / Association for the Advancement of Medical Instrumentation*, vol. 29, no. 3, pp. 213–219, Jun. 1995. 39

[148] F. Kovacs, M. Torok, and I. Habermajer, "A rule-based phonocardiographic method for long-term fetal heart rate monitoring," *IEEE Transactions on Biomedical Engineering*, vol. 47, no. 1, pp. 124–130, Jan. 2000. 39, 43

[149] (2004) Az NKFP 2004. évi pályázat nyertesei–A magzati szívműködés phonocardiografikus vizsgálatára szolgáló telemetrikus rendszer létrehozása. Accessed: 10/05/2012. [Online]. Available: http://www.nih.gov.hu/palyazatok-eredmenyek/nemzeti-kutatasi/2nkfp-2004-nyertesek 39

[150] M. Signorini, G. Magenes, S. Cerutti, and D. Arduini, "Linear and nonlinear parameters for the analysis of fetal heart rate signal from cardiotocographic recordings," *Biomedical Engineering, IEEE Transactions on*, vol. 50, no. 3, pp. 365–374, 2003. 42, 55

[151] M. Ferrario, M. Signorini, G. Magenes, and S. Cerutti, "Comparison of entropy-based regularity estimators: application to the fetal heart rate signal for the identification of fetal distress," *Biomedical Engineering, IEEE Transactions on*, vol. 53, no. 1, pp. 119–125, 2006. 42, 55

[152] H. Cao, D. Lake, J. Ferguson, C. Chisholm, M. Griffin, and J. Moorman, "Toward quantitative fetal heart rate monitoring," *Biomedical Engineering, IEEE Transactions on*, vol. 53, no. 1, pp. 111–118, 2006. 42

[153] P. Hopkins, N. Outram, N. Löfgren, E. Ifeachor, and K. Rosén, "A comparative study of fetal heart rate variability analysis techniques," in *28th Annual International Conference of the IEEE EMBS*, 2006, pp. 1784–1787. 42

[154] F. Magalhaes, J. Marques de Sa, J. Bernardes, and D. Ayres-de-Campos, "Characterization of fetal heart rate irregularity using approximate entropy and wavelet filtering," *Computers in Cardiology, 2006*, pp. 933–936, 2006. 42

[155] M. Akay and H. Szeta, "Analyzing fetal breathing rates using matching pursuits," *Engineering in Medicine and Biology Magazine, IEEE*, vol. 14, no. 2, pp. 195–198, 1995. 42

[156] M. Godinez, A. Jimenez, R. Ortiz, and M. Pena, "On-line fetal heart rate monitor by phonocardiography," in *Engineering in Medicine and Biology Society, 2003. Proceedings of the 25th Annual International Conference of the IEEE*, vol. 4, Cancun, Mexico, 2003, pp. 3141–3144. 43

[157] A. Jimenez, S. Charleston, M. Pena, T. Aljama, and R. Ortiz, "Performance of the hilbert transform in fetal phonocardiography for cardiotacogram generation," in *BMES/EMBS Conference, 1999. Proceedings of the First Joint*, vol. 1. IEEE, 1999. 43

DOI:10.15774/PPKE.ITK.2012.001

[158] D. Gill, N. Gavrieli, and N. Intrator, "Detection and identification of heart sounds using homomorphic envelogram and self-organizing probabilistic model," in *Computers in Cardiology, 2005.* IEEE, Sep. 2005, pp. 957–960. 43

[159] M. Ruffo, M. Cesarelli, M. Romano, P. Bifulco, and A. Fratini, "An algorithm for FHR estimation from foetal phonocardiographic signals," *Biomedical Signal Processing and Control*, vol. 5, no. 2, pp. 131–141, 2010. 43

[160] J. T. McDonnell, "Knowledge-based interpretation of foetal phonocardiographic signals," *Radar and Signal Processing, IEE Proceedings F*, vol. 137, no. 5, pp. 311–318, Oct. 1990. 43

[161] M. Unser and A. Aldroubi, "A review of wavelets in biomedical applications," *Proceedings of the IEEE*, vol. 84, no. 4, pp. 626–638, 1996. 48

[162] J. Abrams, "Current concepts of the genesis of heart sounds i. first and second sounds," *JAMA: The Journal of the American Medical Association*, vol. 239, no. 26, pp. 2787–2789, Jun. 1978. 56

[163] C. Longhini, E. Baracca, C. Brunazzi, M. Vaccari, L. Longhini, and F. Barbaresi, "A new noninvasive method for estimation of pulmonary arterial pressure in mitral stenosis," *The American Journal of Cardiology*, vol. 68, no. 4, pp. 398–401, Aug. 1991. 56, 62

[164] C. Tranulis, L. Durand, L. Senhadij, and P. Pibarot, "Estimation of pulmonary arterial pressure by a neural network analysis using features based on time-frequency representations of the second heart sound," *Medical and Biological Engineering and Computing*, vol. 40, no. 2, pp. 205–212, 1992. 56, 62

[165] A. Bartels and D. Harder, "Non-invasive determination of systolic blood pressure by heart sound pattern analysis," *Clinical Physics and Physiological Measurement*, vol. 13, no. 3, pp. 249–256, Aug. 1992. 56, 62

[166] J. Xu, L. Durand, and P. Pibarot, "A new, simple, and accurate method for Non-Invasive estimation of pulmonary arterial pressure," *Heart*, vol. 88, no. 1, pp. 76–80, Jan. 2002. 56, 62

[167] S. Debbal and F. Bereksi-Reguig, "Automatic measure of the split in the second cardiac sound by using the wavelet transform technique," *Computers in Biology and Medicine*, vol. 37, no. 3, pp. 269–276, 2007. 56, 62

[168] V. Nigam and R. Priemer, "A dynamic method to estimate the time split between the A2 and P2 components of the S2 heart sound," *Physiological Measurement*, vol. 27, no. 7, pp. 553–568, 2006. 56

[169] I. Yildirim and R. Ansari, "A robust method to estimate time split in second heart sound using instantaneous frequency analysis," *Engineering in Medicine and Biology Society, 2007. EMBS 2007. 29th Annual International Conference of the IEEE*, pp. 1855–1858, 2007. 56, 91

DOI:10.15774/PPKE.ITK.2012.001

[170] H. Koymen, B. K. Altay, and Y. Z. Ider, "A study of prosthetic heart valve sounds," *Biomedical Engineering, IEEE Transactions on*, vol. 34, no. 11, pp. 853–863, Nov. 1987. 56

[171] Y. Tang, C. Danmin, and L. Durand, "The synthesis of the aortic valve closure sound of the dog by the mean filter of forward and backward predictor," *Biomedical Engineering, IEEE Transactions on*, vol. 39, no. 1, pp. 1–8, Jan. 1992. 56

[172] A. Baykal, Y. Ziya Ider, and H. Koymen, "Distribution of aortic mechanical prosthetic valve closure sound model parameters on the surface of the chest," *Biomedical Engineering, IEEE Transactions on*, vol. 42, no. 4, pp. 358–370, Apr. 1995. 56

[173] H. Sava and J. McDonnell, "Spectral composition of heart sounds before and after mechanical heart valve implantation using a modified forward-backward prony's method," *Biomedical Engineering, IEEE Transactions on*, vol. 43, no. 7, pp. 734–742, Jul. 1996. 56

[174] D. Chen, L. Durand, and H. Lee, "Time-frequency analysis of the first heart sound. part 1: Simulation and analysis," *Medical and Biological Engineering and Computing*, vol. 35, no. 4, pp. 306–310, 1997. 56, 57

[175] X. Zhang, L. Durand, L. Senhadji, H. Lee, and J. Coatrieux, "Analysis-synthesis of the phonocardiogram based on the matching pursuit method," *Biomedical Engineering, IEEE Transactions on*, vol. 45, no. 8, pp. 962–971, 1998. 57

[176] ——, "Time-frequency scaling transformation of the phonocardiogram based of the matching pursuit method," *Biomedical Engineering, IEEE Transactions on*, vol. 45, no. 8, pp. 972–979, Aug. 1998. 57

[177] T. Leung, P. White, J. Cook, W. Collis, E. Brown, and A. Salmon, "Analysis of the second heart sound for diagnosis of paediatric heart disease," *Science, Measurement and Technology, IEE Proceedings*, vol. 145, no. 6, pp. 285–290, 1998. 57

[178] D. Chen, L. Durand, and H. Lee, "Time-frequency analysis of the first heart sound. part 1: Simulation and analysis," *Medical and Biological Engineering and Computing*, vol. 35, no. 4, pp. 306–310, 1997. 57

[179] P. Flandrin and P. Borgnat, "Time-Frequency energy distributions meet compressed sensing," *Signal Processing, IEEE Transactions on*, vol. 58, no. 6, pp. 2974–2982, Jun. 2010. 59

[180] M. H. Kalos and P. A. Whitlock, "What is Monte Carlo?" in *Monte Carlo Methods*. John Wiley & Sons, Jun. 2009, pp. 1–5. 59

[181] S. Kirkpatrick, C. D. Gelatt, and M. P. Vecchi, "Optimization by simulated annealing," *Science*, vol. 220, no. 4598, pp. 671–680, May 1983. 59

[182] V. Černý, "Thermodynamical approach to the traveling salesman problem: An efficient simulation algorithm," *Journal of Optimization Theory and Applications*, vol. 45, no. 1, pp. 41–51, 1985. 59

DOI:10.15774/PPKE.ITK.2012.001

[183] T. Csendes, L. Pál, J. Sendín, and J. Banga, "The GLOBAL optimization method revisited," *Optimization Letters*, vol. 2, no. 4, pp. 445–454, 2008. 59

[184] A. Noponen, S. Lukkarinen, A. Angerla, and R. Sepponen, "Phono-spectrographic analysis of heart murmur in children," *BMC Pediatrics*, vol. 7, no. 1, p. 23, 2007. 62

[185] F. Kovács, N. Kersner, K. Kádár, and G. Hosszú, "Computer method for perinatal screening of cardiac murmur using fetal phonocardiography," *Computers in Biology and Medicine*, vol. 39, no. 12, pp. 1130–1136, Dec. 2009. 62

[186] H. Shino, H. Yoshida, K. Yana, K. Harada, J. Sudoh, and E. Harasewa, "Detection and classification of systolic murmur for phonocardiogram screening," in *Proceedings of the 18th Annual International Conference of the IEEE Engineering in Medicine and Biology Society*, vol. 1. IEEE, Nov. 1996, pp. 123–124 vol.1. 62

[187] A. F. Quiceno-Manrique, J. I. Godino-Llorente, M. Blanco-Velasco, and G. Castellanos-Dominguez, "Selection of dynamic features based on Time–Frequency representations for heart murmur detection from phonocardiographic signals," *Annals of Biomedical Engineering*, vol. 38, no. 1, pp. 118–137, Nov. 2009. 62

[188] L. D. Avendaño-Valencia, J. I. Godino-Llorente, M. Blanco-Velasco, and G. Castellanos-Dominguez, "Feature extraction from parametric Time–Frequency representations for heart murmur detection," *Annals of Biomedical Engineering*, vol. 38, no. 8, pp. 2716–2732, Jun. 2010. 62, 106

[189] E. Delgado-Trejos, A. Quiceno-Manrique, J. Godino-Llorente, M. Blanco-Velasco, and G. Castellanos-Dominguez, "Digital auscultation analysis for heart murmur detection," *Annals of Biomedical Engineering*, vol. 37, no. 2, pp. 337–353, 2009. 62

[190] E. Delgado, J. Jaramillo, A. F. Quiceno, and G. Castellanos, "Parameter tuning associated with nonlinear dynamics techniques for the detection of cardiac murmurs by using genetic algorithms," in *Computers in Cardiology, 2007.* IEEE, Oct. 2007, pp. 403–406. 62

[191] C. Ahlstrom, P. Hult, P. Rask, J. E. Karlsson, E. Nylander, U. Dahlström, and P. Ask, "Feature extraction for systolic heart murmur classification," *Annals of biomedical engineering*, vol. 34, no. 11, pp. 1666–1677, 2006. 62, 106

[192] P. Johnson, D. Maxwell, M. Tynan, and L. Allan, "Intracardiac pressures in the human fetus," *Heart*, vol. 84, no. 1, pp. 59–63, Jul. 2000. 68

[193] M. Sklansky, A. Tang, D. Levy, P. Grossfeld, I. Kashani, R. Shaughnessy, and A. Rothman, "Maternal psychological impact of fetal echocardiography," *Journal of the American Society of Echocardiography*, vol. 15, no. 2, pp. 159–166, Feb. 2002. 71

[194] D. Kumar, P. Carvalho, M. Antunes, R. P. Paiva, and J. Henriques, "Heart murmur classification with feature selection," in *2010 Annual International Conference of the IEEE Engineering in Medicine and Biology Society (EMBC).* IEEE, Sep. 2010, pp. 4566–4569. 71

DOI:10.15774/PPKE.ITK.2012.001

[195] R. I. Clyman and N. Chorne, "Patent ductus arteriosus: Evidence for and against treatment," *The Journal of Pediatrics*, vol. 150, no. 3, pp. 216–219, Mar. 2007. 75

[196] S. Schmidt, "Detection of coronary artery disease with an electronic stethoscope," PhD Thesis, Dept. of Health Science and Technology, Aalborg University, 2011. 76, 77

[197] R. P. Feynman, R. B. Leighton, and M. Sands, "The flow of wet water," in *The Feynman Lectures on Physics*. New Jersey: Pearson P T R, 1970, vol. 2. 76, 77

[198] H. Nygaard, L. Thuesen, J. M. Hasenkam, E. M. Pedersen, and P. K. Paulsen, "Assessing the severity of aortic valve stenosis by spectral analysis of cardiac murmurs (spectral vibrocardiography). part i: Technical aspects," *The Journal of Heart Valve Disease*, vol. 2, no. 4, pp. 454–467, Jul. 1993. 77

[199] J. Z. Wang, B. Tie, W. Welkowitz, J. L. Semmlow, and J. B. Kostis, "Modeling sound generation in stenosed coronary arteries," *IEEE Transactions on Biomedical Engineering*, vol. 37, no. 11, pp. 1087–1094, Nov. 1990. 77, 78, 90, 106

[200] A. Borisyuk, "Experimental study of noise produced by steady flow through a simulated vascular stenosis," *Journal of Sound and Vibration*, vol. 256, no. 3, pp. 475–498, 2002. 77, 78

[201] Clay Mathematics Institute. (2000) Millennium prize problems. [Online]. Available: http://www.claymath.org/millennium/ 77

[202] C. J. Chen and S. Jaw, *Fundamentals of turbulence modeling*. Taylor & Francis, 1998. 77

[203] Y. Yazicioglu, T. J. Royston, T. Spohnholtz, B. Martin, F. Loth, and H. S. Bassiouny, "Acoustic radiation from a fluid-filled, subsurface vascular tube with internal turbulent flow due to a constriction," *The Journal of the Acoustical Society of America*, vol. 118, no. 2, p. 1193, 2005. 77, 78, 79, 106

[204] A. Borisyuk, "Model study of noise field in the human chest due to turbulent flow in a larger blood vessel," *Journal of Fluids and Structures*, vol. 17, no. 8, pp. 1095–1110, 2003. 77, 78

[205] S. S. Varghese, S. H. Frankel, and P. F. Fischer, "Direct numerical simulation of stenotic flows. part 1. steady flow," *Journal of Fluid Mechanics*, vol. 582, p. 253, Jun. 2007. 77

[206] H. M. Blackburn, S. J. Sherwin, and D. Barkley, "Convective instability and transient growth in steady and pulsatile stenotic flows," *Journal of Fluid Mechanics*, vol. 607, pp. 267–277, 2008. 77

[207] M. Nobili, U. Morbiducci, R. Ponzini, C. Del Gaudio, A. Balducci, M. Grigioni, F. Maria Montevecchi, and A. Redaelli, "Numerical simulation of the dynamics of a bileaflet prosthetic heart valve using a fluid-structure interaction approach," *Journal of biomechanics*, vol. 41, no. 11, p. 2539–2550, 2008. 78

DOI:10.15774/PPKE.ITK.2012.001

[208] A. Yoganathan, K. Chandran, and F. Sotiropoulos, "Flow in prosthetic heart valves: State-of-the-Art and future directions," *Annals of Biomedical Engineering*, vol. 33, no. 12, pp. 1689–1694, Dec. 2005. 78

[209] O. Smadi, I. Hassan, P. Pibarot, and L. Kadem, "Numerical and experimental investigations of pulsatile blood flow pattern through a dysfunctional mechanical heart valve," *Journal of Biomechanics*, vol. 43, no. 8, p. 1565–1572, 2010. 78

[210] R. J. Tobin and I. Chang, "Wall pressure spectra scaling downstream of stenoses in steady tube flow," *Journal of Biomechanics*, vol. 9, no. 10, pp. 633–640, 1976. 78

[211] P. Ask, B. Hök, D. Loyd, and H. Teriö, "Bio-acoustic signals from stenotic tube flow: state of the art and perspectives for future methodological development," *Medical and Biological Engineering and Computing*, vol. 33, no. 5, pp. 669–675, 1995. 78

[212] D. B. Cooper, M. J. Roan, and P. P. Vlachos, "Acoustic source separation for the detection of coronary artery sounds," *The Journal of the Acoustical Society of America*, vol. 130, no. 6, pp. 4158–4166, 2011. 78

[213] N. Owsley and A. Hull, "Beamformed nearfield imaging of a simulated coronary artery containing a stenosis," *Medical Imaging, IEEE Transactions on*, vol. 17, no. 6, pp. 900–909, Dec. 1998. 78

[214] R. M. Rosen, S. P. Parthasarathy, A. F. Turner, D. H. Blankenhorn, and E. J. Roschke, "Phonoangiography by autocorrelation," *Circulation*, vol. 55, no. 4, pp. 626–633, Jan. 1977. 78

[215] J. Semmlow and K. Rahalkar, "Acoustic detection of coronary artery disease," *Annual Review of Biomedical Engineering*, vol. 9, no. 1, pp. 449–469, 2007. 80, 89

[216] T. Idzenga, J. Pel, and R. van Mastrigt, "Toward an acoustic noninvasive diagnosis of urinary bladder outlet obstruction," *IEEE Transactions on Biomedical Engineering*, vol. 55, no. 6, pp. 1764–1771, Jun. 2008. 80, 89, 90, 91

[217] J. F. Dammann and C. G. R. Sell, "Patent ductus arteriosus in the absence of a continuous murmur," *Circulation*, vol. 6, no. 1, p. 110–124, 1952. 80

[218] Encyclopedia of Children's Health. Patent ductus arteriosus. Accessed: 16 Aug 2012. [Online]. Available: http://www.healthofchildren.com/P/Patent-Ductus-Arteriosus.html 81

[219] A. V. Oppenheim, R. W. Schafer, and J. R. Buck, *Discrete-Time Signal Processing*, 2nd ed. Prentice Hall, Jan. 1999, pp. 336–337. 87

[220] R. Skelton, N. Evans, and J. Smythe, "A blinded comparison of clinical and echocardiographic evaluation of the preterm infant for patent ductus arteriosus," *Journal of Paediatrics and Child Health*, vol. 30, no. 5, pp. 406–411, 1994. 99